İSTANBUL TECHNICAL UNIVERSITY ★ INSTITUTE OF SCIENCE AND TECHNOLOGY

DESIGN AND MANUFACTURE OF POLYMERIC NANOFIBER MEMBRANES VIA ELECTROSPINNING METHOD

M.Sc. Thesis by
Tuncay GÜMÜŞ

Department : Polymer Science and Technology

Programme : Polymer Science and Technology

JUNE 2009

İSTANBUL TECHNICAL UNIVERSITY ★ INSTITUTE OF SCIENCE AND TECHNOLOGY

DESIGN AND MANUFACTURE OF POLYMERIC NANOFIBER MEMBRANES VIA ELECTROSPINNING METHOD

M.Sc. Thesis by
Tuncay GÜMÜŞ
(515071020)

Date of submission :   04 May 2009
Date of defence examination: 01 June 2009

Supervisor (Chairman) :   Prof. Dr. Ali DEMİR (ITU)
Members of the Examining Committee :   Prof. Dr. A. Sezai SARAÇ (ITU)
Prof. Dr. Zeki AKTAŞ (AU)

JUNE 2009

İSTANBUL TEKNİK ÜNİVERSİTESİ ★ FEN BİLİMLERİ ENSTİTÜSÜ

ELEKTROSPİNNİNG YÖNTEMİYLE POLİMERİK NANOLİF MEMBRAN TASARIMI VE ENDÜSTRİYEL ÜRETİMİ

YÜKSEK LİSANS TEZİ
Tuncay GÜMÜŞ
(515071020)

Tezin Enstitüye Verildiği Tarih : **04 Mayıs 2009**
Tezin Savunulduğu Tarih : **01 Haziran 2009**

Tez Danışmanı : **Prof. Dr. Ali DEMİR (İTÜ)**
Diğer Jüri Üyeleri : **Prof. Dr. A.Sezai SARAÇ (İTÜ)**
Prof. Dr. Zeki AKTAŞ (AÜ)

HAZİRAN 2009

FOREWORD

Worldwide conventional manufacturing technologies seem to have reached an end due to limitations in production techniques, material selections and properties. Nanotechnology, as a young challenger, is said to be the revolutionary solution to the limitations in the material properties and indirectly in the production techniques. Nano manipulation of materials has already been providing extraordinary features. Therefore, from now on nanotechnology phenomenon may not be regarded as a futuristic prediction anymore, because it is already a reality in our daily life. This is one of the reasons why I have chosen to research on "nanofiber production" as a branch of nanotechnology. Electrospun nanofibers having nanometer diameters and incredibly large surface area will determine the destiny of all fiber, membrane and composite based materials.

In this work, electrospun nanofibers are produced from synthetic polymers at both laboratory scale and industrial scale. With a commercialization point of view, superior nanofiber based samples are produced. It is hoped that these products will be utilized by the national textile and energy industries. Therefore, I believe this investigation will be a candle to the researchers and manufacturers interested in this area since there is great lack of documentation.

May 2009   Tuncay Gümüş

                                                                              Textile Engineer

TABLE OF CONTENTS

x

ABBREVIATIONS

AC	: Alternative Current
ASTM	: American Society for Testing and Materials
CNC	: Computer Numerical Controlled
DC	: Direct Current
DEC	: Diethyl carbonate
DMAc	: Dimethyl acetamide
DMC	: Dimethyl carbonate
DMF	: Dimethyl formamide
DSC	: Differential Scanning Calorimetry
EC	: Ethylene carbonate
ECM	: Extra Cellular Matrix
GBL	: Butyrolactone
HEPA	: High Efficiency Particulate Air
HEV	: Hybrid Electric Vehicles
HMT	: Hybrid Membrane Technology
HVAC	: Heating Ventilating and Air Conditioning
ISO	: International Organization for Standardization
LED	: Light Emitting Diode
LIB	: Lithium Ion Battery
MCMB	: Meso carbon micro bead
MIT	: Massachusetts Institute of Technology
PA	: Polyamide
PAA	: Poly(acrylic acid)
PAH	: Poly(allylamine hydrochloride)
PAN	: Polyacrylonitrile
PC	: Polycarbonate
PCL	: Polycaprolactone
PE	: Polyethylene
PEG	. Polyethylene glycol
PEMFC	: Polymer electrolyte membrane fuel cell
PET	: Polyethylene terepthalate
PLA	: Polylactic acid
PLGA	: Poly(lactic-co-glycolic acid)
PS	: Polystyrene
PTFE	: Polytetrafluoroethylene
PU	: Polyurethane
PVA	: Polyvinyl alcohol
PVC	: Polyvinyl chloride
PVdF	: Polyvinylidene fluoride
PVP	: Polyvinyl pyrrolidone
QKM	: Quartz Crystal Microbalance
SEM	: Scanning Electron Microscopy
THF	: Tetrahydrofurane
TPU	: Thermoplastic polyurethane

US   **:** United States
USA   **:** United States of America
WVTR   **:** Water Vapor Transmission Rate

LIST OF TABLES

LIST OF FIGURES

DESIGN AND MANUFACTURE OF POLYMERIC NANOFIBER MEMBRANES VIA ELECTROSPINNING METHOD

SUMMARY

Electrospinning process aims to obtain nanometer diameter polymeric fibers by means of high voltage electrical forces. Polymer solutions are exposed to electric fields that transfer the solution from one point to another during solvent evaporation by decreasing the diameter of the fiber to nanometer levels.

Basic electrospinning process and its fundamental aspects are discussed in this work. Process parameters of electrospinning are studied in detail so that a basic understanding of the nature of the process is achieved. The conventional electrospinning setups suggested in the current scientific literature is composed of one needle to be charged by high voltage and a collector plate to be grounded. At the beginning of this work, the conventional setup with one needle/collector had been successfully utilized. Afterwards, to challenge the critics about limitations in electrospinning process production rate, multi needle systems have designed and manufactured to increase the output of the system. 2, 4, 9, 16 and 24 needled electrospinning systems were installed and run successfully in five months period.

At the second stage of the work, industrial scale electrospinning systems with 40, 50, 100 and 256 needles are designed, manufactured and run successfully. Thermoplastic polyurethane (TPU) polymer solutions are prepared and fed into the industrial scale system. The final industrial scale electrospinning configuration with 256 needles is able to coat a one-meter wide fabric with nanofibers having diameters of 50-400 nm.

By the help of multi needle systems, it is now possible to coat a fabric with nanowebs to be used in commercial product development stages of the work. Since, the targeted products such as *Performance Fabrics* and *Battery Separators* are to be developed; TPU and PAN (Polyacrylonitrile) nanofiber webs with 50x40 cm dimensions have been produced. After several nanofiber samples production, first models of nanofiber based Performance Fabric and Battery Separator which are commercially competitive are obtained. These resulting sample products are characterized in accordance with the specific applications.

ELEKTROSPİNNİNG YÖNTEMİYLE POLİMERİK MEMBRAN TASARIMI VE ENDÜSTRİYEL ÜRETİMİ

ÖZET

Elektrospinning prosesinin amacı yüksek voltaj kullanılarak nanometre çapında polimerik lifler elde etmektir. Elektrik alan kuvvetlerine maruz bırakılan polimer çözeltisi bir noktadan başka bir noktaya ilerlerken üzerindeki çözelti buharlaşır ve jetin çapı azalarak nanometre mertebelerine iner.

Bu çalışmada elektrospinning işleminin farklı temel yönleri incelenmiştir. Prosesin doğasını daha iyi anlamak amacıyla proses parametreleri üzerinde detaylıca çalışılmıştır. Literatürdeki mevcut elektrospinning düzenekleri elektrik yüklenmiş tek bir iğne ve topraklanmış bir toplayıcıdan oluşmaktadır. Çalışmada ilk olarak tek iğneli elektrospinning işlemi başarıyla gerçekleştirilmiştir. Daha sonraki beş aylık periyodda 2, 4, 9, 16 ve 24 iğneli sistemler tasarlanmış ve başarıyla çalıştırılarak elektrospinning işleminin üretim hızı gibi kısıtlamaları aşılmaya çalışılmıştır.

Çalışmanın ikinci aşamasında 40, 50, 100 ve 246 iğneli elektrospinning sistemleri tasarlanmış ve başarılı bir şekilde çalıştırılmıştır. 256 iğneden oluşan nihai pilot üretim sistemine termoplastik poliüretan çözeltisi beslenerek, bir metre eninde içerisinde 50-400 nm çapında lifler bulunan bir kumaş üretilebilmektedir.

Çok iğneli elektrospinning sistemlerinin yardımıyla, çalışmanın ticari ürün geliştirme süreçlerinde kullanılmak üzere nano ağlardan oluşan kumaşlar elde etmek mümkün hale gelmiştir. TPU ve PAN nanoliflerinden oluşan ve 50 cm X 40 cm boyutlarındaki yüzeyler *Performans Kumaş* ve *Batarya Separatör Malze*mesi geliştirilecek ürünler olarak seçilmiştir. Çok sayıda nanolif numune üretildikten sonra ticari eşlenikleriyle rekabet edebilir nanolif tabanlı performans kumaş ve batarya separatörlerinin ilk modelleri elde edilmiştir. Ortaya çıkan numune ürünlerin, son kullanım amaçlarına yönelik karakterizasyonu yapılmıştır.

1. INTRODUCTION

In 2000, the American National Science Foundation forecasted that nanotechnology market will have one billion US Dollar capacities and nanotechnology related industries would employ 200 million people by 2015. Despite these numbers are based on data from government documents, the foresights may always contain faults as with every growing technology. Thus, a few industry and corporations related with nanotechnology had emerged in seven years after the launch of National Nanotechnology Initiative in the United States. The research and development activities on this area have been progressing very intensively. Therefore, capacity of "Global Nanotechnology Market" in 2015 revised as 2.95 billion US Dollars in case semiconductors are counted [1]. These forethoughts are huge numbers as it is thought that the capacity of consumer goods was around 900 billion US Dollars and the industrial production was about 3 trillion US Dollars in the U.S.A. in 2005 [2].
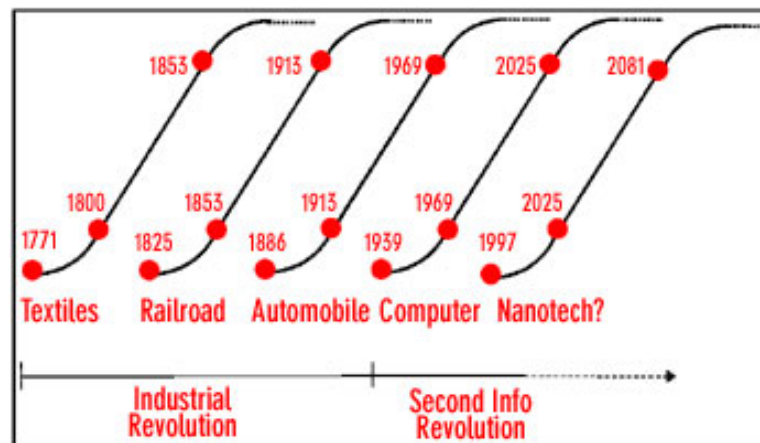
Figure 1.1 : Growth and development of the innovations and technologies [3].

Norman Poire, an economist from Merrill Lynch, argues that growth innovations drive the economy by supporting his thesis with some important revolutions. It is stated that it takes about 28 years for a new technology to become widely accepted which then it goes through a rapid development period for about a half century. Finally, it becomes widely knowable one century after the birth. As illustrated in

Figure 1.1, Poire thinks that nanotechnology which have been in the emerging period will shape the industry in forthcoming century [3].

The studies on nanotechnology are carried out by various disciplines together or individually. It also has started to find some applications in textile industry. Today many nanotechnology applications, from fiber to finishing such as nanofiber production and nano dressing, take part in research topics of scientist in this industry. Nanomaterials have been started producing as nanoparticles. One of the most important advantage of nanomaterials is high surface area to volume ratio. Porous, selectively permeable, high surface area materials can be used in various applications. Therefore, nanofibers are potential materials for applications, which require high surfaces.

A fiber having a diameter below one micrometer may be defined as a nanofiber. As these nanofibers can be manufactured from organics such as synthetic or natural polymers, they also can be produced from inorganic materials such as metals or ceramics [4].

Nanofibers can be obtained by high capacity processes such as meltblowing, spunbonding, bi-component (island-in-the-sea) fiber spinning as well as particular methods for instance self-assembly and nanolithography. However, cost, production rate, fiber structure, fiber diameter distribution, orientation factors are the causes, which limit the usage of these production systems. At this point, electrospinning method which has high production rate and low cost becomes advantageous [5].

Nanofiber production in filament form can only be realized by electrospinning and electroblowing methods. Both of these methods are based on electrostatic fiber spinning. Metals, ceramics, polymers, particles, additives can be used as raw materials for electrospinning process. Moreover, complex nanofiber structures such as core-shell, hollow, highly porous, crimped, bi-component nanofibers can be obtained by using special methods [6, 7].

2. ELECTROSPINNING PROCESS

2.1 Nanofibers and Electrospinning

Diameters of nanofibers are much smaller than human hair (Figure 2.1). The paramount advantage of nanofibers is to have extremely high surface area to volume ratio. For example, when 10 μm and 100 nm polyethylene fibers are compared, 13 km microfiber (with 10 μm diameter) is produced from one gram polymer while 130,000 km nanofiber (with 100 nm diameter) is obtained from the same amount of polymer. These microfibers construct 0.4 m^2gr^{-1} surface area while nanofibers make 40 m^2gr^{-1}. In denier numbering system, 9000 meters of one gram fiber is defined as one denier so, 10 μm fiber equals 1 denier and it equals to 10^{-4} denier for 100 nm of nanofiber [6].
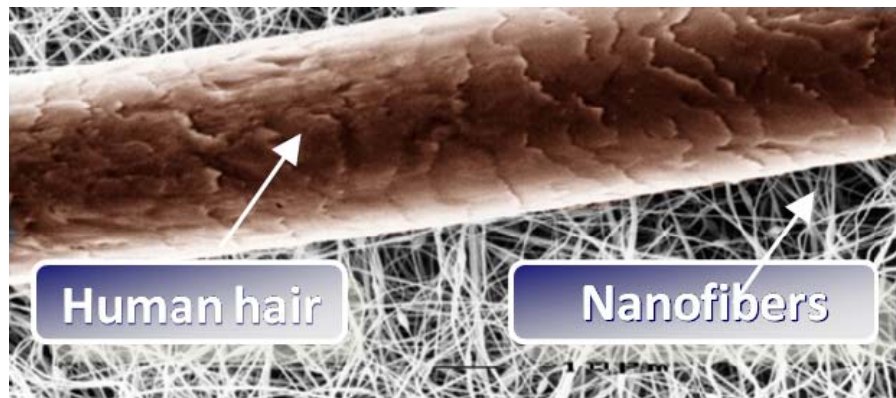
Figure 2.1 : Human hair and nanofibers.

Principle of electrospun nanofiber production method is based on thinning of viscoelastic fluid material by drawing it in a path, under internal and external forces. In solution and melt spinning production methods fibers are made thinner under mechanical forces, while in electrospun fiber production, fluid material is oriented by electrostatic forces during solidification, so nano-sized fibers are obtained. Nanofiber filament is produced as long as material is fed to the system that is also principle of conventional fiber spinning methods.

A laboratory electrospinning set-up (as seen in Figure 2.2) basically and commonly consists of polymer solution, solution feeding system, high voltage power supply and collector plate. By some means, a polymer droplet is formed on the needle with a feeding rate about 1-7 ml/h. High voltage which have potential more than a few kilovolts is applied to this polymer droplet on the tip of needle.
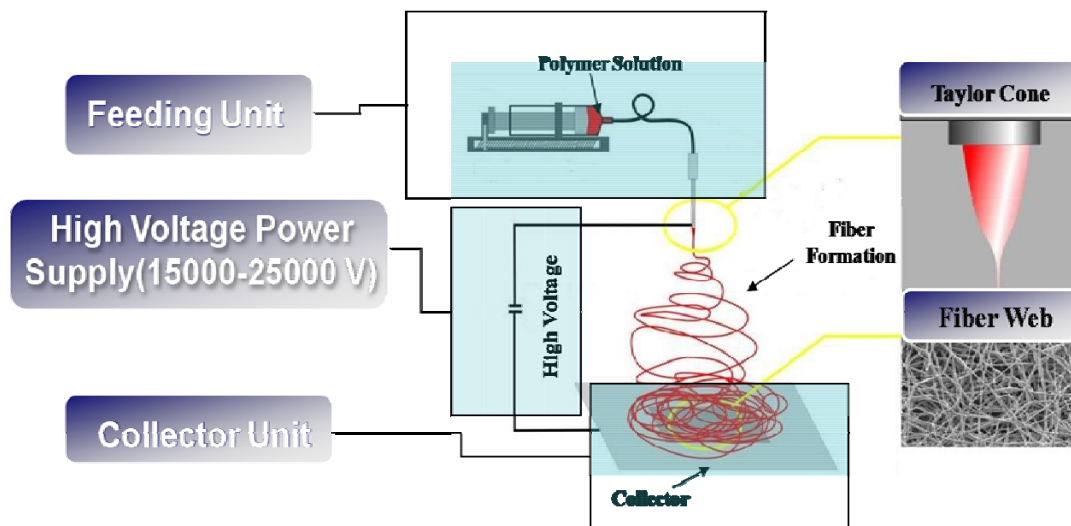
Figure 2.2 : Electrospinning set-up.

A collector, which is grounded or charged with opposite potential, is placed at a suitable distance from the needle. The semi-spherical droplet under surface tension forces forms a conical shape into direction of the collector by the effect of electrostatic forces opposing to surface tension, this cone is named as "Taylor cone". When the voltage is increased a little more, a polymer jet ejects from droplet and it started to travel to the collector. Jet moves into a linear path for the first several centimeters, and then it continues its travel on a helical path because of the high stress difference between internal and external forces. During this time, viscoelastic jet becomes thinner by drawing and it also solidifies. The helical motion of jet in unstable region is defined as "whipping". In addition, this phenomenon provides the nonwoven and porous structures from fibers accumulated on the collector [8-10].

It is possible to produce melt electrospun fibers from thermoplastic polymers such as polypropylene or polyethylene. Because it requires more drawing ratios and solidifies quickly, melt electrospinning process contains difficulties in practice [8].

2.2 Electrospinning History

Though electrospinning is a topic, which is actively researched, fundamental of process goes back to 1700's. Gray was the first person who worked on the activity of water droplets under electrostatic forces in 1731 [11]. At the end of 1800's Larmor explained the movements of dielectric liquids under electric charges by electrodynamics theory [12]. This theory made contributions to electrospinning which was firstly experimented by Cooley and Morton in the first decade of 20th century. In addition, the first patent about electrospinning was published by Cooley in 1902 (see Figure 2.3). However Cooley's set-up as seen in Figure 2.3 was not a fiber spinning process, fluids are collected onto a drum as dispersed particles by using electrostatic forces [13]. In the same year, Morton patented a process that he produced liquid particles under positive or negative high electrical potential [14]. Hagiwara in 1929 designed a viscose fiber production system by electrospinning [15].
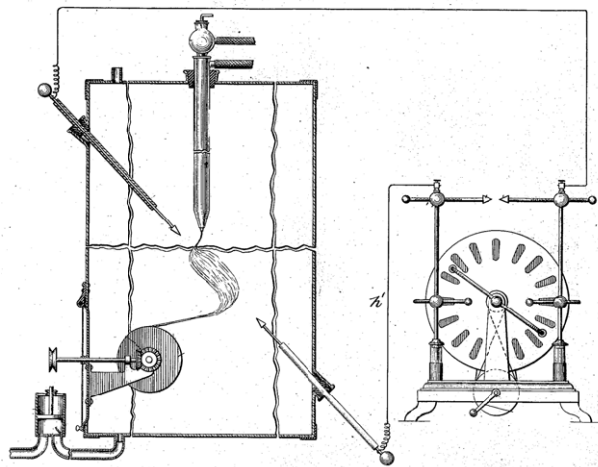
Figure 2.3 : Cooley's electrospinning set-up [13].

The first patent for electrospun fiber production, which is commonly acknowledged, was published by Formhals in 1934. In the Formals' patent, a solution was prepared by solving cellulose acetate in ethylene glycol, then a high voltage about 5-10 kV was applied to the solution by a rough drum. He accumulated the fiber onto another drum then he managed to collect fibers as a bunch from this drum [16]. Formhals used various systems and he published eleven patent applications in following ten years [6].

Vonnegut and Neuber, in 1952, managed to produce regular droplets having diameters about 100 μm by employing high voltage. They used water that conduct high voltage in a capillary glass tube which has a hole diameter smaller than 1 mm. They applied 5-10 kV high voltage to a copper wire which does not have any contact to water [17].

Drozin invented that some liquids are dispersed under high voltage conditions in 1955. He used an electrospinning set-up which was similar to Vonnegut and Neuberin's system, he investigated the characteristic of droplets in different conditions [18].

In 1966, Simons achieved producing very thin and light nonwovens by application of electrospinning set-up, which is also published as a patent application. Fiber webs in different structures were obtained by polymers such as cellulose esters and ethers, vinyl, acrylic, polystyrene, polyurethane, polycarbonate solved in chloroform, ketone based solvents which have different dielectric constants [19].

In 1969, Taylor made investigations on liquid droplets, electrically charged polymer jets, and derived a theory as a result of his observations (see Taylor's electrospinning set-up in Figure 2.4). In this theoretical model, it is showed that a stable fluid droplet becomes unstable under the effect of critical voltage. Taylor also reflects on the Zeleny's theory and he argued that instability starts when internal and external forces equally affect the polymer droplet [20].

He set up a test equipment in order to show voltage value the liquid from capillary tube is required as seen in Figure 2.4. Polymer in C reservoir is activated by applying potential difference between B and E plates. If voltage is increased, at first, droplet take a convex form by quitting from A, D metal tube. Then, a little increase in voltage moves the jet from A tube to B plate [20].
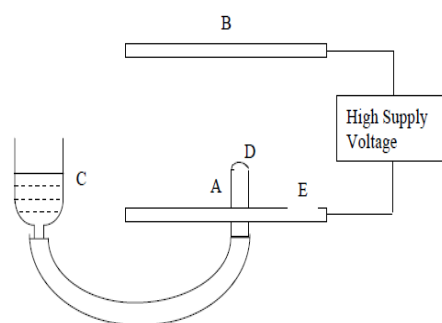
Figure 2.4 : Taylor's electrospinning set-up [20].

In 1971, Baumgarten produced acrylic microfiber by electrospinning method. In the experiment a solution was prepared with commercial copolymer contains 43.6% acrylonitrile, 56% methyl acrylate and 0.4% sodium styrene by solving it in dimethyl formamide. In order to display the events taking place between needle tip and collector plate, a camera and a flasher are placed into the electrospinning set-up as seen in Figure 2.5. It is observed that the shape of the polymer droplet becomes semi-cylindrical from conical if viscosity is increased. Additionally, it was verified that linear jet length increase with increasing viscosity and this jet length is directly proportional to fiber diameter. In addition to these, the number of jets increases with increasing flow rate, however fiber diameter does not change. All these phenomena are supported by the experimental photographs (see Figure 2.5) [21].
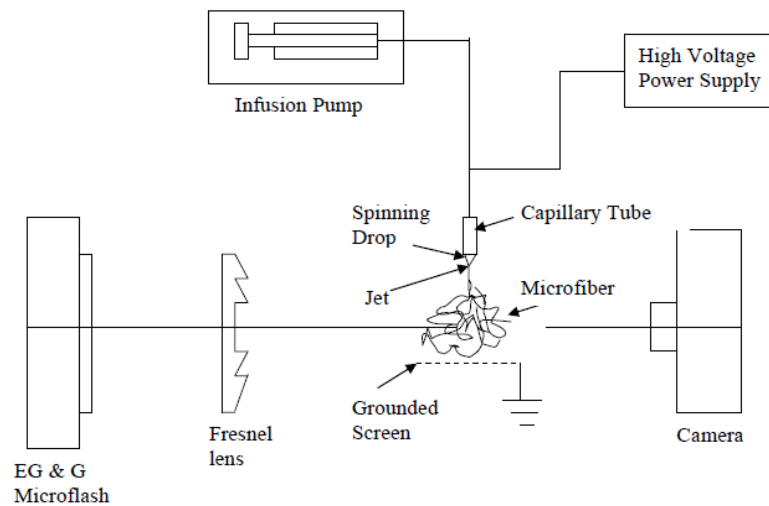
Figure 2.5 : Electrospinning apparatus with photographic setup [21].

In 1977, Martin et al. manufactured two and three-dimensional prosthesis from organic materials such as PTFE (polytetrafluoroethylene), polyurethane, polyvinyl alcohol, polyvinyl pyrrolidone, polyethylene oxide by electrospinning method. Fiber webs, collected onto a non-conductive conveyor belt, are taken from belt in order to be used as medical prosthesis, wound dressings and tissue scaffolds as seen in Figure 2.6 [22].

In 1978, Simm et al. who worked for Bayer in Germany published a patent about an electrospinning design, which produces electrospun polystyrene fiber webs for filtration applications. Solution is fed from a reservoir by a pump to the rotary nozzle, so at the nozzle tip a high voltage is applied to the solution as seen in Figure 2.7.
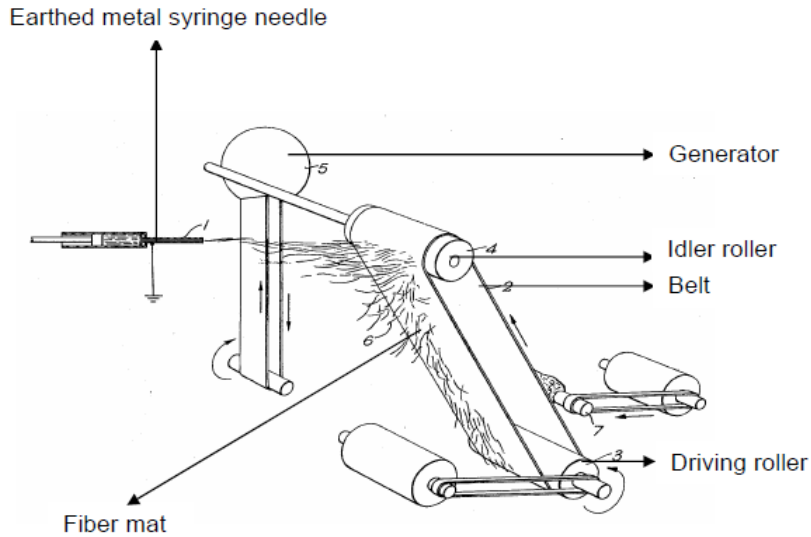
Figure 2.6 : Continuous electrospun fiber production by Martin et al [22].

At the both sides of the nozzle, two conveyor belts are placed as collector. Simm et al. observed that temperature, humidity and solution conductivity affect the diameter of electrospun fibers. Electrospun fiber web is produced as a composite material by laminating it with a suitable filter paper [23].

Lorrando and Manley made experiment on polyethylene and polypropylene by combining electrospinning and melt spinning process to produce melt electrospun fibers. In this novel production system, high pressure forces which is required for conventional melt spinning replaced low pressure and electrostatic forces [24].
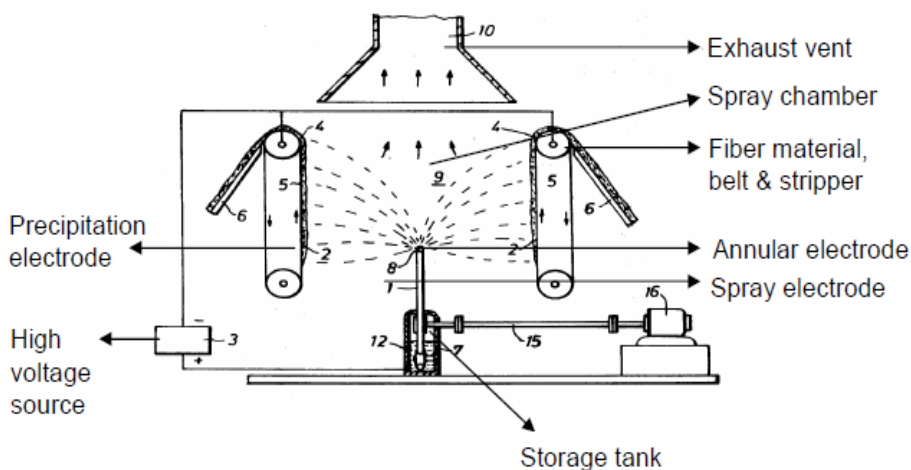
Figure 2.7 : Apparatus for the production of fiber fleeces by Simm et.al.[23].

As electrospun fiber was compared to the fibers produced by conventional melt spun fibers, its orientation was low and some beads were also generated on the fiber

8

surface. The level of voltage and melt viscosity directly affects the diameter of fiber. It is determined that finer fibers can be produced with higher voltage values and higher temperatures. As for spinneret diameter, it was stated that spinneret diameter does not constitute a factor on fiber diameter [24].

In 1982, Bornat patented a design for manufacturing electrospun tubular products to use as medical products. In this system (as seen in Figure 2.8), biocompatible polymers such as PTFE, polyurethane, polyamide, polyacrylonitrile, polyvinyl alcohol, pyrrolidone, polyethylene oxide were preferred. High potential difference is generated between polymer solution loaded needles and a rotating grounded rod, which is also used as collector. Fibers are accumulated on to this rotating rod to form tubular nanofiber webs for medical applications. The final products are constructed with porous web containing fine fibers [25, 26].
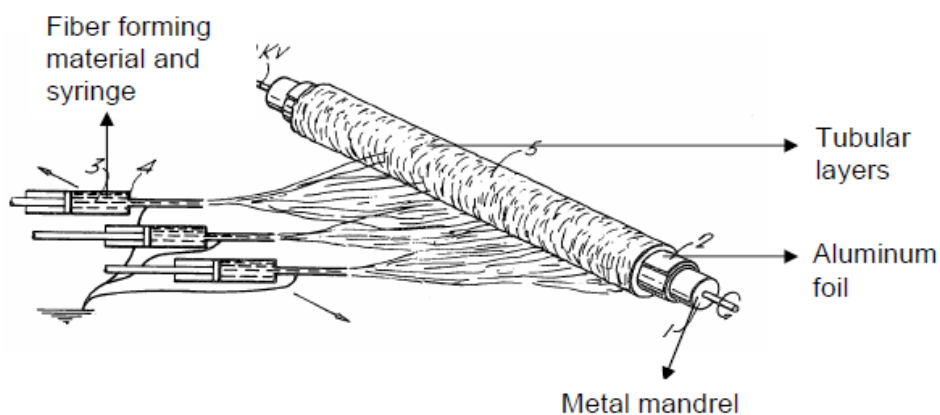
Figure 2.8 : Apparatus for preparing tubular fiber webs [25].

In 1982, Donaldson Inc. incorporated nanofibers into filters to increase the efficiency of filtering small particles. The first electrospun fiber product was introduced to the market by the trade name Ultra-Web®. Electrospun nonwoven mesh incorporated with catalyst has been used in clothing to provide protection from chemical and biological hazards [27].

After an interruption for a decade or so, a major upsurge in research on electrospinning took place due to the increased knowledge on the application potential of nanofibers in different areas such as high efficiency filter media, protective clothing, catalyst substrates and adsorbent materials. Research on nanofibers gained momentum due to the work of Doshi and Reneker [28]. Doshi and Reneker studied the characteristics of polyethylene oxide (PEG) nanofibers by

varying the solution concentration and applied electric potential. The jet diameters were measured as a function of distance from the apex of the cone and they observed that the jet diameter decreases with the increase in distance. They found that the solution with viscosity less than 800 centipoises (cP) was too dilute to form a stable jet and solutions with viscosity more than 4000 cP were too thick to form fibers [29].

2.3 Electrospinning Theory

It is stated that five forces act on polymer solution or melt during electrospinning process (Figure 2.9). These forces make fluid droplet a mobile jet and they move the jet towards to collector at high acceleration rates [30]. Forces are shown in the equation below,

In this equation, "l" is the distance between spinneret and collector.

$$Ft = Fo + Fc + Fve + Fcap + Fg = -m.(\frac{d^2 l}{dt^2})$$

(2.1)

F_o: Electrostatic force generated by the electric field. This force is the resultant force of electrostatic forces between charged spinneret and collector. It goes through droplet with force

$$Fo = q \times E = q \times \frac{V_0}{l}.$$

(2.2)

In the equation, q is quantity of charge on droplet, V_o is applied voltage, and l is needle to collector distance.

F_c: repulsive coulomb force acting on droplet from internal droplet forces. This force acts as a repulsive forces into droplet generated from droplet molecular structure. So, it is defined as

$$Fc = e^2/l^2$$

(2.3)

In the equation, "l" provides stretching of the jet generated on the needle in two directions.
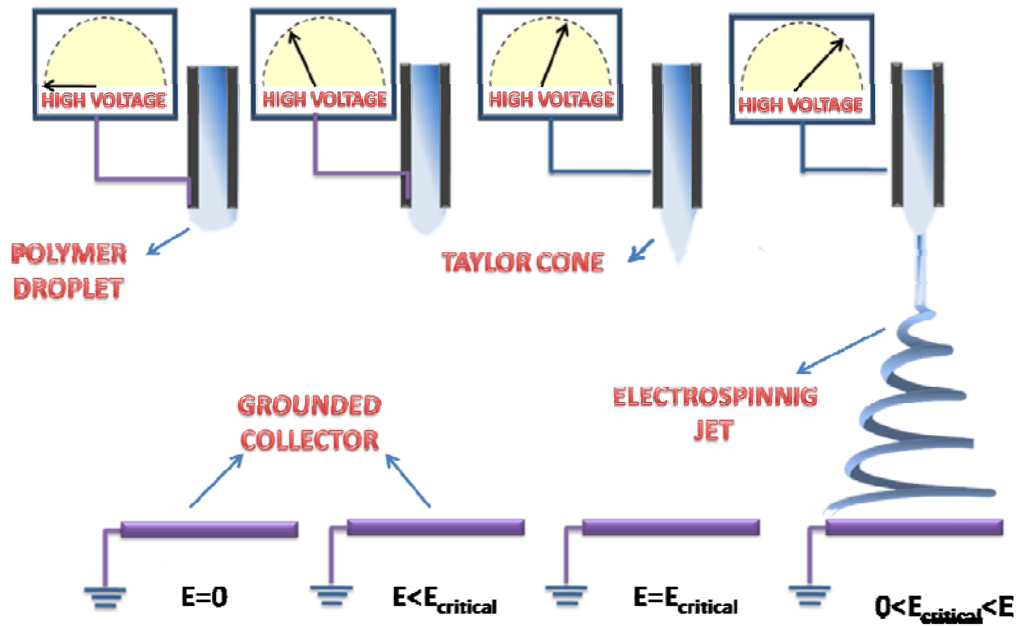
Figure 2.9 : Schematic diagram showing balance of external and internal forces.

F_{cap} **(Surface tension):** hinders the stretching of droplet and jet, it makes the polymer droplet stable. This is characteristics of viscous fluids.

F_{ve} **(Viscoelastic force):** hinders the stretching of polymer jet and decreases the fluidity of liquid polymer. It depends on the frictional and contact forces between polymer chains.

Fg **(Gravitational force):** It positively or negatively affects the total force on the droplet or jet depending of electrospinning set-up direction, from down to top or from top to down, during the travel of jet from needle to collector [31].

In comparison to other forces, the gravitational force is negligibly smaller. Therefore, electrospinning occurs because of the force differences between internal forces such as surface tension, viscoelastic forces of the polymer jet and the electrostatic forces, which acts on the jet in the opposite direction of internal forces. For especially solution electrospinning process, when a small volume of a polymer solution, which is stable under the effect of internal forces, is charged with electric, charged molecules are slowly prompt these polymer droplet unstable. At the point where internal forces equal to external polymer droplet takes a conical shape called Taylor cone. Then the balance between internal and external forces is disturbed with a small increase of in electrostatic forces, a jet generates from droplet and begins to travel to the collector. The difference between internal and external forces increases as much

as jet approach to collector that provides thinning of the jet at a very high draw spinning ratio. At this section, the jet travels by forming a helical path (Figure 2.10), this motion of the jet is called whipping instability, which not only enhances the draw ratio but also, provides much longer time for solidification of viscous jet. At the end of this travel, solidified polymer jet is accumulated on the collector as a continuous filament having diameter smaller than one micron. In brief, it can be said that a polymer solution having suitable properties is spun and solidified under electrostatic forces, so a continuous filament, which has nano size diameter is produced by a hybrid process composed of electrospray and dry spinning named electrospinning [31].
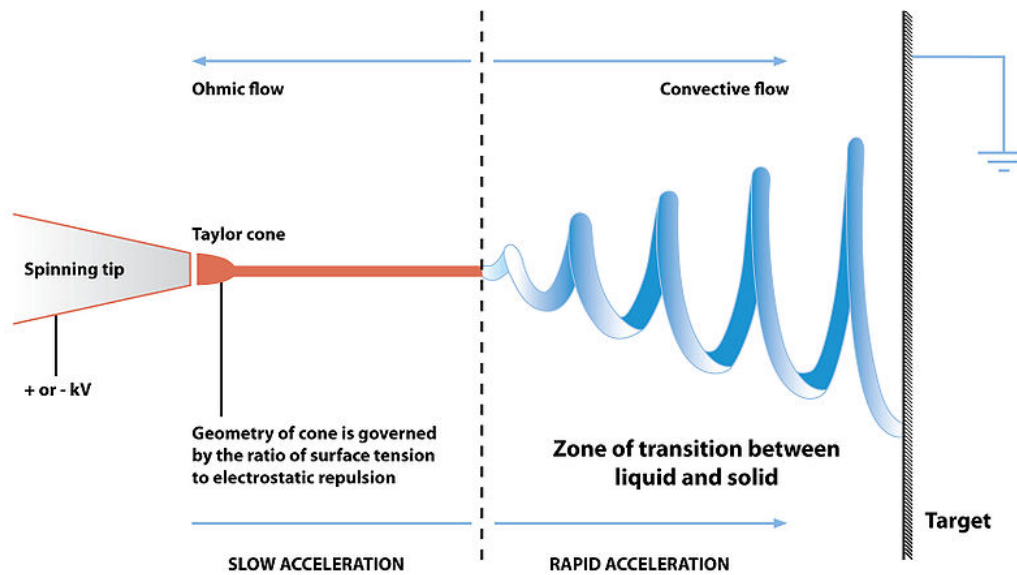
Figure 2.10 : Taylor cone and electrospinning jet [32].

2.4 Factors Affecting Electrospinning Process and Nanofiber Properties

There are a number of parameters that determine internal and external forces. These can be classified as solution properties (concentration, viscosity, molecular weight, and surface tension), process parameters (voltage, needle to collector distance, flow rate, needle dimensions) and ambient parameters (temperature, humidity).

2.4.1 Solution properties

Solution properties directly affect the fiber morphology, production rate, and producibility in electrospinning process. Concentration, viscosity, surface tension,

solvent properties, solution conductivity and solution temperature are significant parameters, which specify the solution properties.

2.4.1.1 Viscosity

Viscosity describing the intermolecular interactions in polymer solutions is the most important parameter that determines fiber diameter and morphology in electrospinning method. For polymer-solvent systems, concentration plays the biggest role on the viscosity by decreasing or increasing the intermolecular interactions. Therefore, a linear relation exists between these two parameters. In addition to this, the interactions between the polymer molecules with solvent, organic or inorganic additives are other factors that affect the viscosity [33].

In order to produce nanofiber by electrospinning process, the viscosity of the solution has to be within a strictly defined range. If viscosity is too high, the electrostatic forces are not able to generate a jet from the polymer fluid or the fibers with diameter in micron range can only be produced. In contrary, a polymer solution with lower viscosity generates nano- and micro-particles instead of fibers. Hence, this process is called electrospraying. During a production with electrostatic forces from a suitable solution viscosity around 1-200 poise, sufficient viscoelastic force is provided, any discontinuity does not exist on the jet, as a result, nanofibers can be obtained by evaporation of solvent from the jet [34]. While all other parameters are kept constant, the viscosity and the surface tension are the prime factors which set this production range [35].

As seen in Figure 2.11, the relation between viscosity and the fiber diameter is claimed to be exponential [36]. Because polymer chains have increasing mobility and intermolecular interactions are weaker in low viscosity solutions, stronger instabilities occur during electrospun fiber production. Consequently, the jet is subject to higher elongation, so fibers with smaller diameters are produced. When viscosity is increased, polymer molecules obtain more stable structure that results in coarser fiber diameters because of lower elongation ratio of the jet [33].

13
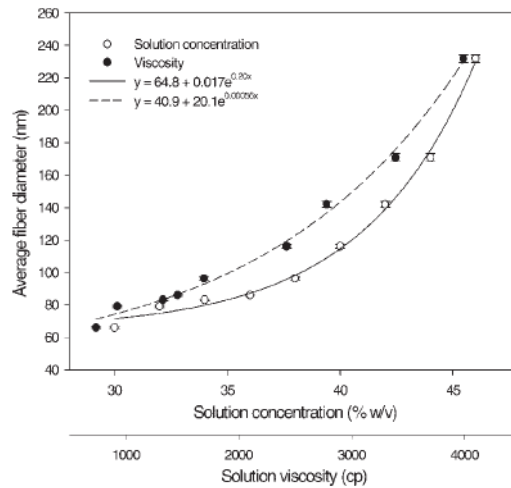
Figure 2.11 : Average diameter of PA fibers as a function of concentration and the viscosity of solutions [36]

In addition to the homogeneity of the solution, the variation in the process parameters during fiber production process, the instability of the jet during the travel from spinneret to collector and the splaying of the jets are the factors that shape characteristics of the fiber diameter distribution. In general, the experiments show that decreasing viscosity results in obtaining more homogeneous fiber diameters. On the other hand, the electrospun fiber production with high viscosity solutions produces a broad fiber diameter distribution. Bimodal or trimodal peaks are observed on graphics of the fiber diameter distributions. The reason for this result is that some of the jets are broken into small jets during fiber production; however, some others stay as they are. This is a problem experienced frequently in the electrospraying [33].
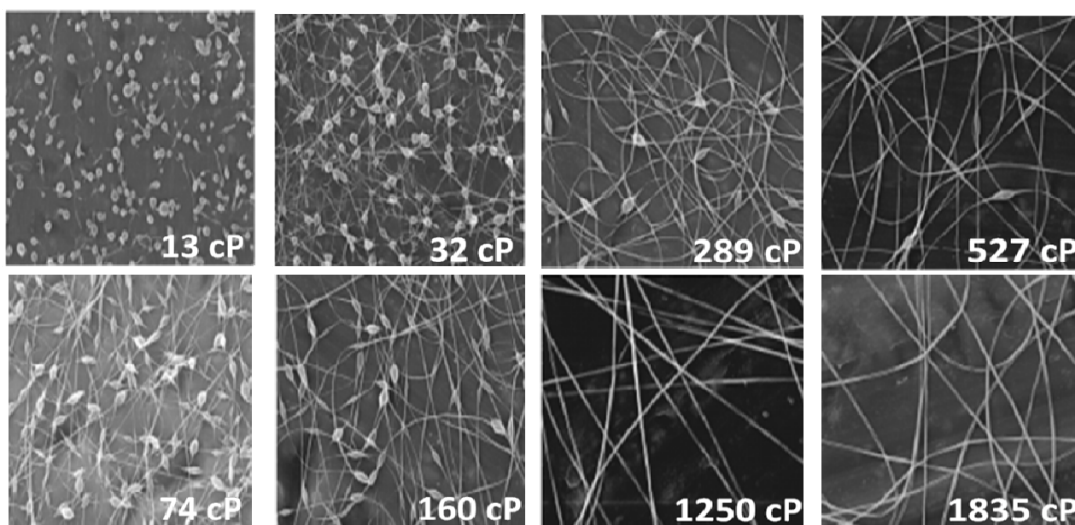
Figure 2.12 : Morphology of beaded fibers versus solution viscosity. Electric field is 0.7 kV/cm, The horizontal edge of each image is 20 microns [37].

Another effect of viscosity on the fiber morphology is the defects called "bead formation". Bead formation is a disorder resulting from jet irregularly due to the reasons stated above. In addition to this, size and structure of beads can differ. As seen from Figure 2.12, the beading behavior of fibers electrospun from high viscosity solutions is lower than less viscous solutions [37].

As seen from Figure 2.12, increasing viscosity decreases the number of bead defects on fibers, and spherical bead defects are generated from lower viscosity solutions. On the other hand, the beads obtain elliptical shapes with increasing viscosity. At the end, the smooth fibers are electrospun from much higher viscous solutions without any bead formation [37].

2.4.1.2 Concentration

The solution concentration is one of the most important parameter for electrospinning process, it is necessary that solutions with suitable concentration and viscosity must be used in order to produce nanofibers by this method.
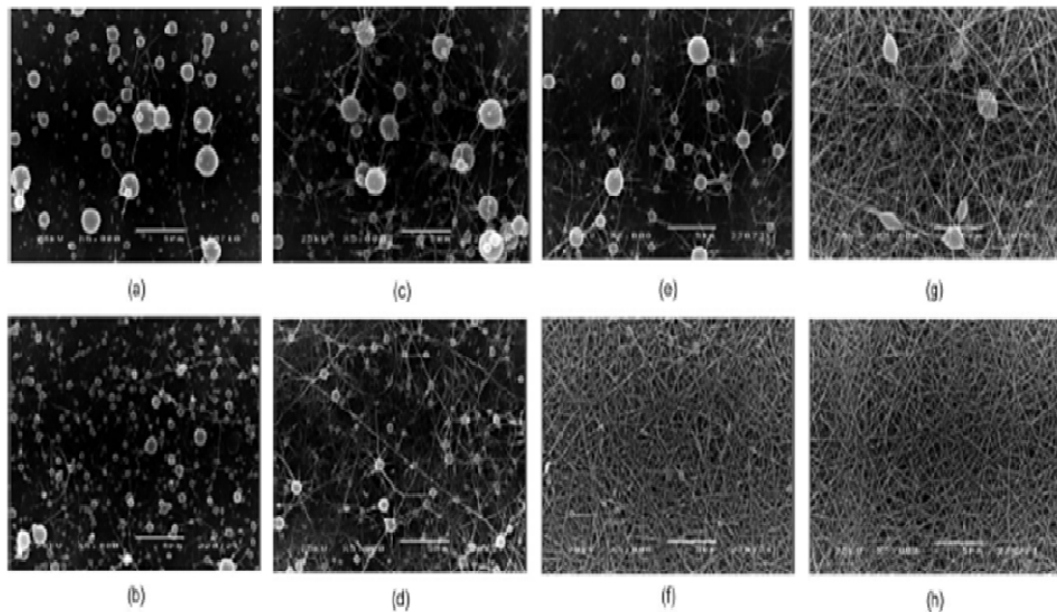
Figure 2.13 : SEM images of PA6/formic acid solution with different concentration a)10% b)14% c) 16% positive d) 16% negative e)18% positive f) 18% negative g) 26% positive h) 26% negative [38].

If concentration is too low, the jet can not withstand the electrostatic forces due to low viscoelastic force that result in breaking of jets. As a result, discontinuous fibers or even particles are formed. Thus, an electrostatic process is called electrospray occurs which is widely used in the ink-jet printing process, electrostatic powder

painting, electrostatic paint spraying. On the other hand, if concentration or viscosity is within a suitable range, molecular contacts and friction between polymer chains increase. These internal forces exhibit resistance to the electrostatic forces that inhibit jet breaks or bead defects and also make fiber thinner by providing electrostatic forces to elongate the jet [38].

In Figure 2.13, PA 6 (polyamide 6) nanofibers are shown which have different concentrations ranging between 10-26% w/v. For every material used to produce nanofiber by the electrospinning process has limit values of concentration [38]. Even particles or fibers coarser than one micron can be produced at the outside of these limits. As examples, 10-46% for PA, 4-10% for PEO, 1-4% for PLLA are favorable concentration ranges in order to get regular nanofibers. At this point, it has to be stated that the molecular weight is also another factor. [38-40].
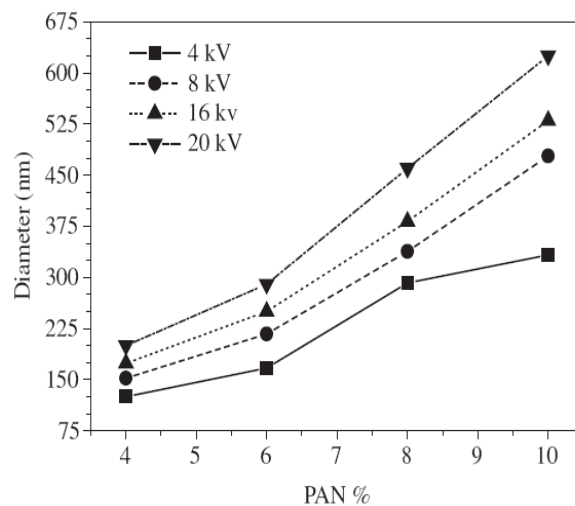
Figure 2.14 : Fibers diameter variation as a function of precursor solution concentration and applied voltage [41].

The fiber diameter is linearly proportional to the concentration. An increase in concentration increases the fiber diameter as seen in Figure 2.14. In order to electrospin uniform nanofibers, highly concentrated solutions must be used. [41].

2.4.1.3 Molecular weight

Molecular weight is one of the parameter that directly affects the viscosity of the material. Increasing the molecular weight results in an increase in the length of the polymer chains as well as an increase in the chain interactions and a decrease in distance between molecules. Generally when a high molecular weight polymer is

16

solved by a solvent, the viscosity of the solution is higher than the solution prepared from the low molecular weight of same polymer [38].

Experimental work is carried out by 100,000 and 300,000 molecular weight PLLA, fiber diameters electrospun from 4.5%wt concentration of high molecular weight equals to 9 wt% concentration of low molecular weight solutions. Molecular weight plays an important role on determining the solution concentration and fiber diameter (see figure 2.15) [39].
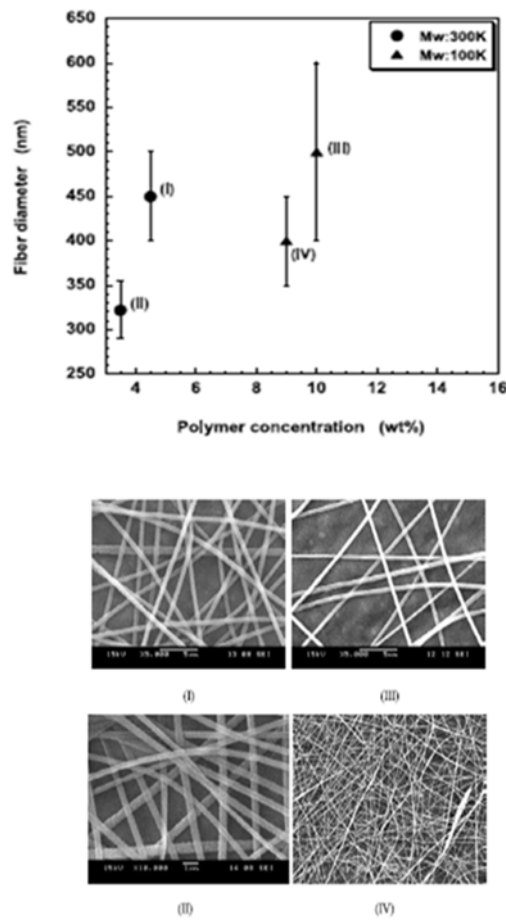
Figure 2.15 : Molecular weight effects on the morphology of the electrospun PLLA fibers [39].

2.4.1.4 Surface tension

Viscoelastic forces protect polymer droplet against irregular forces during electrospinning. The surface tension tends to keep the polymer droplet in minimum surface area, in contrast the electrostatic forces push them to elongate and even to break the polymer jet in order to disperse the polymer droplet into structures having maximum surface area [37].
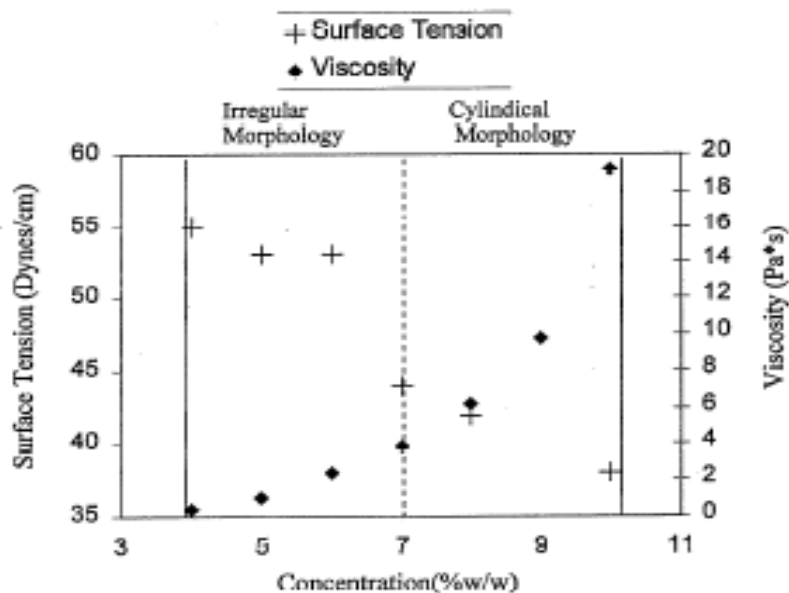
Figure 2.16 : Concentration dependence of solution surface tension and solution viscosity for PEO-water solutions [28].

Experiments carried out with PEO showed that the surface tension severely decreases with increasing concentration ratio. As it is showed in Figure 2.16 smoother fibers are obtained because of the regular solidification during travelling of the jet to the collector as surface tension decreases [40].

2.4.1.5 Solvent

Solvent used to make polymer chains mobile and open affects the solution viscosity, the surface tension and the solution conductivity. Thus, interactions between viscoelastic forces, surface tension, electrostatic forces and evaporation, phase inversion can be changed in respect of solvent and solvent systems [38, 42].
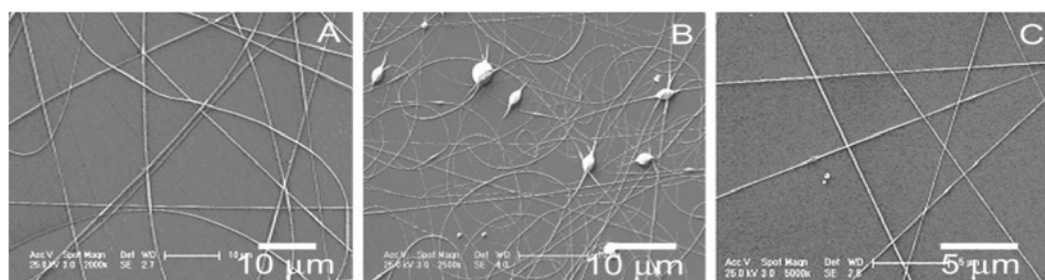
Figure 2.17 : SEM images of 4% PVP (w/v) nanofibers spun in different solvents; A) ethanol B) DMF C) ethanol/DMF [42].

The effect of the solvent properties such as surface tension, viscosity, charge density, boiling point on PVP nanofiber morphologies is observed by an experiment in which ethanol, DMF and ethanol/DMF solvents were used. Increasing amount of ethanol

added to the system increases the viscosity of solution; however, reduction in surface tension occurs. That provides producing shapely regular and smooth nanofibers. As DMF ratio of solvent is increased. The so called "bead defects" are generated as a result of reducing viscosity and also increasing the surface tension. Fibers in Figure 2.17-A having diameter of 300 nm can be made thinner about 200 nm as in Figure 2.17-C by adding suitable DMF to the ethanol which provides conductivity and suitable viscosity and surface tension values to the solution [42].

2.4.1.6 Additives

Additives such as salts, surfactants, plasticizers, polyelectrolytes added to the polymer/solvent systems can alter the electrospun fiber diameter, morphology, diameter distribution and physical properties of fiber web. Because of this, they affect the internal, external forces and phase separation in electrospinning process.

In the observations by adding salt to the solution, it is observed that nanofibers with smaller diameters are generally produced. However, this result can not be generalized as that every salts give similar results, because each salt has different, specific chemical structure and molecular size. In consequence of this observation, a salt, which gives favorable results for polymer solutions, could not form similar effects for other solutions in electrospun fiber production. Each salt specifically react with polymer and solvent molecules with different intensity that results in various changes in viscosity, surface tension and conductivity [33].

The effect of different salts on electrospun PAN nanofiber properties is experimentally investigated by Qin, et al.[43]. It was observed that salts added 1%wt to the solution increases conductivity of the solution to superior levels as seen in Figure 2.18. It is also stated that viscosity and shear strength are slightly affected by the salts added to the solution. Added salts to PAN/DMF solutions more than 4% give limited decrease to viscosity and shear strength properties of the solution [43].
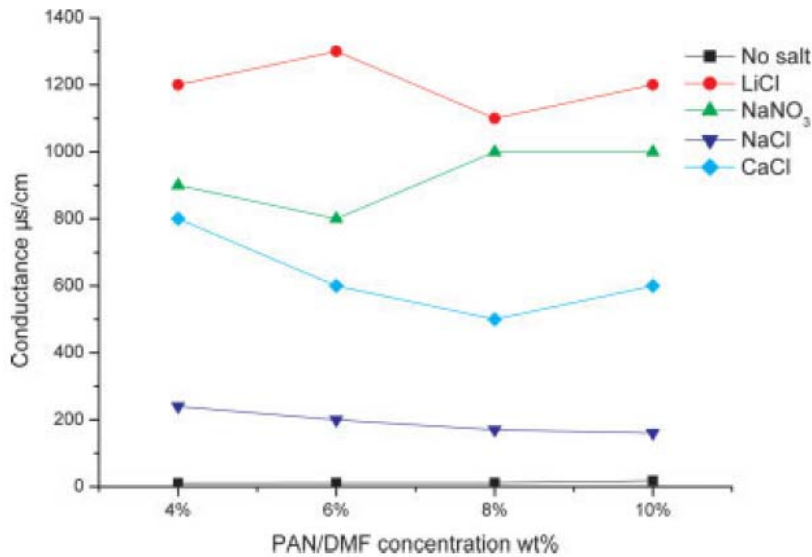
Figure 2.18 : Comparison of conductance of solutions with different kinds of concentration and added salt [43].

In Table 2.1, it is argued that, final nanofiber diameter is directly proportional to the solution conductivity as a result of velocity of jet increasing by the effect of solution conductivity increment [43].

Table 2.1 : Mean values of fibers electrospun by solutions with different salts [43].

Salt	Average fiber diameter (nm)
LiCl	473
NaNO$_3$	462
CaCl$_2$	444
NaCl	410

In addition to this, ion diameters of salts play important role on the diameter of electrospun fibers. Smaller diameter ions have higher charge capacities. In addition, mobility of ions in the electric field is higher. A study executed on PLDA with different salts which have 1% salt concentration by Zong et al. [44] showed that NaCl salt produces thinner nanofibers than NaH$_2$PO$_4$ and KH$_2$PO$_4$ solutions do. The researchers explained this result on the difference in the atomic diameters of ions [44].

Salt ratio added to the solution could be as diverse as ranging from 0.01% to 1% . It is stated that a slight amount of salt in the polymer solution significantly affects the electrospun fiber diameter. However excessive salt contents than these ratios could

give different results such as coarser diameter because of increasing velocity of the jet during travel from needle to collector or thinner fibers as a result of increasing columbic forces. It is found that fiber diameter distribution realizes in narrower range by adding salt to the solution. Also, production rate can be scaled up by increasing solution conductivity with salts which has up to 10 mS cm^{-1} values [33].
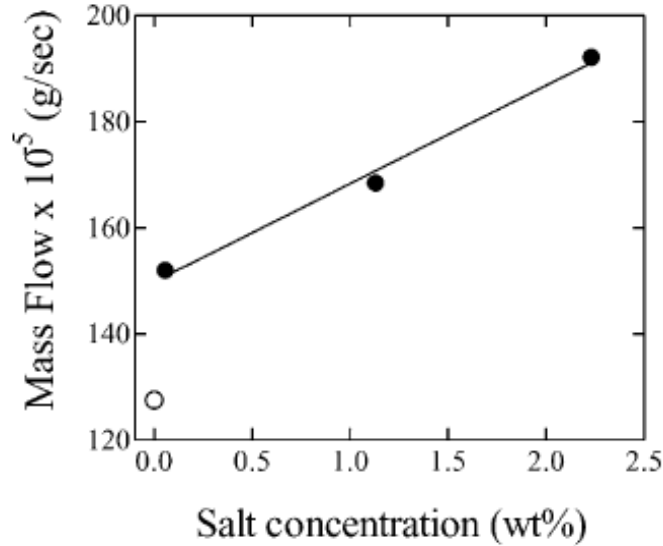
Figure 2.19 : Effect of salt concentration on jet current [45].

Although it is stated that a linearly proportional relation exists between production rate and solution conductivity, excessive solution conductivity provokes jet activity, thus this intensity of coulomb forces on polymer jet increases as seen in Figure 2.19. Extra low or extra high solution conductivity could cause disorders in electrospun fiber production [33].

In the electrospinning process, polyelectrolyte materials can perform similar effects by increasing charge density, which also provided from adding salts to polymer solutions. Son et al. [46] managed producing thinner and bead free fibers by adding PAA and PAH polyelectrolyte materials with different ratios to 7 wt% of PEO/water solution. Despite the fact that only small differences occur in viscosity and surface tension as seen in Figure 2.20, the solution conductivity tremendously increases by adding polyelectrolyte material to polymer/solvent system.

While average fiber diameter is about 360 nm for PEO solution without any additive, 150 nm diameter of fiber is produced by adding 4% PAA or PAH to the solution. In this experiment, despite little concentration decrease due to the addition of the

polyelectrolyte, smoother fibers are produced because of providing higher spinning force resulting from an increase in charge density. It is proved that bead defects are observed in fibers produced from 7 wt% concentrated PEO solution, however there is no bead defect seen on fibers electrospun from PAA or PAH polyelectrolyte added solutions [46].
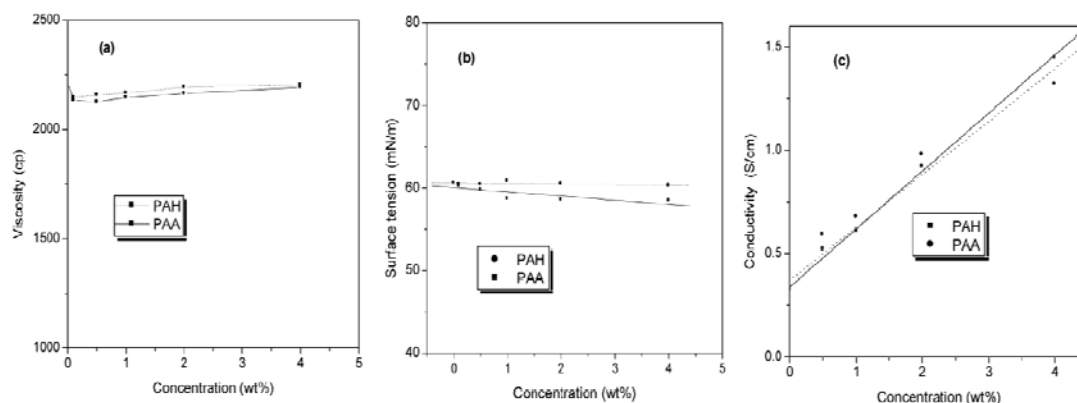
Figure 2.20 : Changes in (a) viscosities, (b) surface tensions, and (c) conductivities of 7 wt% PEO/water solutions with different amounts of PAH and PAA [46].

It is also possible to produce thinner and smoother nanofibers by surfactants that can be used in polymer solutions. Jung et al. [47] carried out an experiment in order to observe effects of surfactants on solution properties and fiber diameter. They added to PVA/water solution anionic, cationic, amphoteric, and non-ionic surfactants in various ratios. Each surfactant reacts with solutions in different ways. Therefore, solution properties such as viscosity, surface tension, conductivity of different surfactant added solution differs from the others. As a result of their study, they have stated that 4% amphoteric surfactant added solution gives thinner and smooth fibers.

2.4.1.7 Solution temperature

If a polymer solution is heated up at the constant concentration, the polymer chains opens up, interactions between polymer chains decrease, thus viscosity declines. By decreasing viscosity, external forces face with weaker viscoelastic forces; electrostatic forces easily draw the polymer jet during electrospinning. Table 2.2 taken from Kataphinan's study shows properties of polyamide 6/formic acid solutions at different temperatures and fiber properties obtained from this solutions [48].

Table 2.2 : Viscosity, surface tension, conductivity and nanofiber diameter of 20%wt PA6/formic acid solution at different temperatures [48].

Solution Temperature (^{0}C)	Viscosity (cp)	Surface Tension (mN.m^{-1})	Conductivity (mS.cm^{-1})	Fiber Diameter (nm)
30	517	43.2	4.2	98.3± 8.2
40	387	42.3	3.9	94.0± 6.3
50	284	41.8	3.8	91.8±7.2
60	212	41.1	3.4	89.7±5.6

Despite solution conductivity slightly decreases, more reduction in viscosity value occurs which results in producing 10% thinner fiber [48].

Experiment conducted by Demir et al.[45], polyurethane-urea nanofibers were produced at 30 ^{o}C have 179.2 nm diameter values, however nanofibers having 92.2 nm diameters can be produced from solution at 60 ^{o}C. In addition to this, it has determined that increasing temperature provides electrospinning of smoother fibers and increases fiber production rate.

2.4.2 Process Parameters

In the electrospinning process, regular and very thin fibers can be produced as long as a balance in process parameters (voltage, needle to collector distance, flow rate, spinneret geometry, and polarity) provided.

2.4.2.1 Applied voltage

A polymer droplet under the effect of viscoelastic and surface tension forces is prompted by electrostatic forces in the electrospinning process. The resistance of these forces to each other provides elongation of the jet to nano size diameters. To produce finer nanofibers, voltage applied to system must be adjusted very precisely. In fact, to generate a jet from droplet, which is under the effect of remarkable surface tension forces, a critical voltage value is necessary at a distance from the needle. Voltage, which is lower than this value, is not sufficient to drive the polymer droplet.

Experiment made by Lee et al. in conditions of 13 wt% PS/DMF-THF concentration, 12 cm needle to collector distance, shows that up to voltage value of 15 kV spherical beads on fibers obtain elliptical shapes. After 15 kV, beads reshape themselves into

spherical forms as voltage increases. The polymer jet is drawn by higher electrostatic forces up to 15 kV results in higher elongation of fiber. However, values over a critical voltage (15 kV in this case) draw ratio of the jet decreases because of higher velocity of the jet in the electrospinning area. As a result, the fiber diameters become coarser, the number and the diameter of the beads on fiber also increase (see Figure 2.21) [34].
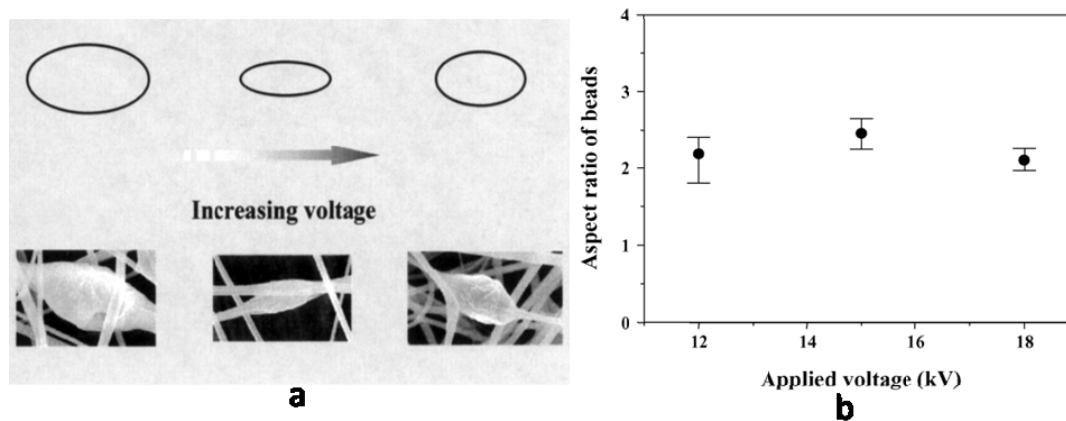
Figure 2.21 : (a) The change of bead morphology and (b) the aspect ratio with the applied voltage (PS dissolved in the mixture of THF/DMF, 50/50 (v/v)). The solution concentration and needle to collector distance are 13 wt%, 12 cm, respectively [34].

Increasing voltage accelerates the drawing velocity of the fiber, while the current created between the needle and the collector hinders the whipping instability. Decreased whipping instability means coarser or beaded fibers.

Additionally, if solution feeding rate is much lower from the applied voltage can draw, a Taylor cone is generated inside the capillary of the needle, hence polymer jet rapidly accelerates to the collector. This phenomenon increases the drawing effect. The increased whipping in the electrospinning process also cause production disorders and results in jet breaks and bead defects on fiber web [45].

High voltage does not only affect the physical properties of the fiber, but also it changes the crystallinity of the fiber because polymer molecules are aligned in well organized manner by the electric field. If applied voltage is increased, the polymer jets get faster. This causes a reduction in the amount of amorphous area of the fiber because reducing travel time of the jet also limits the required orientation time for the fiber [49].
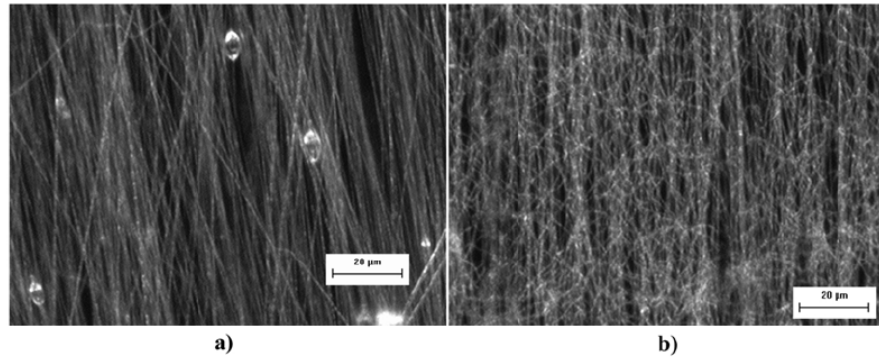
Figure 2.22 : Optical microscope images of PEO nanofiber web produced by a) AC b) DC electrospinning [50].

The type of the high voltage power supply such as voltage generators working in DC or AC mode, affect the process parameters. Consequently, it can affect the diameter and the morphology of the fibers or fiber webs. If an AC power supply is used on the system, forces that determine the whipping instabilities become weaker which has a positive role on elongation and solidification of fiber. Fibers electrospun by AC high voltage power supply are aligned on the collector as parallel to each other because jet which is charged with alternative current moves to collector faster and takes longer distance than direct current (DC) charged jet does as shown in Figure 2.22. As a result of these, fibers which is produced by AC current power supply, are coarser and more wet when it is compared to electrospun fibers accumulated by DC power supply [50].

2.4.2.2 Needle to collector distance

In order to make thinner a macro size jet by elongation and solidification, it requires 5 meter length from spinneret to winding in dry spinning fiber production process though polymer solution temperature is close to the boiling point. By this arrangement, a 40 μm diameter of fiber can only be manufactured [51]. However, one or two decimeters space is effective for producing fibers with nano size from a polymer at room temperature by electrospinning process.

Needle to collector distance and applied voltage are the factors, which determine the electrical field forces acting on polymer droplet. Increasing the distance between the two charged poles, parabolic decrease is shown in electric field forces. The effects of needle to collector distance on production of electrospinning process are similar to the voltage effect, but it acts conversely. Additionally, a decrease in distance between

two polar point increases the electric field which causes electrospinning of coarser, semi solidified, bead defected fibers [33].

An exact linear relation between needle to collector distance and fiber morphology may be established as stated for the voltage effect. It is difficult to generate a polymer jet from solution droplet with much long needle to collector distance because sufficient electric field is not provided at long distances. On the other hand, essential time and path for solidification and elongation can not be supplied with much short needle to collector distances. The needle to collector distance defines the reaching time of jet to collector, solidification amount and whipping instability of jet [33].

2.4.2.3 Flow rate

In electrospinning process, for every voltage value applied to the solution, there must be a certain flow rate, which can response to that voltage which drives the solution from feeding zone. If the flow rate is higher than a certain value that a definitive voltage can not drive it properly, fibers with coarse diameters and beaded structures are obtained [44].

It is more difficult to solidify the polymer jet at high flow rates. The residual solvent on the jet can convert a fiber web into a film layer when jet reaches the collector due to dissolving of the fiber. High flow rates cannot be employed in order to provide enough solidification [52].
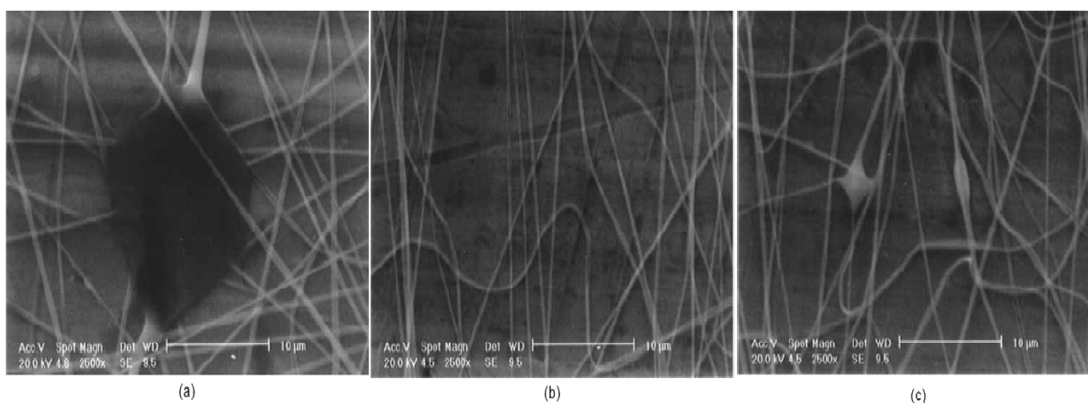
Figure 2.23 : Effect of feeding rates of 15 wt% PAN/DMF solution on nanofiber morphology (voltage: 10 kV, needle to collector distance: 15 cm) feeding rate: (a) 4 mlh^{-1}; (b) 2 mlh^{-1}; (c) 1 mlh^{-1} [53].

A regular flow rate is necessary to control diameter distribution of the final fiber. If solution is fed to the system less than the electrostatic forces can spin, solution

solidifies in needle tip, which causes choking up of the needle. Conversely, polymer solution leaks from needle if solution flow rate is kept at higher value than critical point. This irregularity of feeding rate carries out different size of fiber diameter, in other words fiber diameter distribution increases. In addition to this, it is possible to increase production rate by concurrently raising voltage and flow rate [33].

It is stated that increasing or decreasing feeding rate in a specific flow rate range affects the fiber diameter and morphology. Jalili et al. made an experiment with PAN/DMF solution, beads and high diameter distribution on fiber is observed with 4 ml/h flow rate resulted from electric field does not completely respond to the flow rate (see Figure 2.23). Smooth and homogenous fibers are obtained when 2 ml/h flow rate is applied. While flow rate is decreased to 1 ml/h, solution flow becomes slower against voltage, so bead defects and fiber diameter irregularities take place on fiber web [53].

2.4.2.4 Spinneret geometry

Surface tension of droplet exiting from spinneret increases with decreasing spinneret inner diameter. If applied voltage is kept at a constant potential, the acceleration and mean velocity of the jet decrease because of the increased surface tension. It becomes easier that jet breaks into smaller jets and gets thinner by decreasing velocity of the jet. Thus, spinnerets with smaller diameters are preferred (see Table 2.3). However running of the electrospinning process becomes difficult if inner diameter of spinneret is smaller than 0.5 mm because of excessive increase in surface tension [49].

Table 2.3 : Effect of needle diameter on fiber diameter [49].

Fiber diameter distribution (µm)	Different spinneret diameters and fiber diameters (%)		
	0.7 mm	0.9 mm	1.2 mm
0-1	62	46	19
1-2	25	48	34
2-3	9	6	8
3-4	3	0	15
4-5	1	0	13
5-6	0	0	5
6-7	0	0	6
Average fiber diameter	1.0	1.1	2.6

In study of Maccosay et al., electrospun fibers were produced by using number 18 (Inner Diameter: 0.83 mm, Outer Diameter:1.23 mm), number 22 (ID:0.4 mm, OD:0.7 mm) and number 26 (ID:0.1, OD:0.45) needles in same conditions, and diameter of 10-12 fibers are measured on SEM photographs of electrospun fiber web.
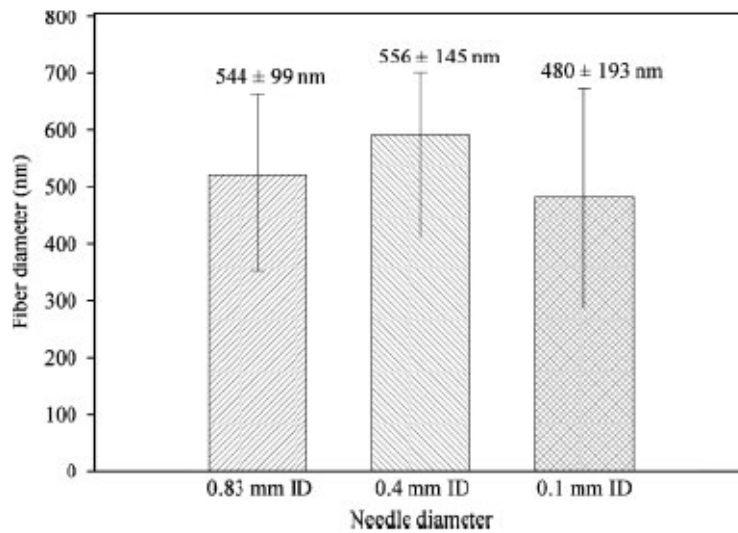
Figure 2.24 : Effect of inner needle diameter to fiber diameter [54].

According to the available information in the literature, it is stated that inner diameter of needle is correlated with fiber diameter, however results showed above exhibit that a correlation between needle inner diameter and fiber diameter does not clearly exist (see Figure 2.24) [54].

Mo et al. made an experiment with different needles having diameters between 0.4 mm to 1.2 mm, they demonstrated that fibers produced with 1.2 mm diameter needle have bead defects and needle was clogged, on the other hand, smooth and thinner fibers were produced with needle, which has 0.4 mm inner diameter. Also smoother and thinner fibers can be produced from high viscosity solutions by using thinner spinnerets [55].

2.4.2.5 Polarity

Polarity of applied voltage has some effect on the fiber diameter, fiber morphology and fiber web properties. In Supaphol et al. experiment with PA 6, it is seen that wider fiber webs can be obtained from solutions, which are processed with negative polarity. Additionally, negative polarity makes fiber more flattened. This claim is supported with SEM photographs. Supaphol et al. explained the reason that amino

groups in the tail groups of PA 6, which is solved in formic acid produces ammonium cations in solution. Solution is affected by negative polarity more than positive because of molecule diameter difference between this cations and formic acid anions, so whipping instability makes stronger effect on solution when negative polarity is applied [38].

(a)   (b)   (c)   (d)
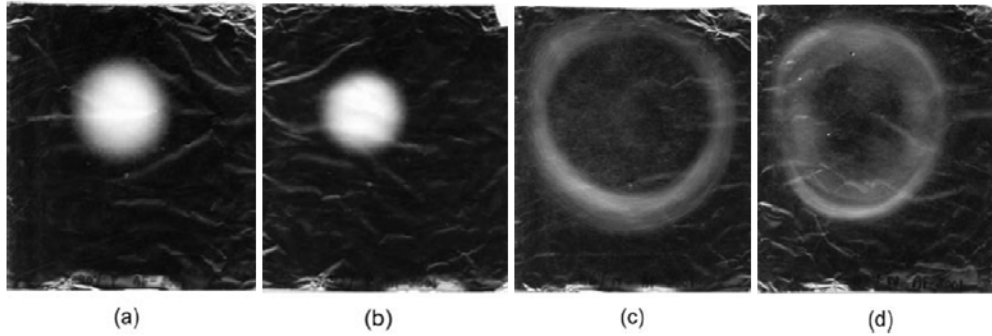
Figure 2.25 : Optical scanner images of as-spun mats from solutions of PA-6-20 in 85% v/v formic acid at the concentrations of (a) 40 and (b) 42% w/v under positive polarity and at the concentrations of (c) 40 and (d) 42% w/v under negative polarity. The electrostatic field strength used was 21 kV/10 cm and the collection time was 30 s [38].

Mit-uppatham et al. made an experiment with PA 6 and they stated that fibers produced under negative potential are coarser than fibers electrospun by positive voltage. It is also stressed that this is a result of increasing mass transport which is carried out by electrostatic forces when negative voltage is applied (see Figure 2.25) [56].

Kilic et al. made two different electrospinning production processes with PVA/water solution by using only positive polarity power supply. For the first electrospinning set-up, solution feeding spinneret is charged and collector is grounded, for the second as the adverse of first experiment set-up, collector is positively charged and needle is grounded. Consequently, it is determined that average fiber diameter produced in first set-up is thinner than the other [57].

2.4.3 Ambient parameters

2.4.3.1 Humidity

Ambient humidity can change polymer solution properties during electrospinning process. At high humidity rates, liquid condensation may occur on fiber in a regular

electrospinning process conditions. Thus, ambient humidity can affect the fiber morphology of polymers which is solved in volatile solvents [58].

Smooth fibers are obtained with humidity lower than 50% in an experiment conducted with polysulfone/tehtrahydrofurane solution. An increase in the humidity rate after this limit results in generating spherical pores on fibers, and diameter of pores increases with increasing ambient humidity [59].

In study of Kim et al., effect of various humidity values that changes from 10% to 70% on fiber diameter by using polystyrene solution. The result of experiment show that fiber diameters increases with increasing relative humidity as it is shown in Table 2.4 [30].

Table 2.4 : Average fiber diameters corresponding to different humidity ratios [30].

Relative Humidity (%)	Average fiber diameter (nm)
10	130
30	240
50	290
70	380

No electrostatic charging on the surface of polymer solution is underlined as a reason of increasing fiber diameter with increasing relative humidity. In other words, electric field, which is deficient to elongate the polymer jet, diminishes with increasing humidity or electrostatic forces can not exactly act on the surface of polymer jet.

In Figure 2.26, the morphology of nanofibers produced under different humidity values is showed. A conclusion can be drawn from these SEM images that increasing humidity makes nanofibers coarser [60].
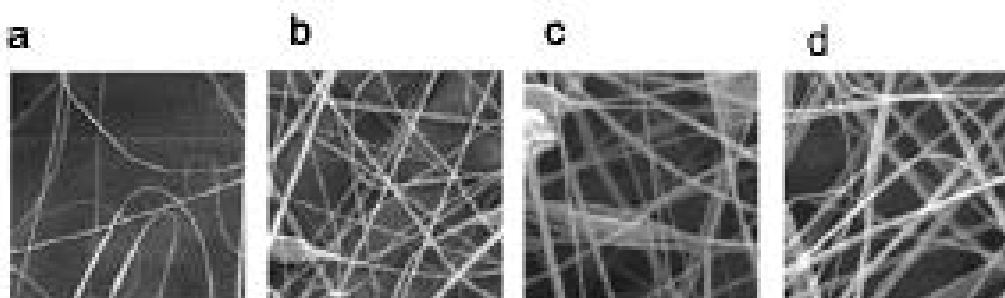
Figure 2.26 : SEM images for the change of morphology as a function of relative humidity: 7%wt polymer concentration, relative humidity of (a) 10%, (b) 30%, (c) 50%, and (d) 70% [60].

2.4.3.2 Ambient temperature

Evaporation rate of solvent slows when the ambient temperature is low. Polymer jets do not completely solidify when they arrive at the collector, so diameter of nanofibers gets higher. If ambient temperature is high, time that is needed for polymer jet splaying and jet elongation can not be completed because of higher solidification rates. As a result of this, fiber diameters and fiber diameter distributions become higher. In conclusion, fibers can be made thinner with optimum temperature ranges, which adjusted for evaporation of solvent on the jet and getting thinner of fiber. In Table 2.25, diameter distribution of electrospun fibers produced under various temperature conditions are given. It is seen that a suitable temperature range for electrospinning is between 22-26 $^{\circ}$C [49].

Table 2.5 : Average diameters and diameter distributions of nanofibers produced at different ambient temperatures [49].

Fiber distribution (µm)	Fiber distribution at different temperatures (%)				
	18 $^{\circ}$C	22 $^{\circ}$C	26 $^{\circ}$C	30 $^{\circ}$C	34 $^{\circ}$C
0-2	15	22	26	11	18
2-4	37	55	27	40	25
4-6	19	12	14	14	18
6-8	20	6	13	13	12
8-10	9	5	20	6	10
10-12	0	0	0	16	17
Average fiber diameter	4.5	3.5	4.5	5.4	5.6

2.5 Applications of Electrospun Nanofibers

The first commercial product of electrospinning process came on to the market in 1982. Research on product development and potential applications have been exponentially increased since 1990's with increasing number of studies on electrospinning. Today there are a lot of products exist in the market, besides numerous scientific research on nanofibers are continuously being conducted around the world. Filtration, medical, energy, technical textile materials, protective materials are some of the major research areas.

2.5.1 Filtration

High specific surface area of nanofibers and porous, nonwoven microstructure of electrospun fibers make nanofiber products a good candidate for especially liquid and solid filtration. In fact Ultra-Web$^®$ [61] is the first electrospun nanofiber product launched to the market in 1982 by Donaldson company [61]. Electrospun nanofibers have usage potential in air filtration, dust collector units, automotive filters, HVAC systems and liquid filtration.

Today, desired air quality have been increasing in particular places such as in industry, business, daily life, clean rooms, hospitals, schools, thus necessity of development of filter materials which can reply to this air quality demand have occurred. Nanofiber materials, which can satisfy these properties, are used in many applications by constructing them with other filter materials as a composite product. Global companies such as Donaldson, DuPont, are pioneer manufacturers of nanofiber filter materials. Nanofibers are five hundred times thinner than fibers used in conventional filter products. Generally, thinner fibers provide higher filtration efficiency because better inertial impaction and interception effect in air filtration [27, 62].

In Figure 2.27, effect of fiber diameter on filtration efficiency is showed. Filtration efficiency of nanofiber filters better than filters having micron diameter fibers for every aerosol sizes. Additionally, it can be seen that with thinner fibers, smaller aerosol particles can be intercepted. The fact, dust holding capacity and filtration life of nanofiber filters are better than conventional filters, is demonstrated by laboratory tests and experiences obtained in industry [63].

While fiber diameter decrease causes an increase in pressure drop, this increase is balanced by making an improvement in values of direct interception and inertial impaction. Therefore, submicron particles can be filtered with better filtration efficiency at the same pressure drop or with lower pressure drop values at the same filtration efficiency.

Another characteristic of the nanofiber filters is that they catch the particles on the surface of filter, i.e., they make surface filtration.
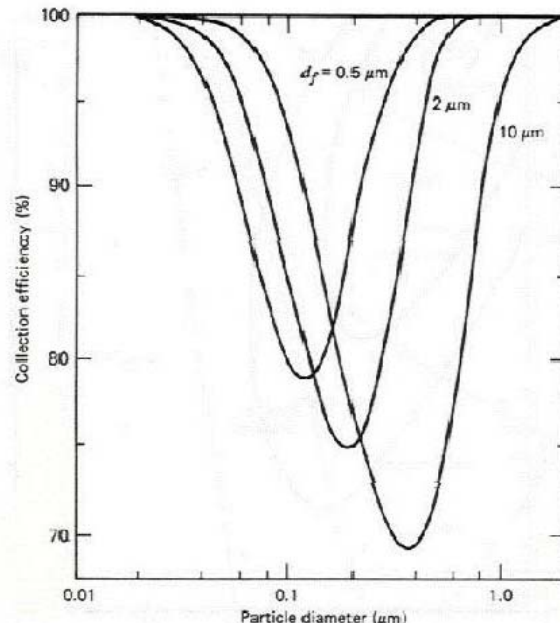
Figure 2.27 : The effect of fiber size on filter efficiency as a function of particle sizes [63].

HVAC filters manufactured from glass fibers hold the contaminants along the filter thickness [63].

Nanofiber filters, on the other hand, sieves the particles on the surface of filter, thus it enhances the dust holding capacity and provides a longer lifetime by cleaning them with backward air flushing (see Figure 2.28).
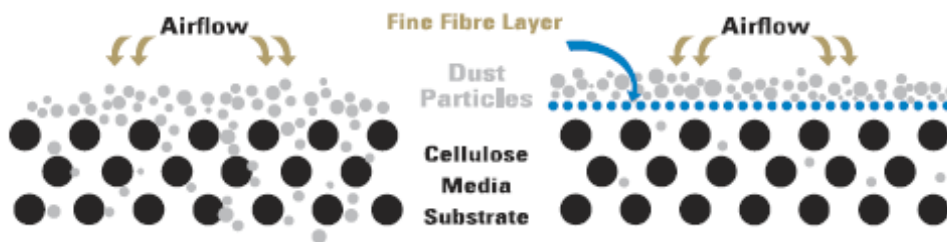
Figure 2.28 : Schematic filtration mechanisms of conventional and nanofiber filter media [61].

Air quality of indoor places has big importance for the aspect of both human health and working performance of machine and devices. HEPA filters are the most developed filter systems that are used in automobile engines, automobile cabins and hospitals. In a study where nanofiber and HEPA filters are compared, it is stated that nanofiber filter media containing 100 nm diameter fibers exhibits better filtration efficiency than HEPA filters (see Figure 2.29). Also, nanofiber materials gives more

favorable results about pressure drop values which directly affect energy consumption [64].
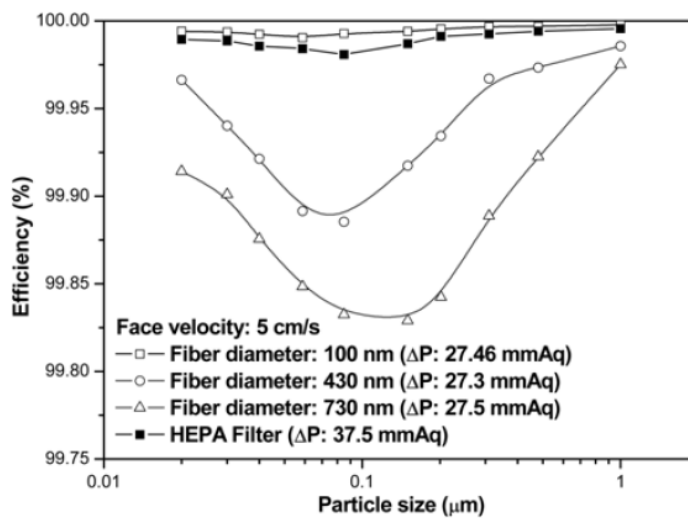
Figure 2.29 : Filtration efficiency of the Nylon 6 nanofiber filters and the HEPA filter as a function of particle size for various fiber diameter [64].

Usage of nanofiber filter materials has been increasing in liquid filtration day by day. Finetex [61] and DuPont [64] firms started to manufacture membranes for this application. Potential application area of these membranes can be counted as pharmaceutical industry, microelectronics, water purification, food, beverage and medical [62, 65].

2.5.2 Medical

Nanofiber materials with a few nanometers to micrometers diameters can be produced via synthetic or natural polymers, which have various morphologies through improvement in electrospinning process. This nanofiber products can be used as tissue and organ scaffolds, tissue regeneration materials, drug delivery systems, biocompatible and biodegradable implants, wound dressings, protective materials etc [5].

Natural and synthetic polymers in nano structures such as nanorods, nanofibers, nano hollow fibers and nanotubes are used in various applications of medical and pharmacology. Biological systems such as proteins, viruses, bacteria, dimensionally take place in nano scale and they show similar characteristics with nano structures that are the reasons for that they find various application area. Many viruses, for example, Tobacco Mosaic, and Marburg have shapes that resembles nanotubes [9].

Natural and synthetic polymer based nanofibers are available in medical applications, and research on this materials are kept going. Natural or synthetic polymers such as polyglycolites, PLA, PCL, various copolymers, some polyurethanes, collagens, gelatins, chitosans, silks, and alginates are used for medical purposes.

Electrospun nanofiber scaffolds have properties,

- High water vapor transmission
- Permeability
- Surface comfortable
- Bacteria protective [9].

Scientific researches have been conducted on medical applications of nanofibers, besides a few commercial products have been launched to the market. One of them is ECM (Extra Cellular Matrix) which is developed by co-operation of Surmodics and Donaldson companies [66].

Synthetic ECM of Surmodics seen in Figure 2.30 is a synthetic, durable and new generation tissue scaffold that mimics the tissue in the body by its shape and matrix structure. Synthetic ECM is user friendly, cheap, practically applied in short time that is determined with data obtained from cell researches and cell related applications. Nanofiber structure of this product benefits from the nanofiber technology of Donaldson Company named Ultra-Web®. Two types of this product are produced as nanofiber mixed, non-coated and nanofiber mixed, polyamine coated [67].
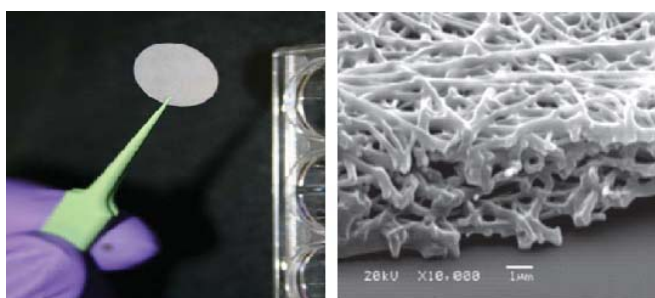
Figure 2.30 : Surmodics nanofiber extra cellular matrix [66].

Structure of electrospun nanofiber provides surface of web mimicking the tissue that results in physiologically formation of cells and forcing cell-to-cell adhesion. The polyamine coating is applied due to replying desired cell functions and conjoining biomolecules to each other with covalent bonds. Synthetic ECM is sterilized by

exposing it to rays via electron beam process. Material is durable about 384 days as far as it is not exposed to direct sunlight [67].

Another material that correspond to synthetic ECM has come into market under trade name NovaMesh® developed by Nicast Company (see Figure 2.31). NovaMesh® has advantages for instance it is durable to tissue adhesion and it provides positive contributions to tissue reproduction. It serves good properties such as,

- resistant to adhesion of tissue in body,
- increases tissue reproduction and tissue growth in body,
- nanofiber layer that biologically mimic tissue,
- practical for laparoscopic applications,
- it does not shrink.
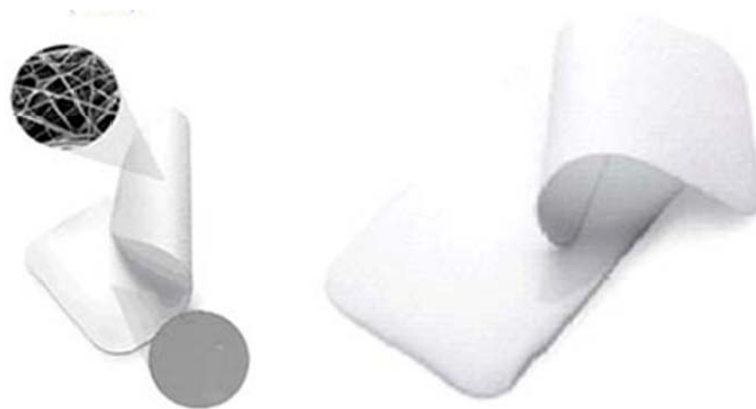
Figure 2.31 : NovaMesh® nanofiber extra cellular matrix [68].

NovaMesh nanofiber scaffold can be produced in standard and special sizes. Also it is manufactured from polyurethane carbonate which is biocompatible with human body [68].

One of the interesting application area of nanofiber products is huge wounds resulted from combustion or frictional injuries (see Figure 2.32). It is determined that huge wounds give quick healing results when they are especially covered with a biopolymer based, thin nanofiber web. It is said that nano porous structure of this wound dressings allow gas transmission, also it resist the penetration of destructive organisms such as bacteria and viruses. It also planned that these nanofiber materials, which has a 100 meter square surface area from 1 gram of polymer, can be used in homeostatic wounds because of their high liquid adsorption and drug delivery capacity values [9].

Figure 2.32 : Nanofiber wound dressing [69].

When nanofiber materials are compared to current commercial wound dressing products, the scar risk after the rehabilitation quite decreases. Nano sized fiber structure accelerates skin growth, and be adding drugs into structure that can be inject to nanofiber web provides a controllable healing. For example, antibiotic embedded nanofibers are available in literature. PU nanofiber wound dressing is commonly used because of high oxygen permeability and barrier properties. Also it is verified with histological results that epitelization rates of nanofiber products are much more higher when they are compared with other control groups during treatment period [70].

In the research conducted by Rho et al., collagen 1 type nanofiber wound dressings are tested on mice. They get good results in the beginning phase of treatment.

In addition to this, nanofibers produced from mixture of collagen, silk, polyethylene oxide can be used as wound dressing. Additionally biodegradable polymers, suitable for electrospun nanofiber production, can be used for wounds are available. PLA, PLGA copolymers, PCL, chitin, chitosan are only some examples of the biodegradable polymers [71]. Commercially, HemCon has begin producing nanofiber wound dressings by using nanofiber technology of Elmarco Company [72].

Additionally, Smith and Reneker have developed a direct electrospun nanofiber coating process onto wounded skin and it is called "portable electrospinning device". In this device, high voltage is generated from standard batteries. It is possible to inject active agents or different polymers in respect of wound type [9].

2.5.3 Energy

Attention to clean energy systems that can be replaced by current energy resources have been increasing because of run out of fossil energy resources and increasing

carbon emissions around the world. Polymer batteries, fuel cells, photovoltaic cells, wind power stations and geothermal resources are the examples that are thought as alternatives. Nanofibers having high surface area and high porosity can be used in polymer batteries, photo voltaic cells and proton exchange membrane fuel cells.

Polymer batteries are developed for laptops and mobile telephones; they are also lighter and smaller energy storage devices than lithium ion batteries. Polymer batteries need to improve electrolyte absorption, physical and chemical resistance, energy density properties, in this way the market ratio of polymer batteries can increase [10].

Polymers such as Pad (polyvinylidene fluoride), PAN (polyacrylonitrile) and PVC (polyvinyl chloride) are used for polymer batteries. It is estimated that electrospun polymer nanofibers are used for this applications because of nano size porous structure. Porous structure of nanofiber membrane provides high electrolyte absorption. Additionally, high surface are of the nanofiber web makes contribution to ion conductivity. Significant properties of polymer batteries with nanofibers are:

- high ion conductivity
- high resistance between to layer
- high electrochemical balance [5].
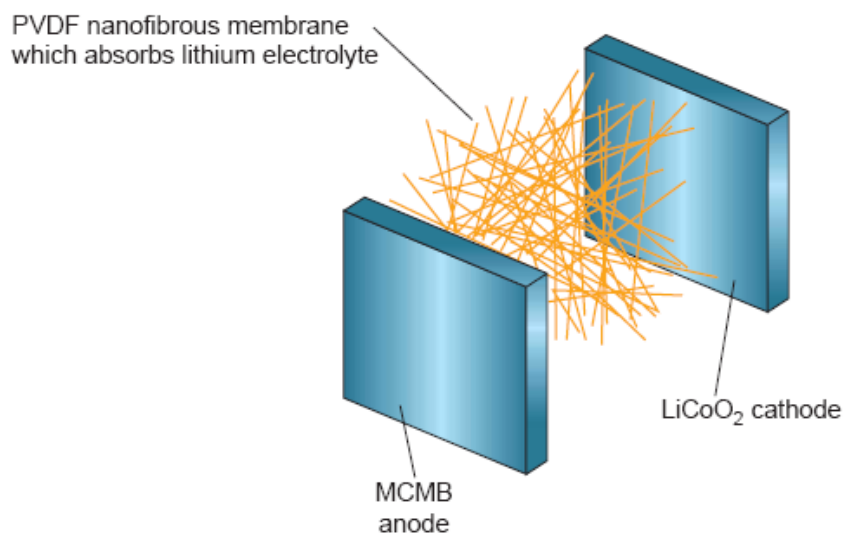
Figure 2.33 : Polymer battery assembled by sandwiching PVdF nanofiber membranes between a mesocarbon micro bead (MCMB) anode and a $LiCoO_2$ cathode [5].

As shown in Figure 2.33, a polymer battery is designed which contains two electrodes and PVdF nanofiber web. PVdF membrane having 450nm average fiber diameter and 1 micron pore diameter is embedded into 1:1:1 mixture of 1 M LiPF$_6$ in (EC)/dimethyl carbonate(DMC)/diethyl carbonate (DEC) solution, after that it is placed in argon atmosphere for one hour. Then, nanofiber membrane containing electrolyte solution is constricted between two steel electrodes, and this prepared system is wrapped with a polyethylene coated aluminum foil via vacuum. It is observed that electrolyte absorption of PVdF nanofibers is better because of good wettability properties and high surface area of nanofibers; also, they keep the 80% percent of electrolyte solution, which they absorb at first. Electrolyte solution absorption is affected by average nanofiber diameter, moreover thinner fibers absorbs more electrolyte solutions besides provide better ion conductivity [5].

Resistance between two electrode layer and electrolyte absoption of nanofibers are other property of polymer batteries constructed with nanofibers. Nanofiber membrane swells when it absorbs electrolyte. At this time, fiber diameter increases on the other hand, solution quantity and contact area of nanofiber surface decline. In addition, resistance between two layers generally increases with increasing storage time. Researchers reveal the result that resistance between two layers of PVdF nanofiber electrolyte with lithium electrodes gains a bit increase with increasing storage time, but this value is smaller than other gel polymer electrolytes. In conclusion, batteries with higher charge density than conventional polymer batteries can be produced with nanofibers because of its high surface are [73].

Fuel cells are energy systems that they convert the fuel into electrical energy via electrochemical reactions and they do not need any recharging. When anode supplies fuel and cathode makes oxidation, fuel cells permanently work as battery. Fuel cells are also harmless, silent, renewable energy converting devices like as a battery. To operate the fuel cell, hydrogen-oxygen or hydrogen-air is necessary. A fuel cell is constructed with an electrolyte placed between two central electrodes. Air flows over cathode surface. When electrons are transmitted to cathode via an external circuit, hydrogen ions moves to the electrode on which oxygen ions are available via electrolyte. Water is obtained from the reaction of hydrogen, oxygen ions and electrons. The flow of electron on external circuit produces electrical energy (see Figure 2.34) [10].

Electricity generation in fuel cells realizes through the chemical reaction of hydrogen at the anode and oxygen at the cathode protons are transmitted through an electrolyte membrane that contains distilled water, while electrons are transmitted from the anode to the cathode. The key properties of electrolyte membranes are high proton conductivity and shielding of electron transport.
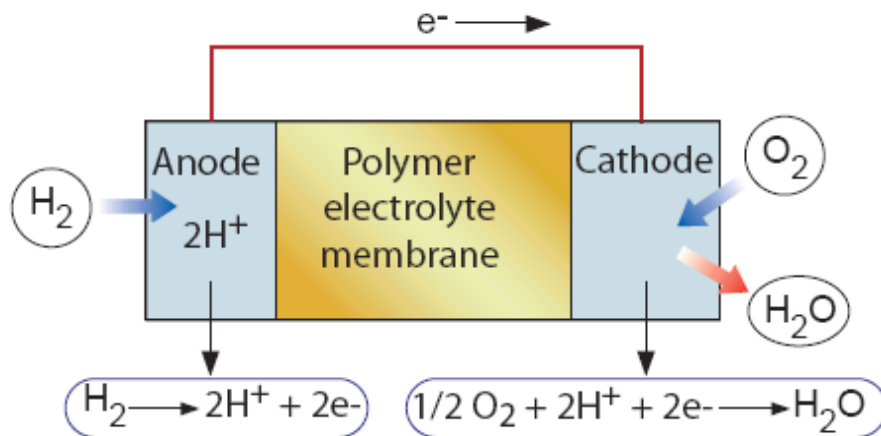
Figure 2.34 : Schematic diagram of a fuel cell containing nanofiber membrane [5].

As the membrane needs to hold distilled water for proton conductivity, water retention of the membrane is also important. Nafion® (DuPont), a perfluorosulfonic acid polymer film, has been widely used so far. However, Nafion® membranes are expensive at up to \$800/kg. For the same membrane area, electrospun Nafion® fiber membranes require less material than conventional Nafion® fuel cell membranes, thereby reducing cost. Porous nanofiber membranes are also able to hold distilled water, thus enhancing proton conductivity. Therefore, such nanofiber membranes have the potential to be used in PEMFCs [5].

Table 2.6 : Properties of nanofiber membrane produced by DuPont [74].

Thickness	20-70 μm
Porosity	40-90%
Pore Size	<1μm
Ionic Resistance	0.3-1.2 ohms/cm^2 in 2 M LiCl/methanol
Frazer Air Permeability	<5 cfm/ft^2 at 125 Pa
Shrinkage	<5% at 180°C for 2 hours
Wettability	Wets in typical aqueous/organic electrolytes

Besides scientific researchers have been going on the energy applications of nanofibers, DuPont Company release the semi permeable membrane products for lithium-ion batteries, alumina electrolytic capacitors, alkaline cells and two-face-electrochemical capacitors. Properties of nanofiber membrane are given in Table 2.6 below [74].

Japan Vilene Company has also research on commercially producing battery separators by electrospinning method [75].

2.5.4 Protective applications

It is desired from protective materials not only they are effective against to bacteria, viruses and toxic, chemical, biological substances but also they provide comfortability to user. For example, it is widely required property that a barrier cloth in order to be used against to chemical agents can transfer the moisture, which is produced by user.

Developing warfare technology makes necessary the increase of soldier equipments. Equipments used by soldiers are required as lighter, air impermeable, water vapor permeable, durable to chemicals and as much as reactant to chemical and biological agents. Because nanofiber webs have very small pore diameters and high porosity, they do not transfer chemical and biological agents in aerosol form besides they do not discomfort user. Additionally nanofiber materials are much lighter as they are compared with conventional textile materials. A research had realized with cooperation of MIT and US Army, which has a 50 million $ budget, its target was minimizing the size of soldier equipments also increasing their quality. Thus, it was desired to minimize deaths and injuries that can be take place during a battle. By the frame of this project, researches on nanofiber military materials were realized [30].

In Singapore, a research called development of protective mask against biological agents were conducted by Military Science and Technology Agency with Ramakrishna's group. In the study, instead of active carbon, nanofiber composite is used for mask as an alternative to HEPA filter with active carbon coal respirators. Metal nanoparticles such as silver, magnesium oxide, titanium, nickel embedded on nanofiber surfaces were effective to resist paraoxane and dimethyl phosphanate [5].

In addition to developments in military technology, nanofiber materials are used to enhance quality of humans in daily life. An allergen barrier fabric, which is

especially required by asthma sufferers, launched to market by DuPont in 2006 can be an example. Although commercial barrier materials available in the market have good results for allergen protective, they are though, bad handle and uncomfortable materials. Furthermore, pillows produced from vinyl, polyurethane and micro porous coatings requires holes for air transmission. In addition, pillows and mattresses constructed with these materials have short usage life. Spunbond/meltblown/spunbond olefin fabrics are also used as allergen barrier fabrics, but pore size of these materials is much more than microorganisms [76].

Pillows and mattresses of DuPont HMT technology contains microporous polymeric layer, which are constructed with fibers having 50 nm to 1 micron diameter. The nanofiber layer has pores between 0,01 micron to 10 microns diameter. Feature of the nanofiber product is given in Figure 2.35 below with a comparative chart containing other barrier materials [76].
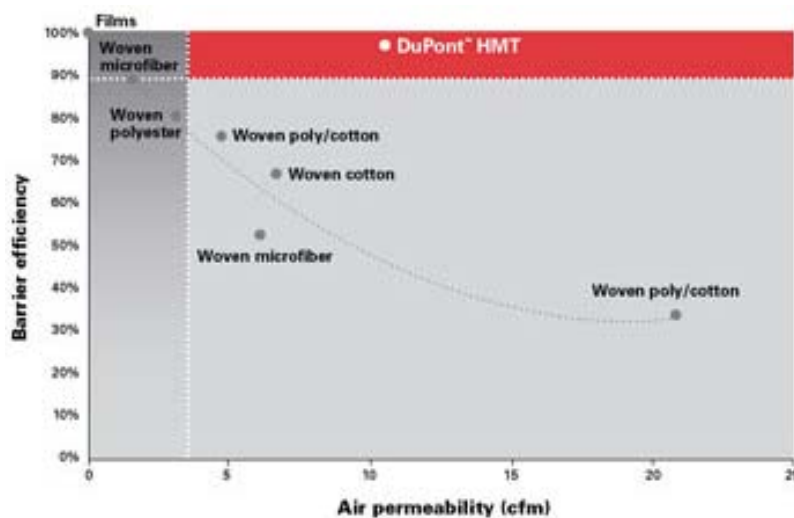
Figure 2.35 : Barrier efficiency and air permeability of nanofiber barrier fabric [76].

Although hospitals are sterilized, they accommodate various bacteria and viruses. In addition, people who use the places are under risk. AntimicrobeWeb® is a mask as barrier material produced by Elmarco Company. Mask is produced by the combination of three, four or five nanofiber layers, an active nanofiber layer, spunbond and meltblown layers. For example, it can be seen on the figure, if it is said from inner to outer, one layer spunbond fabric, one layer meltblown fabric, than one layer nanofiber layer, one active nanofiber layer and a outer textile fabric for covering these layers (see Figure 2.36). At this point, layer called active nanofiber is

constructed by antimicrobial nanofibers. Antimicrobial effect is provided by adding silver nitrate to the solution [77].
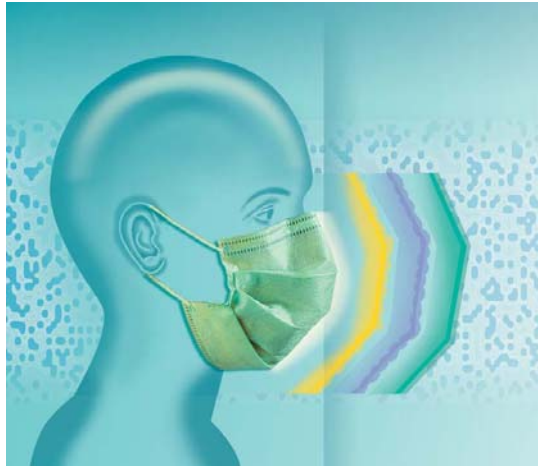
Figure 2.36 : AntimicrobeWeb® nanofiber mask [77].

Subsequent nanofiber layer only contains polymeric nanofibers. Polyvinyl alcohol, polyurethane and polyamide polymers can be applicable for this product. The suitable range of nanofiber density is between 0.1-0.

3 gr/m^2. Filtration efficiency of this mask for bacteria, fungi and viruses is 99.9% that is officially registered by international laboratories [77].

2.5.5 Sensors

The role of sensors is to transform physical or chemical responses into an electrical signal based on the targeted application. So far, electrospun polymer nanofibers have been investigated as gas sensors, chemical sensors, optical sensors and biosensors. It is considered that high sensitive sensors can be assembled by nanofibers, which possess high surface to volume ratio. Except sensitivity of sensors, quick response time with a targeted material is also expected to nanofiber sensors [30].

It is exactly known that sensitivity of quartz crystal microbalance (QKM) sensors is directly related with material coated onto it. Film surfaces have one-dimensional structure on the other hand nanofibers have three dimensions. When it is seen to the reaction of nanofiber and film QKM sensor which has same thickness coating at 40% humidity to 1 ppm of ammonium, frequency change of nanofiber sensor is four times faster when it is compared to film coated sensor. The reason of this that surface area of electrospun nanofiber is twofold of film coated surface. Because surface area of

coating material provides more adsorption surface area, sensors of this materials are more quick [78].

3. ELECTROSPUN NANOFIBER WATERPROOF BREATHABLE MEMBRANES AND RELATED EXPERIMENTAL WORK

3.1 Introduction

In 1950's membrane researches emerged because of the need of water demineralization. Production of membranes in different structures and rising demands for membranes resulted in using of membranes in various applications. Today, membranes are widely used in food, beverage production, recycling of process water in the industry, oil and gas refinery, fuel cells, performance clothes even baby diapers.

Water resistant breathable membranes are generally barrier materials, which resist water up to a certain value and also prevent transition of water vapor. This type of membranes are used in sport clothes, raincoats and protective clothes more than 30 years [79].

A human body makes a kind of refrigeration during physical activity via perspiration. If water vapor is not sufficiently transferred, humidity between body and cloth increases. That humidity discomfort the body even it may cause deaths resulted from hypothermia. In other words, if water vapor between body and cloth is not transferred outside, it becomes denser, body may not supply the heat transferred to this liquid, so that phenomena can produce mortal circumstances. The water vapor transfer capability of cloth or material is known as breathability. Water vapor transfer is defined as "the weight in gram of water vapor that passes thorough one square meter of a material in a day" [80].

Water vapor transfer of a cloth directly affects performance of user. One of common reason of job diseases of fire fighters is heart attacks because of heat differences, which is resulted from decreasing of liquid body substance occurring by perspiration. In 1982, according to statistics of fire deaths in America, deaths resulted from burns are 2.6% on the other hand, the reason of 46.1% of deaths occurred is heart attacks. So, it is vital that water, air and heat resistant should be also breathable.

The usage of barrier materials for the same purposes may be dated back to antique ages. In those days, they were obtained via coating fabrics with wax, vegetable and animal oil. Today, polyvinyl chloride and polyurethane coated waterproof products are substantially used in various forms. Especially apparel forms of these products, which are laminated to textile fabrics, can not satisfy the user requirements because they also resist the transfer of water moisture. Therefore, attention to the selectively permeable materials is increasing day by day.

The usage of breathable materials in shoes, tents, bed coverings, buildings, surgical costumes and wound dressings is continuously increasing [79].

3.2 Types of Waterproof Breathable Materials

Breathable barrier materials can be classified into three main groups. These are densely woven fabrics, microporous membranes and hydrophilic nonporous membranes.

3.2.1 Densely woven and nonwoven fabrics

The first effectively breathable waterproof fabric is Ventile fabrics, which was developed for military purpose during the Second World War. In Ventile fabrics, yarns spun by special method from particularly selected long fibers are used. Then an Oxford woven fabric is produced from these yarns in order to decrease the size of holes in the woven fabric. When fabric is wetted, fibers close the holes via swelling, so some pressure is necessary for passing water from the fabric (see Figure 3.1) [80].
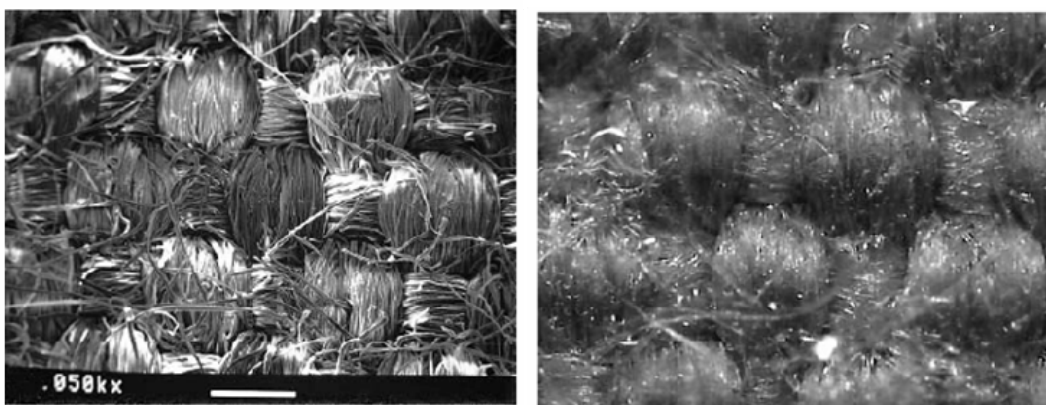
Figure 3.1 : Densely woven dry and wetted waterproof fabrics [80].

By the existence of synthetic fibers especially microfibers, breathable waterproof woven fabrics were started to produce from these fibers (see Figure 3.2). Polyester and polyamide microfilaments come into prominence with water repellency properties [81]. Today, in addition to this fabrics, much more qualified fabrics are produced with silicone or fluorocarbon finishing processes [80].
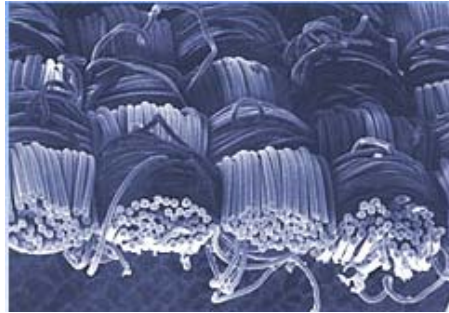
Figure 3.2 : Toray Entrant® waterproof densely woven fabric [81].

In addition to the densely woven fabrics, a nonwoven fabric such as Tyvek® developed by DuPont in 1955 and put it on the market ten years later is a waterproof breathable material. This barrier material is a type of nonwoven fabric which is produced from polyethylene via flash spinning method and it is used as water isolation in buildings and as protective clothing in chemical sector (see Figure 3.3). Tyvek® product has various types which has different water resistance and water vapor permeability values [82].

Figure 3.3 : Tyvek® water resistant breathable fabric a) SEM photograph of Tyvek® b)Tyvek® weather barrier c) Tyvek® protective apparel [83-85].

3.2.2 Microporous membranes

Microporous membranes are breathable water resistant materials which have pore diameters ranging from 1 to 50 micron and they are laminated or directly coated on to fabrics. PTFE, polyurethane, acrylic and polyethylene membranes are the most

widely used types. Polyurethane is the most preferred type of membrane because of its toughness and conformity to cutting and sewing processes [86].

As visually compared in Figure 3.4, microporous membranes having 2-3 micron diameter pores do not prevent passing a 100 micron diameter water droplet while they provide easily passing 0.0004 micron (0.4 nm) diameter water vapor molecule [86].
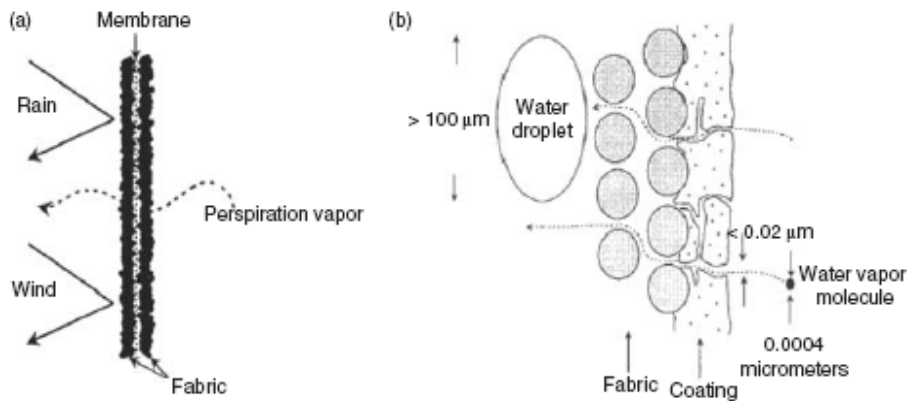
Figure 3.4 : Moisture vapor regulation through fabrics: (a) typical microporous membrane system and (b) microporous coating [86].

First microporous breathable waterproof membrane was developed in 1976 by W. Gore and it came into market under the name of Gore-Tex®. Gore-Tex® membranes are fabricated by highly crystalline PTFE [87].
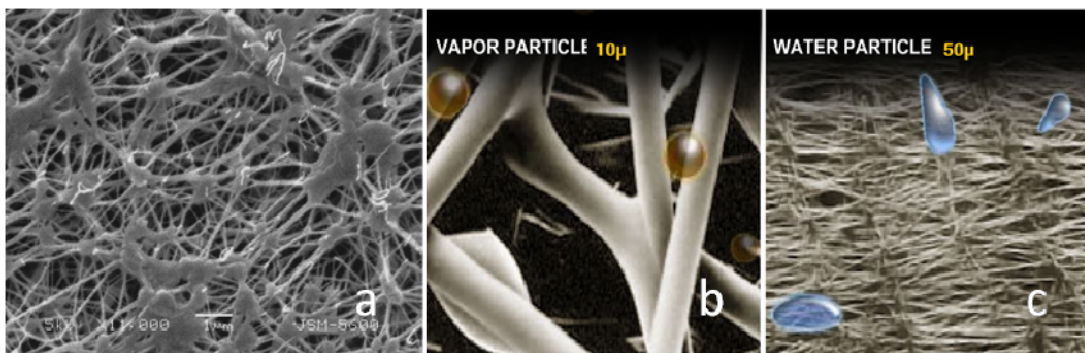
Figure 3.5 : Gore-Tex® microporous waterproof breathable membrane a) SEM photograph b) water vapor transfer mechanism c) water resistance mechanism [88, 89].

Gore-Tex® membranes seen in Figure 3.5 are also known as expanded film membranes. These membranes are extruded as film then it is drawn in lengthwise and crosswise about 300%. During this process, pores begin to be formed by deformation of amorphous sections in polymer network. Crystalline sections, which

are more stable, construct the joint points of occurring pores. By this way, 1,4 billion pores are constructed in one inch square of a Gore-Tex® membrane. Parameters below determine the porosity and strength of membrane:

- Crystallinity of membrane must be high (above 98%)
- Temperature and stretching speed: high temperature and high stretching speed make the membrane more homogenous, more fibrous, and tougher and increase the length between nodes.
- Temperature and thermal process time: Amorphous structure of polymer increases during thermal process above melting point.
- Hydrophobic structure of polymer provides membrane high water resistance. So hydrostatic head and water vapor permeability values of Gore-Tex® membranes are so good. In addition, amorphous sections of polymer reinforce the crystalline sections without any change in microstructure.

Film produced by stretching method can be easily laminated to textile material because of thin structure and toughness [86].

Micro porous polyurethane membranes are produced by a method called "phase inversion" in which a non-solvent liquid is added a solution system obtained from a polymer and a solution. "Wet coagulation" and "phase separation" are also production methods, which are based on phase inversion principle [90].

In wet coagulation method, a solution is prepared by solving polyurethane in dimethyl formamide. Then this solution is coated onto fabric which is sequently exposed water vapor by passing through a post treatment chamber. Organic solvent leaves polymer by mixing with water vapor, so polymer precipitates and a membrane coating having micro pores is obtained. Consequently, fabric is washed for removing residual solvent. Finally fabric is squeezed by passing through a rolling press and it is dried [80].

Some additives can be added to the polymer solvent system in order to enhance performance of this membrane types. Water repellent agents and non-ionic surfactants added to coating solution increase water resistance value of membrane coating. 0.1 μm silicium dioxide or magnesium oxide particles added to polyurethane resin about 1% increase water vapor transmission, also membrane surface take a shape like honey comb which is constituted by 1-20 μm pores [86].

In thermal coagulation method, polyurethane is solved in a methyl ethyl ketone and water. Hence, an emulsion is prepared having 15-20% polymer content. Emulsion pat is coated onto one surface of a fabric. Then, coated fabric is passed through two-step drying process. In the first step, low temperature is applied to remove the solvent. In the second step, temperature is increased in order to vaporize the water which fill the pores after entering phase inversion process with solvent [86].

3.2.3 Microporous coatings

In foam coating method polyurethane and polyurethane/acrylic acid esters mixtures are dispersed in water and it is lathered. The foam is also stabilized with some additives. Then foam is coated onto fabric and it is replaced drying process to form micro pores (see Figure 3.6). Finally, low pressured calendaring is applied to coated fabric to tighten the foam coating. Because number of micro pores much more in this method, the water resistance of membrane is promoted by applying fluoro carbon finishing. It can be said that this process is eco friendly because any solvent is not used in this type of membrane production [80].

Increasing foaming speed and using hydroxyl cellulose as stabilizing agent enhances the water vapor transmission and water resistance values [86].
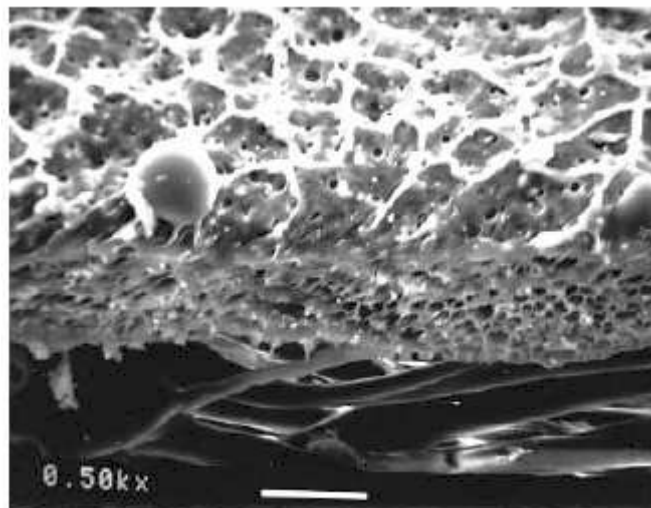
Figure 3.6 : SEM photograph of microporous coating on a fabric [80].

3.2.4 Hydrophilic Films

Hydrophilic films are non-porous waterproof breathable materials, which is produced from chemically modified polyurethane or polyester. Hydrophilic feature of membrane can be expressed by chain reactions between film and water vapor

molecule. Film is constructed by carbon, hydrogen and oxygen atoms on polymer chains. By addition of hydroxyl and carboxyl to polymer chain, polymer makes better interaction with water molecules, so it gains breathability properties. Hydrophilic hydrogen groups on polymer chain transfer water vapor molecules from sections where RH is high to low RH sections [86].
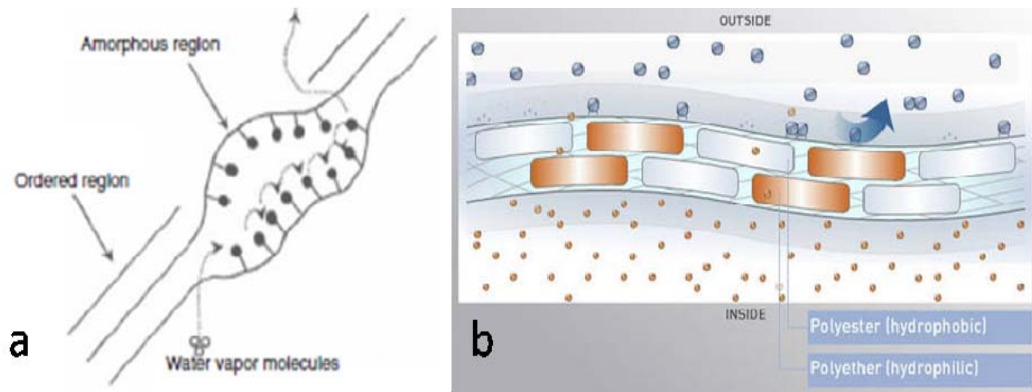
Figure 3.7 : a) Schematic diagram of hydrophilic membrane b) water resistance and water vapor transfer mechanism of hydrophilic membrane [80, 91].

In polymer chains, polyether soft segments which are amorphous and hydrophilic permits water vapor transmission. On the other hand, urethane and ester segments have crystalline structure and they are the parts providing toughness to the film. Water vapor transmission can be raised by adding polyethylene oxide and amino acid groups to the chemical structure of film. Amorphous sections constructing the soft segments behave as inter molecular pores which resist water but provide water vapor transmission (see Figure 3.7) [91].

Some advantages of hydrophilic films with regard to microporous membranes can be compiled as below:

- Micro porous membrane production via wet coagulation method necessitates coagulation bath, washing lines and DMF recycling unit. Moreover, the method have difficulties on producing regular pores below 3 μm and providing balance between water vapor permeability and water resistance properties. On the other hand, hydrophilic film coating can be produced by conventional coating equipments.

- Body fat and detergent contaminants and surfactants used for cleaning can clog the pores of micro porous membranes. In addition to this, the pore diameter of micro porous membranes increases when they are drawn. In any

event, water vapor permeability and water resistance properties of membrane are negatively affected. On the other hand, this is not valid for hydrophilic membranes.

- Hydrophilic laminated PU films or PU coatings are more effectively adhered to textile material, more resistant to chemicals and cheaper than micro porous membranes.

- Hydrophilic membranes have some advantages such as high strength, high toughness, good air impermeability, durable to many chemicals, good odor barrier properties, good adherence to textile material because of its small thickness, high water vapor permeability.

In addition to these advantages, hydrophilic films have same disadvantages stated as below:

- Hydrophilic membranes must absorb a little water vapor to start water vapor permeability.

- When film is wetted, connection between film and fabric can break by swelling.

- Hydrophilic film laminated fabrics give coolness sense when they are exposed to rain because they stop water on the surface [86].

3.3 Membrane Related Experimental Work

3.3.1 Materials

Commercial-grade pellets of polyether based thermoplastic polyurethane (Elastollan® 1185A10) and polyester based thermoplastic polyurethane (Elastollan® B64D11) were obtained from ENPAŞ Endüstriyel Hammaddeler San. Pazarlama A.Ş., properties of thermoplastic polyurethane pellets are given below (see Table 3.1)

N, N-dimethyl formamide (DMF), ethyl acetate (Bereket Kimya Tıp Teknik Tic. ve San. Ltd. Şti.) were used as solvent. Silicone oil and sodium chloride (Bereket Kimya Tıp Teknik Tic. ve San. Ltd. Şti) were used as additives for electrospinning solution (Table 3.2).

Three electrospinning solutions were prepared by dissolving the polymer in DMF. Solutions were stirred at 110 $^{\circ}$C for 24 hour with added sodium chloride. Then ethyl

acetate and poly(methylphenylsiloxane) were added at 80 °C and the solution is stirred for four hours.

Table 3.1 : Properties of thermoplastic polyurethane pellets [92, 93].

			B64 D11	1185A10
Physical	**Test Method**	**Unit**	**Value**	**Value**
Density	ISO 1183	grcm^{-3}	1.24	1.12
Hardness	**Test Method**	**Unit**	**Value**	**Value**
Shore Hardness (Shore D)	ISO 868		61	36
Mechanical	**Test Method**	**Unit**	**Value**	**Value**
Tensile Modulus	ISO 527-2	MPa	320	45
Tensile Strain (Break)	ISO 527-2	%	450	600
Elastomers	**Test Method**	**Unit**	**Value**	**Value**
Tensile Stress	ISO 37			
100% Strain		MPa	19	6
300% Strain		MPa	35	10
Tear Strength	ISO 34-1	kNm^{-1}	180	70
Compression Set	ISO 815			
23°C		%	35	25
70°C		%	50	45
Impact	**Test Method**	**Unit**	**Value**	**Value**
Charpy Notched Impact Strength	ISO 179			
-30 °C		kJm^{-2}	6	No Break
23 °C			No Break	No Break

Table 3.2 : Composition of the electrospinning solutions.

	ES 1	ES 2	ES 3
Polymer	Polyether based TPU	Polyester based TPU	Polyester based TPU
Polymer (wt%)	15	15	13
DMF (wt%))	60	60	60
Ethyl Acetate (wt%))	25	25	20
NaCl (wt%))	0.01	0.01	0.008
Poly (methyl phenylsiloxane) (wt%)	-	-	7

In order to deposit the electrospun nanofiber web on to a fabric, nonwoven fabrics as substrate material obtained from Mogul Tekstil. The chosen substrate was 100% polyester, lightweight and highly porous spunbond nonwoven. The thickness of the nonwoven substrate is 0.28 mm, its weight is 60 grm^{-2} and its air permeability is 122 cm^{3}s^{-1}cm^{-2}.

3.3.2 Electrospinning Process

The electrospinning process was performed with a 10-needle electrospinning setup (see Figure 3.8). The setup consists of two pipe-needle system, each pipe has five needles. Solution was fed to the pipe-needle system by a syringe pump (Asena Alaris GH, Cardinal Health Inc.), a high voltage power supply capable of 0–100 kV (ES100P-20W, Gamma High Voltage Research, Inc.) and a grounded rotating drum cylinder as a collector.
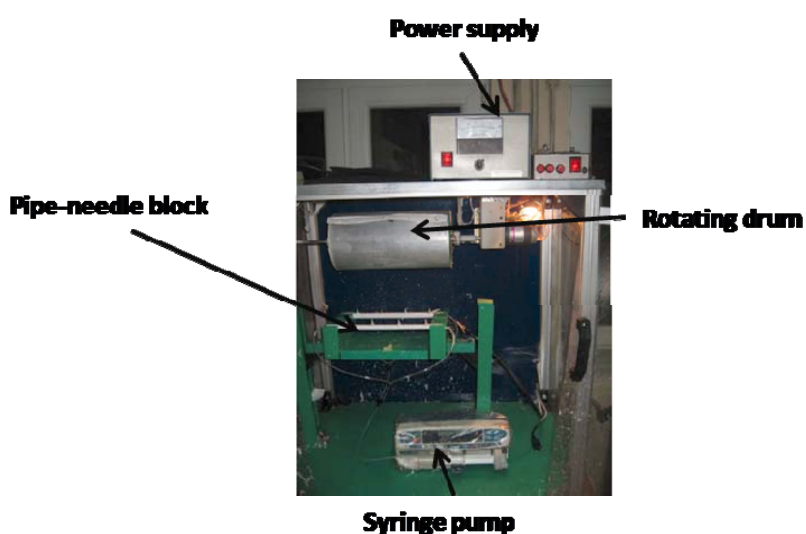
Figure 3.8 : The electrospinning set-up with 10 needles.

TPU/DMF solutions were loaded into a syringe and an electrode was clipped onto the needles. The syringe pump was used to control constant volumetric feed rate. Thermoplastic polyurethane solutions were electrospun under various conditions such as electric potential, needle to collector distance and flow rate to establish optimum production conditions. The experimentally established optimum process conditions for studied electrospinning solutions (ES) are given in Table 3.3.

Table 3.3 : The experimentally established electrospinning conditions for different solutions.

Electrospinning conditions	ES 1	ES 2	ES 3
Voltage (kV)	50	47	43
Needle-Collector Distance (cm)	20	20	15
Flow rate per needle (mlh^{-1})	1	1	2,5
Substrate	Spunbond PET (85 grm^{-2})	Spunbond PET (85 grm^{-2})	Spunbond PET (85 grm^{-2})

3.4 Characterization

3.4.1 Fiber morphology

A scanning electron microscope (JEOL JSM-6390 LV) was used to visualize the TPU nanowebs and to measure the diameters of nanofibers on these nanowebs. SEM photographs were obtained with different magnifications. Fiber diameters of nanofibers were measured by CATIA 3D design program using SEM photographs.

3.4.2 Resistance to water penetration

The hydrostatic head supported by a fabric is a measure of the opposition to the passage of water through the fabric. A specimen is subjected to a steadily increasing pressure of water on one face, under standard conditions, until three droplet penetrations occur through the specimen. The pressure at which the water penetrates through the fabric at the appearance of the third droplet is noted. The water pressure may be applied from below or from above of the test specimen. The type of the chosen alternative for the water application should be stated in the test report. The result is immediately relevant to the behavior of fabric articles which are subjected to water pressure for short or moderate periods of time [94].

A test apparatus as seen in Figure 3.9 was designed and manufactured according to BS 20811 standard (Determination of resistance to water penetration –Hydrostatic pressure test).

Figure 3.9 : Test apparatus for resistance to water penetration.

The designed and manufactured test apparatus confirms the requirements of the standard in the following aspects:

- An area of the fabric of 100 cm^2 is subjected to steadily increasing water pressure from below or from above the fabric.

- No leakage of water takes place at the clamps during the test period

- The specimen does not slip from the clamps.

- Any tendency for penetration to occur at the clamped edge of the specimen is minimized.

- Distilled or fully deionized water is used with the test specimen at 20±2 °C.

- The rate of increase of water pressure is chosen to be 10±0,5 or 60±3 cmH_2Omin^{-1}.

- A manometer is connected to the testing head.

- the pressure value when forth droplet is observed on the specimen is defined as water penetration resistance of material [94].

3.4.3 Water vapor transmission rate (WVTR)

WVTR was measured according to "ASTM E 96-00 B Water Method". Three test apparatus were designed and manufactured according to this standard as seen in Figure 3.10 [95].

Test dishes were filled with distilled water to a level of 19±6 mm from the specimen. The air space thus allowed has a small vapor resistance, but it is necessary in order to reduce the risk of water touching the specimen when the dish is handled. The dishes were manufactured from high molecular weight polyethylene. Specimen is attached to the dish.

Figure 3.10 : Test dishes for water vapor transmission.

The test dish filled with distilled water and covered with specimen is weighed and it is placed in an atmosphere where relative humidity 50±2% and temperature 21±1 0°C. In addition, air continuously circulated throughout the chamber, with a velocity sufficient to maintain uniform conditions at all test locations. It is stated in the standard that air velocity over the specimen shall be between 0.02 and 0.3 ms^{-1}. Test specimens had been left in the test chamber for two days. Then the dishes weighed again. Weight difference shows water vapor transmission of specimens for two days.

3.4.4 Air permeability

The air permeability is defined as the velocity of an airflow passing perpendicularly through a test specimen under specified conditions of test area, pressure drop and time. Air permeability of membranes and membrane laminates were measured according to "ISO 9237 Determination of the permeability of fabrics to air by an air permeability tester (Textest FX 3300-III)" as seen in Figure 3.11. It is based on the rate of flow of air passing perpendicularly through a given area of fabric is measured at a given pressure difference across the fabric test area over a given time period [96].

Figure 3.11 : Textest Fx 3300-III air permeability tester [97].

Circular specimen holder, with an orifice allowing the test to be carried out on an area of 20 cm^2. Pressure gauge or manometer, connected to the test head to indicate a pressure drop across the specimen test area of 100 Pa with an accuracy of at least 2% [96].

3.5 Experimental Results and Discussions for Membranes

3.5.1 Fiber morphology

Nanofiber webs were produced on a commercial polyester fabric by optimal electrospinning conditions. SEM photographs of nanofiber webs are given in Figure 3.12.
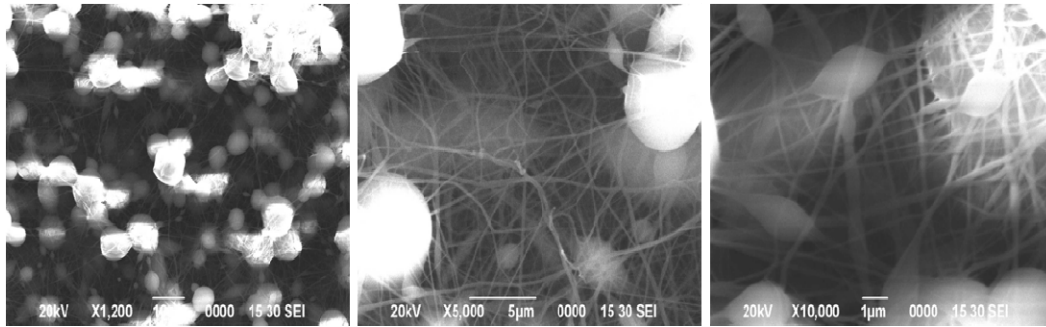
Figure 3.12 : SEM photographs of nanofiber from ES 1 solution at different magnifications.

Nanofiber web obtained from ES 1 (see Table 3.2) solution contains many beads having diameter about 5 μm. Average diameter of nanofibers is 210 nm. Fibers are generally distributed from 100 to 350 nm. A few fibers having diameters 500-550 nm are observed on the nanofiber web. Fiber distribution is from SEM photographs of the specimens, and it is given in Figure 3.13.
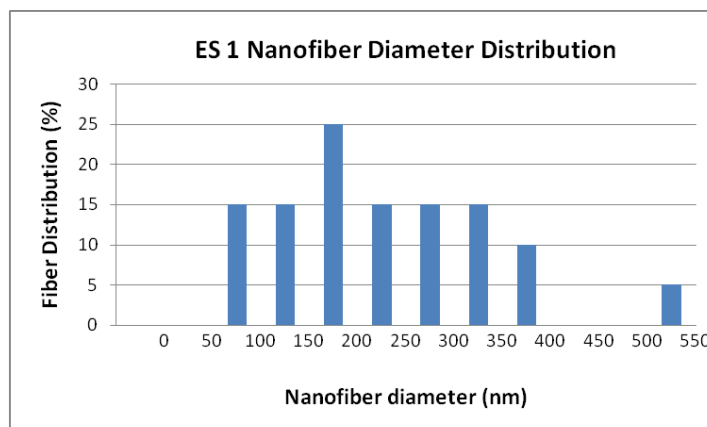
Figure 3.13 : Fiber distribution of ES 1 nanofiber web.

Electrospun fibers obtained from ES 2 solution have fewer beads than ES 1 solution. Nanofibers are smooth and well distributed on the web. SEM photographs of nanofibers obtained from ES 2 solution are given in Figure 3.14.
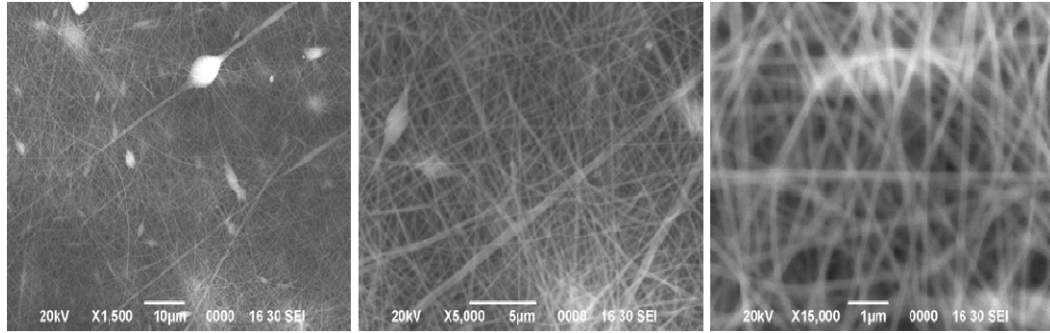
Figure 3.14 : SEM photographs of nanofiber from ES 2 solution at different magnifications.

Fiber diameter distribution from nanofiber web electrospun from ES 2 solution ranges from 150 to 300 nm. Some nanofibers with diameters about 500 nm also exist on the web. Fiber diameter distribution of electrospun nanofibers from ES 2 solution is given in Figure 3.15.
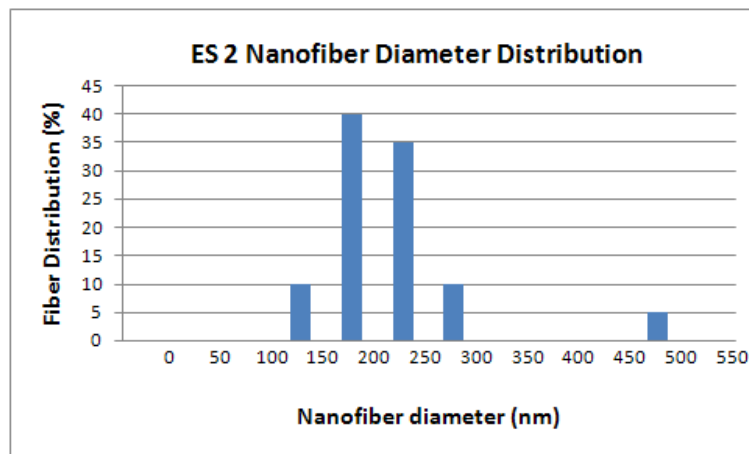
Figure 3.15 : Fiber distribution of ES 2 nanofiber web.

Polymer solution ES 3 contains poly(methylphenylsiloxane) commercially called silicone oil. Many beads are encountered on the SEM photograph of nanofiber electrospun from ES 3 solution. It is thought that these beads are formed due to the existence of poly(methylphenylsiloxane), as the ES 2 solution prepared from the same polymer had given beadless smooth nanofibers. SEM photographs of ES 3 solutions are given in Figure 3.16.
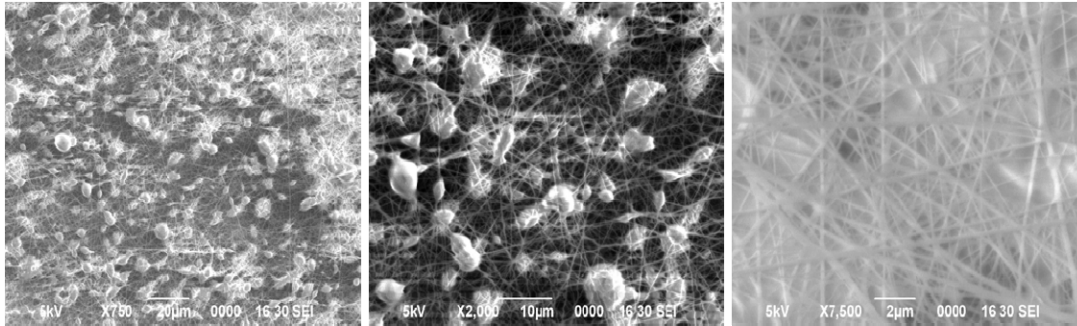
Figure 3.16 : SEM photographs of nanofiber from ES 3 solution at different magnifications.

Fiber diameter distribution of electrospun web from ES 3 solution ranges from 60 to 300 nm (see Figure 3.17). Average diameter of nanofiber web is about 180 nm. Poly(methylphenylsiloxane) enhances the electrospinning process and decreases the average nanofiber diameter. Thus, production rate (grmin^{-1}) of ES 3 solution is approximately 2.5 times more than all other solutions.
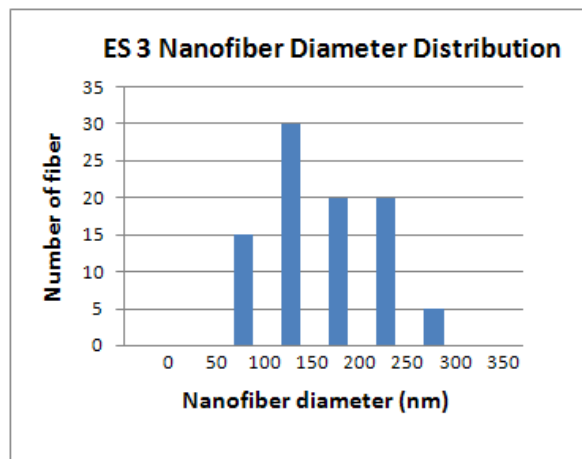
Figure 3.17 : Fiber distribution of ES 3 nanofiber web.

3.5.2 Resistance to water penetration

Water penetration resistance of nanofiber web is compared with the commercially available waterproof breathable products. A Gore-Tex$^{®}$ 65 grm^{-2} membrane laminated warp knitted fabric and Eurodach$^{®}$ 125 grm^{-2} three layer spunbond-membrane-spunbond waterproof material were used as control materials (see Figure 3.18). In addition, a laminated material was manufactured by using nanofiber web from ES 3 solution and a woven fabric by using polyurethane hotmelt adhesive.
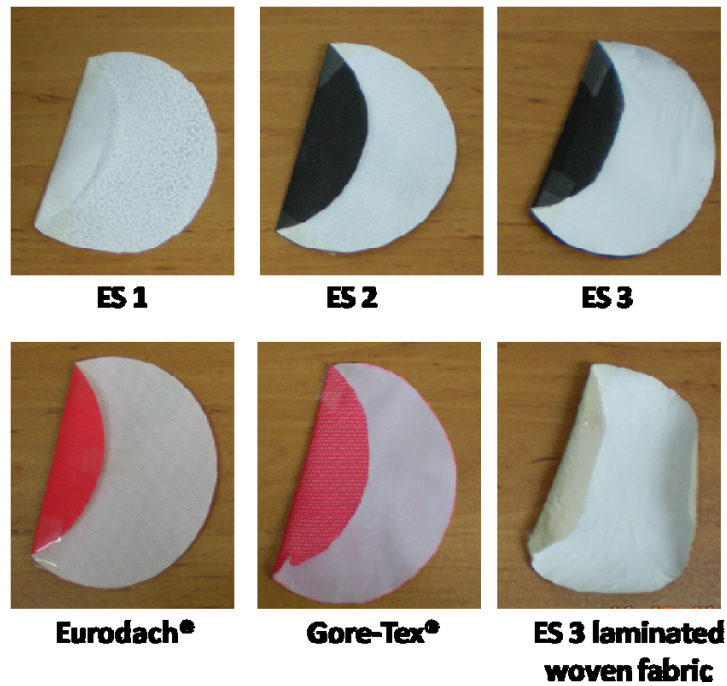
Figure 3.18 : Commercially available and experimentally developed waterproof breathable materials.

Figure 3.19 shows water penetration resistance of experimentally developed nanofiber webs, laminated nanofiber web and control materials. The properties of these materials are explained below:

- ES 1: 60 grm^{-2} PET spunbond + 10 grm^{-2} nanofiber (polyether based TPU)

- ES 2: 60 grm^{-2} PET spunbond + 10 grm^{-2} nanofiber (polyester based TPU)

- ES 3: 60 grm^{-2} PET spunbond + 10 grm^{-2} nanofiber (polyester based TPU+ poly(methylphenylsiloxane))

- Eurodach: 125 grm^{-2} polypropylene spunbond + polypropylene membrane + polypropylene spunbond

- Gore-Tex: 65 grm^{-2} knitted fabric + PTFE membrane

- Laminated ES 3: Woven fabric + 40 grm^{-2} nanofiber web (polyester based TPU+ poly(methylphenylsiloxane))
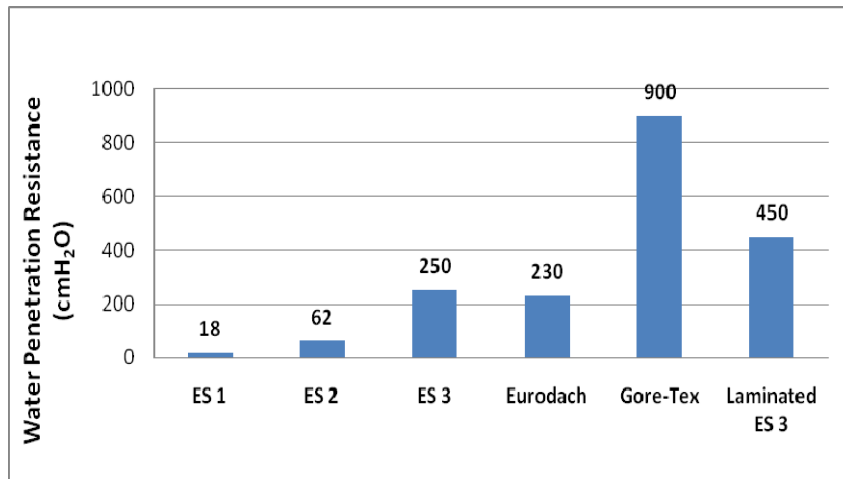
Figure 3.19 : Water penetration resistances of electrospun webs and control materials.

Water penetration resistance of ES 1 nanofiber is 18 cmH$_2$O. It is very low for a membrane material when it is compared to the commercial ones (see Figure 3.19).

Microporous membranes as seen in Figure 3.20 resist water molecules with nonporous sections of their surface, pores on the membrane permit the transfer of water vapor molecules [98]. Nanofiber web also has microporous structure, therefore it can be said that polyether phase of nonporous sections of nanofiber web can not resist the transfer of water molecules at high pressure values.
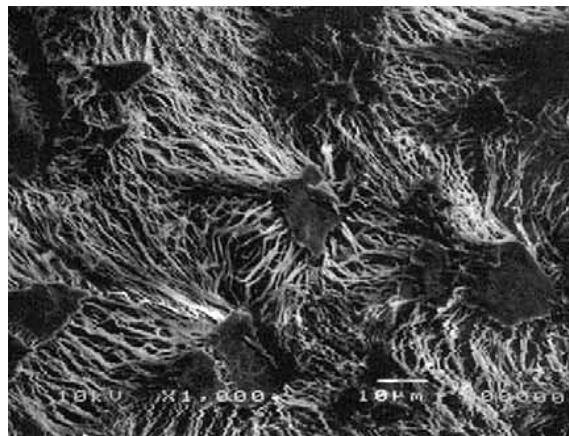
Figure 3.20 : SEM photograph of Gore-Tex PTFE membrane [99].

ES 2 specimen, polyester based thermoplastic polyurethane nanofiber coated on polyester spunbond fabric resist the water penetration up to 62 cmH$_2$O hydrostatic head pressure. Nanofiber web of polyester based thermoplastic polyurethane is more durable to passing of water molecules than polyether based thermoplastic polyurethane.

Water resistance levels of waterproof fabrics are classified as low-water-resistant (30-80 cmH_2O), middle-water-resistant (l0-250 cmH_2O) and high-water resistant (50-3000 cmH_2O) based on the water resistance values [100]. Therefore, ES 2 nanofiber web can be defined as low water resistant fabric.

A 10 grm^{-2} nanofiber web was electrospun from polyester based TPU/DMF-ethyl acetate solution added poly(methylphenylsiloxane) (Specimen ES 3 electrospun from ES 3 solution in Table 3.3) onto 60 grm^{-2} polyester spunbond exhibited 250 cmH_2O water penetration resistance. ES 3 specimen differs from ES 2 specimen by content of 7 wt% poly(methylphenylsiloxane). That content of poly(methylphenylsiloxane) provides 190 cmH_2O water resistance more.

Addition of poly(methylphenylsiloxane) to the solution makes the nanofiber web middle water resistant material. Water resistant value of ES 3 specimen is also higher than the waterproof material Eurodach[®] without any post treatment.

To produce an alternative membrane material to Gore-Tex[®] fabric laminates, nanofiber web was electrospun from ES 3 solution and it was laminated on a woven fabric by polyurethane hotmelt adhesive. However, ES 3 specimen has only 450 cm hydrostatic head pressure, which is much lower than Gore-Tex PTFE. The laminated fabric exhibited 900 cmH_2O water penetration resistance. 40 grm^{-2} nanofiber web electrospun from ES 3 solution laminated onto woven fabric substrate can be defined as high water resistant fabric.

3.5.3 Water vapor transmission rate (WVTR)

WVTR is used as an evaluation criteria for performance of the the fabric material with regard to user comfort. Therefore, a high WVTR value is desirable with a high water penetration resistance. WVTR values of studied specimens are given below (see Figure 3.21).

Vapor transmission rate of all nanofiber web specimens are higher than commercial products Eurodach[®] and Gore-Tex[®]. Eurodach[®] as a commercial product has the lowest WVTR value because of high material density and material type. That waterproof material is composed of polypropylene spunbond layers and polypropylene membrane. Both spunbond layers and membrane, which has low porosity, play a role on decreasing WVTR value. Gore-Tex[®], PTFE laminated knitted fabric has remarkable vapor transmission rates, because it contains a

membrane layer, which has highly microporous structure and has a warp knitted fabric with large holes. Both highly porous membrane and laminated fabric enhance the vapor transmission of Gore-Tex[®].
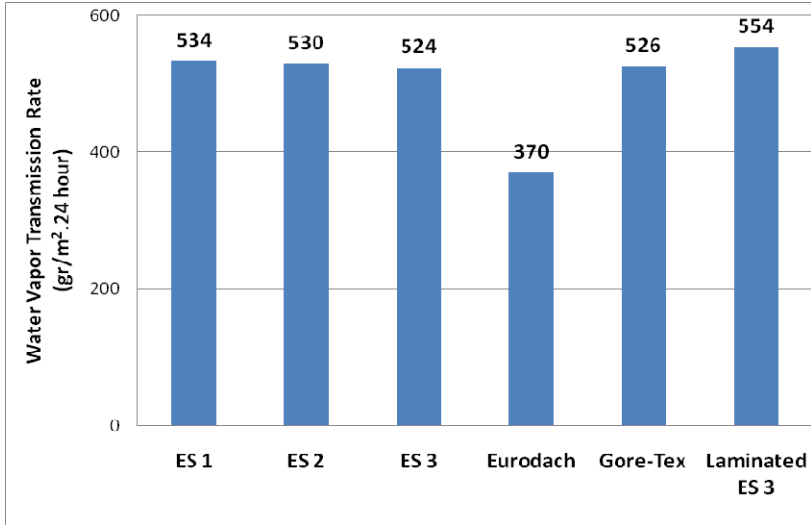
Figure 3.21 : WVTR values nanofiber and commercial membrane materials.

The highest WVTR value was obtained from the ES 3 laminated fabric. It was expected that higher membrane density of ES 3 laminated fabric should give lowest water vapor transfer. Since woven substrate material used for ES 3 nanofiber web was made of cotton, substrates of the other three materials were polyester spunbond nonwovens therefore they have lower WVTR values. High value in WVTR for ES nanofiber webs indicates that open structure plays a major role in transmitting of water vapors through fabrics.
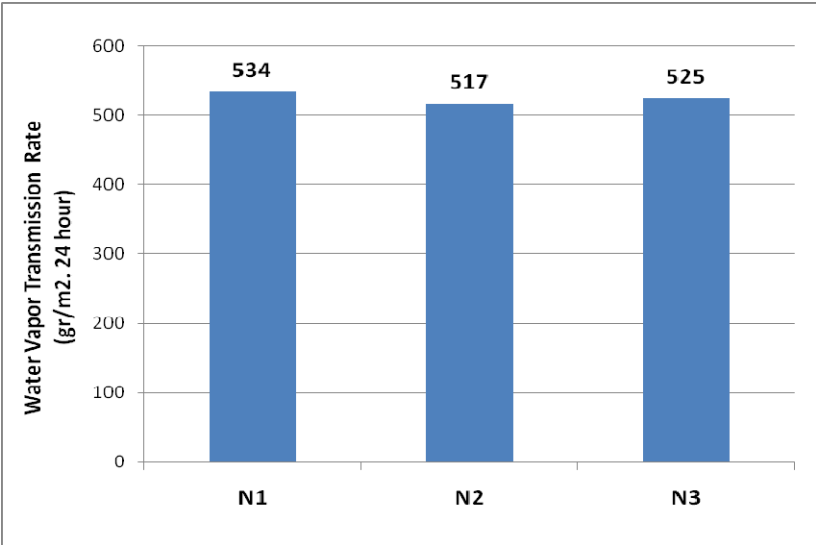
Figure 3.22 : WVTR values of nanofiber webs having different weights N1: 9 grm^{-2}, N2: 12 grm^{-2}, N3: 27 grm^{-2}.

In addition to this, three nanofiber web electrospun from the solution ES 2 onto 60 grm^{-2} polyester spunbond fabrics with different densities were tested to compare WVTR values of nanofiber webs, which have different nanofiber weights.

It can be seen from Figure 3.22 that the weight of the web does not seem to play remarkable role on water vapor transmission rate of nanofiber web. Open pore structure makes nanofiber web highly breathable material even if weight density of nanofiber is high.

3.5.4 Air permeability

Air permeability rates of six specimens were investigated and the results of the tests are given in Figure 3.23. Air permeability is important for waterproof breathable materials because low air permeable products indirectly provide thermal insulation especially in cold circumstances. The number and size of pores in the construction determine the air permeability of a material. Product with no pores is impermeable and offer good protection against wind. But also materials with sufficiently small pores may in practice be almost impermeable to air penetration [101]. So commercial waterproof materials have low air permeability values because of their limited open pore structures.

On the other hand, nanofiber membranes have air permeability values around 3 $ltm^{-2}s^{-1}$, which is high in comparison to the commercial ones.
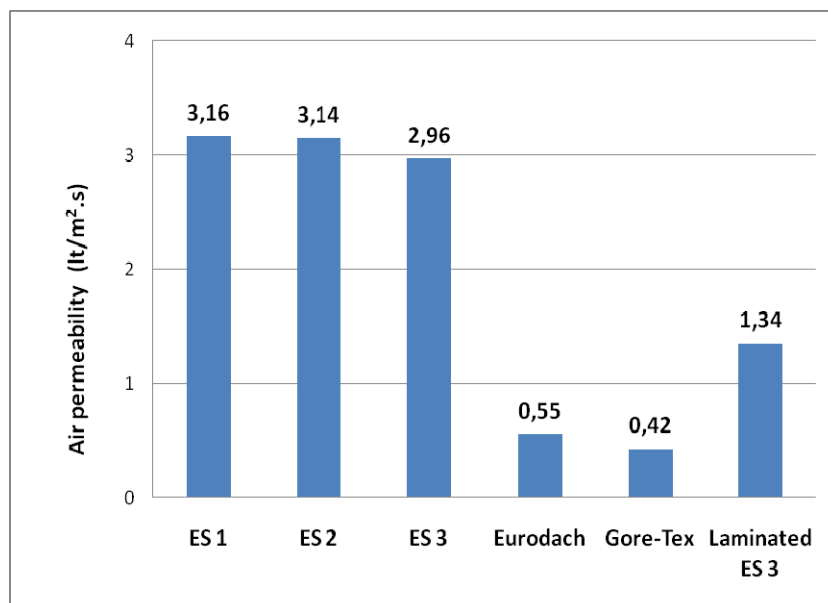
Figure 3.23 : Air permeability rates of nanofiber and commercial membrane materials.

In addition to this, laminated woven fabrics by hotmelt adhesive with 40 gr/m^2 nanofiber web has 1.34 ltm^{-2}s^{-1} air permeability value which is closer to the performance value of the Gore-Tex® and Eurodach® barrier products.

4. NANOFIBROUS COMPOSITE MEMBRANE SEPERATORS FOR LITHIUM-ION BATTERIES AND RELATED EXPERIMENTAL WORK

4.1 Introduction

The energy and the environment will be at the top of global problems facing our society for the next 50 years. At present, fossil fuels are the primary source used to meet the energy demands, nevertheless these resources are finite. Furthermore, processing of fossil fuels leads to global warming due to emissions of greenhouse gases, including carbon dioxide, methane, nitrous oxide and other gases, such as volatile organic compounds and hydro fluorocarbons. The quality of the environment has also deteriorated due to industrialization, which releases many pollutants into the atmosphere. Water and air represent two environmental systems where the most pressing environmental issues persist. Water pollution and dwindling freshwater supplies are often cited as critical global problems. It is estimated that more than 50% of nations in the world will face freshwater stress or shortages by 2025. By 2075, it is further estimated that the number of nations facing these problems will increase to become 75% of all nations [10].

Researchers have been investigating clean energy opportunities such as, using solar energy more efficiently and cost effective generation of electricity, electrolysis of water to generate hydrogen and into electricity with reduced emissions via fuel cells. Efficient use of energy is often connected with energy conservation. Once the electricity is generated, it must be efficiently stored during low demand periods, or for use in portable applications. This highlights the need for electrochemical energy storage devices, via high energy density batteries and/or super capacitors. Then, the storage of hydrogen becomes of interest, particularly when considering the use of hydrogen as fuel for electric vehicles or as a clean burning fuel for vehicles with combustion engines [10].

Lithium-ion (Li-ion) batteries are thought to hold promise for uses from mobile phones and laptop computers through to electric vehicles and the market is forecast

to rise to \$7 billion in 2015. In hybrid and electric vehicles alone, the market could grow from virtually zero in 2004 to around \$1 billion in 2015 [102].

The cathode in this kind of battery is a lithiated metal oxide ($LiCoO_2$, $LiMO_2$, $LiNiO_2$) and the anode is made of graphitic carbon with a layered structure. The electrolyte is made up of lithium salts (such as $LiPF_6$) dissolved in organic carbonates. When the battery is charged, the lithium atoms in the cathode become ions and migrate through the electrolyte toward the carbon anode where they combine with external electrons and are deposited between the carbon layers as lithium atoms. This process is reversed during the discharge process [103].

Lithium-ion batteries, first proposed in the 1960s, came into reality when Bell Labs developed a workable graphite anode to provide an alternative to lithium metal (lithium battery). The first commercial lithium-ion batteries were produced by Sony in 1990. Since then, improved material developments have led to vast improvements in terms of the energy density (increased from 75 to 200 $Whkg^{-1}$) and cycle life (increased to as high as 10,000 cycles). The efficiency of Li-ion batteries is almost 100% which forms another important advantage over other conventional batteries [103].

Although Li-ion batteries take over 50% of the small portable devices market, there are some challenges for making large-scale Li-ion batteries. The main hurdle is the high cost (>\$600/kWh) due to special packaging and internal overcharge protection circuits. [103].

4.2 Lithium-ion Battery Separators

The principle of Li-ion battery (LIB) is based on the "rocking-chair" concept, in which a low potential Li insertion anode as carbonaceous material is matched with a high potential Li insertion cathode. Various materials have been developed for high performance, more safety, low cost and availability considerations. So far, the best choice for electrode reactions for commercial Li-ion batteries is Li intercalation compounds such as $LiCoO_2$ for cathode material and graphite for anode material. The discharge process is the lithium ion moves out of the intercalated carbon and into another lithium intercalation compound

In order to satisfy the human needs of both environmental protection and miniaturization of consumer products, Li-ion batteries have rapidly become the rechargeable battery of choice for many applications and are available in a variety of configuration, size, and capacity [104].

The separator is a critical component in liquid electrolyte batteries, and is placed between the positive electrode and the negative electrode to prevent physical contact of the electrodes while enabling free ionic transport and isolating electronic flow. It mostly is a microporous layer consisting of either a polymeric membrane or a non-woven fabric mat. Essentially, it must be chemically and electrochemically stable towards the electrolyte and electrode materials and must be mechanically strong to withstand the high tension during the battery assembly operation. Structurally, the separator should have sufficient porosity to absorb liquid electrolyte for the high ionic conductivity. However, the presence of the separator adds electrical resistance and takes up limited space inside the battery, which adversely affects battery performance. Therefore, selection of an appropriate separator is critical to the battery performance, including energy density, power density, cycle life and safety.

For high energy and power densities, the separator is required to be very thin and highly porous while remaining mechanically strong. For battery safety, the separator should be able to shut the battery down when overheating occurs, such as the occasional short circuit, so that thermal runaway can be avoided. The shutdown function can be obtained through a multilayer design of the separator, in which at least one layer melts to close the pores below the thermal runaway temperature and the other layer provides mechanical strength to prevent physical contact of the electrodes [105].

4.3 Properties of Separators

4.3.1 Thickness

Separator backweb refers to the porous separating membrane. It is of uniform thickness and has a macroscopically uniform pore distribution. Only in this way can an overall uniform current density be ensured during the operation of the storage battery, achieving a uniform charging and discharging of the electrodes and thus a maximum utilization of the electrode materials.

In practice, the desired electrolyte distribution is achieved by distance-maintaining ribs on the porous backweb; this in addition has the advantage of maintaining a maximum distance between the origin of oxidizing substances located at the positive electrode and the highly porous separating membrane, sensitive due to its large inner surface. The total or overall thickness thus comprises the backweb thickness and the rib height. For achieving a uniform current distribution the thickness is normally specified very precisely and it is acceptable only within rather narrow tolerances. Besides technical difficulties in the production, this also presents a problem in measurement. Since all separator materials are more or less compressible, a specified measuring pressure has to be used. Moreover, the measuring area is also significant. One can easily imagine an extended area touching only the microscopic elevations of the separator, whereas a measuring tip may very well hit "valleys" [106].

4.3.2 Pore size and porosity

An appropriate porosity is necessary to hold sufficient liquid electrolyte for the ionic conductivity between the electrodes. However, too high porosity will adversely impact the shutdown performance because in this case, the pores cannot be closed effectively and the membrane tends to shrink as it melts or softens. The porosity can be measured using liquid or gas absorption methods. Typically, the Li-ion battery separators have a porosity of 40% [105].

The pore size must be smaller than the particle size of the electrode components, including the electrode active materials and the conducting additives. In practical cases, membranes with sub-micron pore sizes have proven adequate to block the penetration of particles since the tortuous structure of the pores assists in blocking the particles from reaching the opposite electrode. Uniform distribution and a tortuous structure of the pores are both highly desirable since the former ensures a uniform current distribution throughout the separator and the latter suppresses the growth of dendritic lithium [105].

4.3.3 Chemical stability

The separator material must be chemically stable against the electrolyte and electrode materials, especially under the strongly reductive and oxidative environments when the battery is fully charged. Meanwhile, it should not degrade and lose mechanical strength. An easy method to verify chemical stability is by calendar life testing [105].

4.3.4 Permeability

Separator should not limit the electrical performance of the battery. Typically, the presence of a separator increases the effective resistance of the electrolyte by a factor of 4–5. The ratio of the resistance of the separator filled with electrolyte divided by the resistance of the electrolyte alone is called MacMullin number. MacMullin numbers as high as 8 have been used in high power Li-ion batteries. For batteries used in hybrid electric vehicles (HEV) and in power tools, the MacMullin number should be lower for the purpose of safety and a long cycle life. Air permeability can be used indirectly to estimate the MacMullin number. Air permeability is expressed by a terms of the Gurley value, which is defined as the time required for a specific amount of air to pass through a specific area of the separator under a specific pressure. The Gurley value can be measured according to ASTM D726. When the porosity and thickness of the separators are fixed, the Gurley value reflects the tortuosity of the pores. The separator with uniform permeability is essential for the long cycle life of a battery. Variations in permeability will result in uneven current density distribution, which has been verified as the main reason for the formation of dendrite Li on the negative electrode [105].

4.3.5 Wettability

The separator should wet easily in the electrolyte and retain the electrolyte permanently. The former facilitates the process of electrolyte filling in battery assembly and the latter increases cycle life of the battery. There is no generally accepted test for separator wettability. However, placing a droplet of electrolyte on the separator and observing whether or not the droplet quickly wicks into the separator is an easy way to indicate sufficient wettability [105].

4.3.6 Dimensional stability

The separator should lay flat and not bow or skew when it is laid out and soaked with liquid electrolyte. The separator should remain stable in dimensions over a wide temperature range [105].

4.3.7 Thermal shrinkage

When the temperature rises to the softening temperature, the membrane tends to shrink, even if the porosity is very low, because of the difference in the density

between the crystalline and amorphous phases of polyolefin materials. For example, the PE can shrink as much as 10% when exposed to a temperature of 120 ^{o}C for only 10 min. The thermal shrinkage should be minimized. For the Li-ion battery, the shrinkage is required to be not more than 5% after 60 min at 90 ^{o}C [105].

4.4 Types of Separators

4.4.1 Microporous membrane separators

Currently, all commercially available, spirally wound lithium-ion cells use microporous polyolefin separators (see 4.1). In particular, separators are made from polyethylene, polypropylene, or some combination of the two. Polyolefins provide excellent mechanical properties and chemical stability at a reasonable cost. A number of manufacturers produce microporous polyolefin separators. Nonwoven materials have not been able to compete with microporous films, most probably because of the difficulty in making thin (25 μm) nonwovens with acceptable physical properties (for example, gauge uniformity, puncture strength). However, nonwovens are used in buton cells and bobbin cells when thicker separators and low discharge rates are acceptable [107].
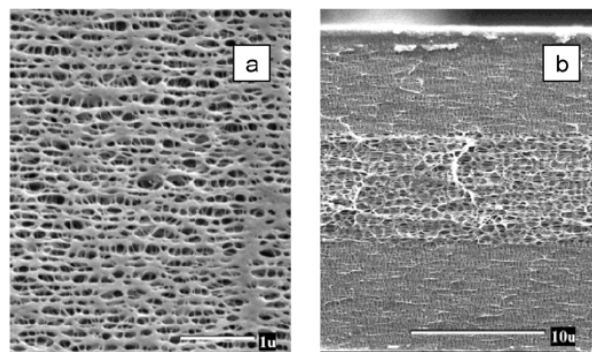
Figure 4.1 : SEM photographs of three layer microporous membrane a) surface b) cross section [107].

The processes for manufacturing micro porous membranes can be broadly divided into wet processes and dry processes. Both processes usually employ one or more orientation steps to impart porosity and/or increase tensile strength.

Wet processes involve mixing a hydrocarbon liquid or some other low-molecular - weight substance with a polyolefin resin, heating and melting the mixture, extruding the melt into a sheet, orientating the sheet either in the machine direction or biaxially, and then extracting the liquid with a volatile solvent [108].

Dry processes involve melting a polyolefin resin, extruding it into a film, thermal annealing, orientation at a low temperature to form micro pore initiators, and then orientation at a high temperature to form micro pores [9, 10]. The dry process involves no solvent handling, and therefore is inherently simpler than the wet process. The dry process involves only virgin polyolefin resins and so presents little possibility of battery contamination [108].

4.4.2 Nonwoven fabric maths

A non-woven separator is a fibrous mat made by bonding numerous fibers together through chemical, physical or mechanical methods. Natural and synthetic materials have been used to manufacture the fibers for non-woven separators. Natural materials include celluloses and their chemically modified derivatives. The synthetic materials include polyolefin, polyamide, polytetrafluoroethylene, PVdF, polyvinyl chloride (PVC), polyester as seen in Figure 4.2 and so forth [105,109].
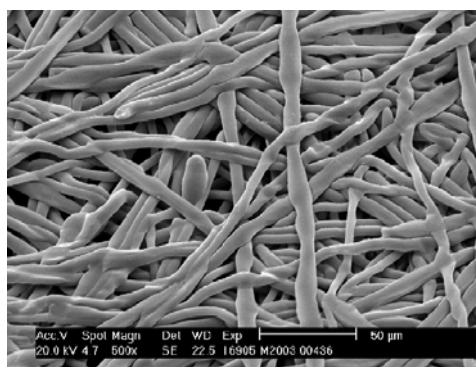
Figure 4.2 : SEM picture of polyester nonwoven separator [109].

The principal bonding methods for the battery separators are resin bonding and thermoplastic fiber bonding. In the former, the resin as an adhesive is sprayed onto the web of fibers, and then dried, heat-cured and in some instances pressed. In the latter, a fusible (thermoplastic) fiber having a lower melting point than the base fiber as the bonding agent is blended with the base fiber to form a web, followed by pressing between two heated rollers to promote bonding of the thermoplastic fibers and the base fibers. To minimize the adverse effect of foreign adhesives on the battery performance, the thermoplastic bonding method is most preferable for the manufacture of battery separator. The fibrous webs can formed either by a wet process such as a paper-making process, a solution extrusion method using a

spinning jet and wet-laid method or by a dry process such as a melt blowing method [105].

4.4.3 Inorganic composite separator

An inorganic composite separator, or "ceramic separator", is a porous web made of ultrafine inorganic particles bonded using a small amount of binder. Due to the high hydrophilicity and high surface of the small inorganic particles, such separators exhibit exceptional wettability with all non-aqueous liquid electrolytes, especially those containing a high content of cyclic carbonate solvents such as ethylene carbonate (EC), propylene carbonate (PC) and butyrolactone (GBL), which have a high dielectric constant and are known to be unable to wet the non-polar polyolefin separators. Meanwhile, these separators have extreme thermal stability and show zero-dimensional shrinkage at high temperatures [105].

The outstanding wettability allows one to use a high content of PC and EC in the liquid electrolytes, which is very helpful to increase the cycleability of the Li-ion batteries at high temperatures, while the extreme thermal stability offers the batteries excellent temperature tolerance, which is critical to large-size Li-ion batteries. In fact, temperature-related safety issues are mostly related to the dimensional shrinking or melting of the separator. Both shrinking and melting of the separator could result in physical contact of the electrodes so that direct chemical reactions between the strongly oxidative cathode material and the strongly reductive anode material occur, and the generated heat causes thermal runaway. Therefore, the inorganic composite separators with excellent wettability and zero shrinkage are highly desirable for the development of large-size Li-ion batteries, especially these for hybrid electric vehicles and power tools [105].

4.5 Experimental Work

Polyolefin microporous films and nonwoven fabrics are the most used material for lithium-ion battery separators. Both separators have disadvantages that porosity and electrolyte wettability of microporous membranes are low and thin membrane structure and small pore size of microporous membranes are the advantages of them. On the other hand, nonwoven separators have higher porosity good electrolyte wettability. But high thickness and large pores are disadvantages of nonwoven

fabrics [110]. Therefore, a new generation separator material, which has good wettability, high porosity with small sizes and has smaller thickness, can be a strong alternative to current battery separators. Polyacrylonitrile nanofiber web can be a good candidate as an alternative material for lithium-ion batteries instead of microporous membranes and nonwoven materials.

4.5.1 Materials

To produce polyacrylonitrile solution, poly(acrylonitrile) powder was obtained from AKSA Akrilik A.Ş. and dimethyl formamide obtained from Bereket Kimya Tıp Teknik Tic. ve San. Ltd. Şti. were used as solvent. Fumed silica nanoparticles, AEROSIL 200 Pharma (See Table 4.1 for its properties), were supplied from Marmara Ecza and Kimyevi Maddeler San. Tic. which have 21 nm diameter.

Table 4.1 : Properties of Aerosil 200 Pharma silica [111].

Properties	Unit	Typical Value
Specific surface area (BET)	m^2g^{-1}	200 ± 25
Tapped density (approx. value) acc. to DIN EN ISO 787/11, Aug. 1983	gl^{-1}	approx. 50
pH Tested according to Ph. Eur., USP/NF		3.5 - 5.5
Chloride Tested according to Ph. Eur.; JP	ppm	< 250; < 110
Heavy Metals Tested according to Ph. Eur.; JP	ppm	< 25; < 40
SiO2 - content Tested acc. to Ph. Eur., USP/NF; JP	wt%	99.0 - 100.5; > 98.0
Loss on Drying (moisture) Tested according to USP/NF; JP	wt%	< 2.5; < 7.0
Loss on Ignition Tested acc. to Ph. Eur.; USP/NF; JP	wt%	< 5.0; < 2.0; < 12.0
As - content Tested according to USP/NF; JP	ppm	< 8.0; < 5.0
Volume Test Tested according to JP	ml	> 70
Fe - content Tested according to JP	ppm	< 500

PAN powders were dissolved in DMF at 10 wt% concentration and solution was stirred at 100 $^\circ$C for 12 hours. Then three PAN/DMF solutions were prepared with 0 wt%, 1 wt% and 2 wt% silica content.

Solutions were coded as below;

- 10 wt% PAN/DMF: PAN-Si00

- 10 wt% PAN/DMF+1 wt% Silica: PAN-Si01

- 10 wt% PAN/DMF+2 wt% Silica: PAN-Si02

Microporous membrane Celgard 2020 was supplied from Celgard LLC (see Table 4.2 for its properties) as control material for nanofiber web separators. Properties of membrane are;

- 20 μm microporous three layer membrane (PP/PE/PP)

- Uniform pore structure with high chemical and thermal stability

- Oxidation resistance for excellent cycling and trickle charge performance

- PE inner layer provides high-speed shutdown

- Excellent resistance to acids, bases and most chemicals

- Zero TD shrinkage reduces internal shorting and improves high temperature dimensional stability [112].

Table 4.2 : Basic film properties of Celgard 2320 [112].

Basic Film Properties	Unit of Measure	Typical Value
Thickness	μm	20
Air permeability	Gurley (JIS) Seconds	530
Porosity	%	30
Pore size (Average diameter)	μm	0.027
TD Shrinkage at 90º C / 1 Hour	%	0
MD Shrinkage at 90º C / 1 Hour	%	5
Puncture Strength	Grams	360
Tensile Strength MD	kgcm^{-2}	2050
Tensile Strength, TD	kgcm^{-2}	165

4.5.2 Electrospinning of PAN/DMF/silica solutions

Electrospinning was performed by the 10-needle electrospinning setup (see Figure 3.8). It consists of two pipe-needle system, each pipe has five needles. Solution was fed to the pipe-needle system by a syringe pump (Asena Alaris GH, Cardinal Health

Inc.), a high voltage power supply capable of 0–100 kV (ES100P-20W, Gamma High Voltage Research, Inc.) and a grounded rotating drum cylinder as a collector.

85 grm^{-2} polyester spunbond fabrics were used as substrate material for PAN/silica nanofibers. Electrospinning of PAN/DMF solution has difficulties because of high conductivity of solution. Fiber bundles generated during electrospinning process and these bundles disturb homogeneity and porous structure of nanofiber web. Optimal electrospinning conditions for three PAN/DMF solutions with different silica content are given in Table 4.3.

Table 4.3 : Optimal electrospinning conditions for PAN/DMF/silica solutions.

Electrospinning parameters	PAN-Si00	PAN-Si01	PAN-Si02
Voltage (kV)	26	34	30
Needle to collector distance (cm)	7.5	10	12
Flow rate (mlh^{-1}needle^{-1})	2	2	1

4.6 Characterization

4.6.1 Fiber morphology

Scanning Electron Microscope (JEOL JSM-6390 LV) was used to characterize PAN nanofiber web and measure the diameters of nanofibers. SEM photographs were obtained at different magnifications. Fiber diameters of nanofibers were measured by CATIA 3D design program using SEM photographs.

4.6.2 Air permeability

Air permeability is defined as velocity of an airflow passing perpendicularly through a test specimen under specified conditions of test area, pressure drop and time. Air permeability of membranes and membrane laminates were measured according to ISO 9237 Determination of the permeability of fabrics to air by an air permeability tester (Textest FX 3300-III). It is based on the rate of flow of air passing perpendicularly through a given area of fabric is measured at a given pressure difference across the fabric test area over a given time period.

A circular specimen holder is used to carry out the test sample with an area of 20 cm^2. Pressure gauge or manometer connected to the test head to indicate a pressure drop across the specimen test area of 100 Pa with an accuracy of 2% [96].

4.6.3 DSC analysis

The DSC analysis was performed at temperature range of 0–400 $^{\circ}$C for PAN/DMF/silica solutions and (-50 $^{\circ}$C) – (200 $^{\circ}$C) for microporous membrane by the rate of 20 $^{\circ}$Cmin^{-1} with Q100 TA Instruments.

4.6.4 Thermal Stability

Thermal stabilities of microporous and nanofiber membranes were measured by replacing them at 120 $^{\circ}$C for 36 hour in a vacuum drying oven. Sizes of membranes were measured before and after thermal process.

4.7 Results and Discussions

4.7.1 Fiber morphology

SEM photographs of pure PAN and PAN/silica nanofibers with various silica contents are give in Figures 4.3, 4.4 and 4.5. All samples exhibit long and straight fibrous morphology, with fiber diameters ranging from 150 to 500 nm. However, deformations exist on nanofibers with increasing silica content of PAN solutions.
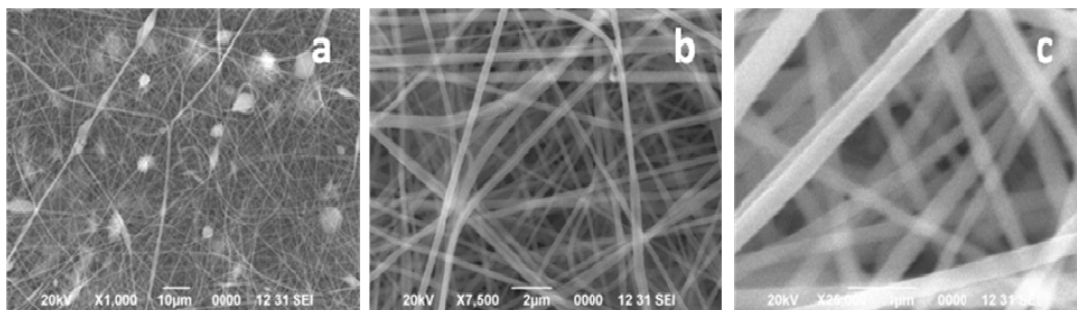
Figure 4.3 : SEM photographs of PAN-Si00 a)1000X b)7500X c)25000X magnification.
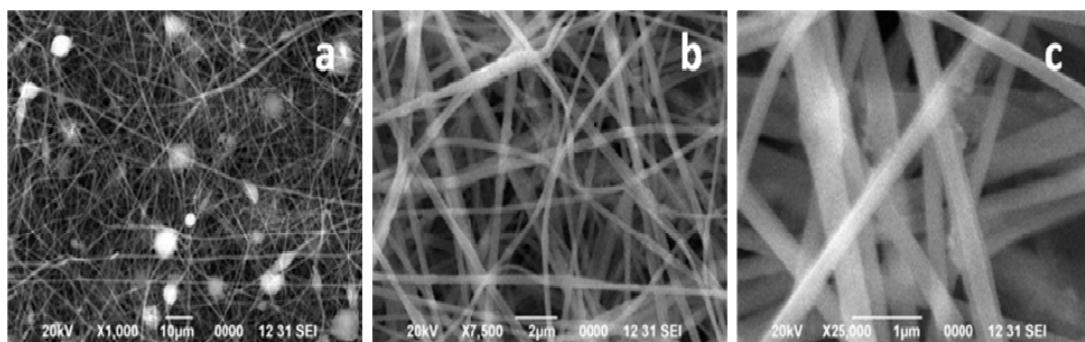
Figure 4.4 : SEM photographs of PAN-Si01 a)1000X b)7500X c)25000X magnification.
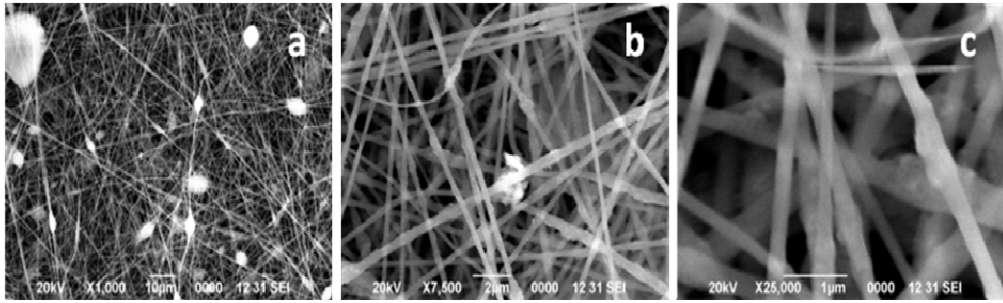
Figure 4.5 : SEM photographs of PAN-Si02 a)1000X b)7500X c)25000X magnification.

Addition of silica to the solution does not constantly affect diameter distributions of web. PAN-Si00 solution, which does not contain silica, has well nanofiber distributed structure (see Figure 4.6). Fiber distribution of nanofiber web, obtained from PAN-Si01 solution, has bimodal structure (Figure 4.7). 550-600 nm diameter fibers are observed in nanofiber web. Fiber diameter distribution of PAN-Si02 solution is better than fibers obtained from PAN-Si01 solution as seen in Figure (4.8).
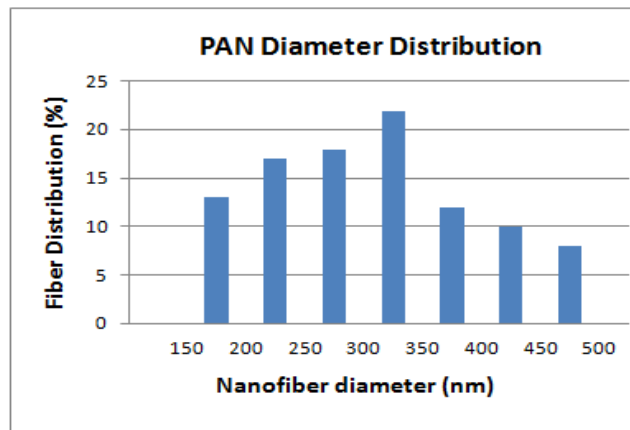
Figure 4.6 : Fiber distribution of PAN-Si00.
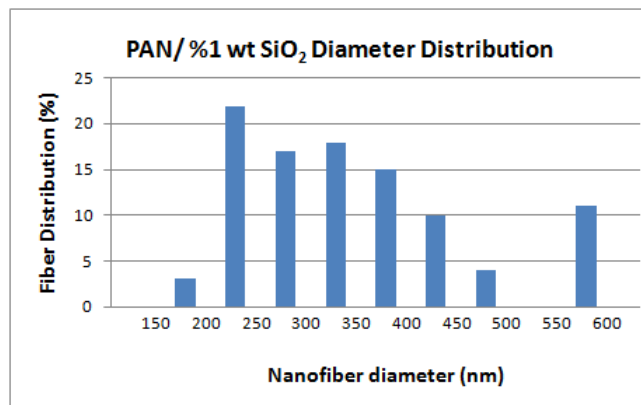
Figure 4.7 : Fiber distribution of PAN-Si01.
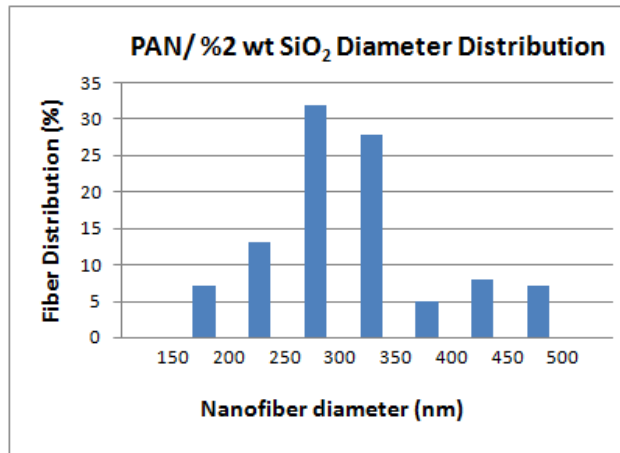
Figure 4.8 : Fiber distribution of PAN-Si02.

Surface of nanofibers become rough with increasing silica content. Agglomeration on the surface of fiber when silica concentration in the solution increases.

4.7.2 Air permeability

Air permeability of PAN/silica nanofibers and Celgard membrane is given in Figure 4.9. Microporous membrane can be defined as air proof material.
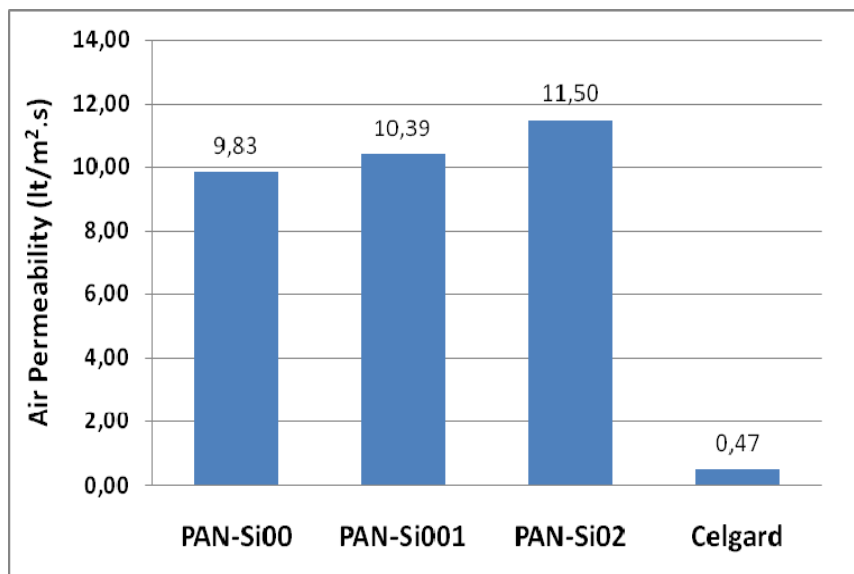
Figure 4.9 : Air permeability of PAN nanofiber webs and Celgard membrane.

PAN nanofiber webs are highly air permeable materials when they are compared with commercial microporous battery separator. Air permeability value of PAN/silica nanofiber increases with increasing silica content. Silica added nanofiber webs possess a bulkier structure than non-silica added webs. Therefore, high air

permeability of silica added nanofiber webs is resulted from this bulky structure of the web.

4.7.3 DSC analysis

DSC graphics of pure PAN and PAN/silica nanofibers obtained from 1 wt% and 2 wt% solution are given in Figure 4.10 and Figure 4.11 respectively. Nanofiber samples give a weak glass transition and a relatively large and sharp exothermic peak. The glass transition temperature and exothermic peak and its onset temperature shift to higher temperatures with increasing silica content. Glass transition of pure PAN nanofiber increases from 102.75 to 104.65 $^{\circ}$C with increasing silica content to 2 wt%. This increase is not so high, because silica nanoparticles are so large when they are compared to polymer chains. It can be said that silica nanoparticles does not affect the movement of polymer chains during the temperature increase.
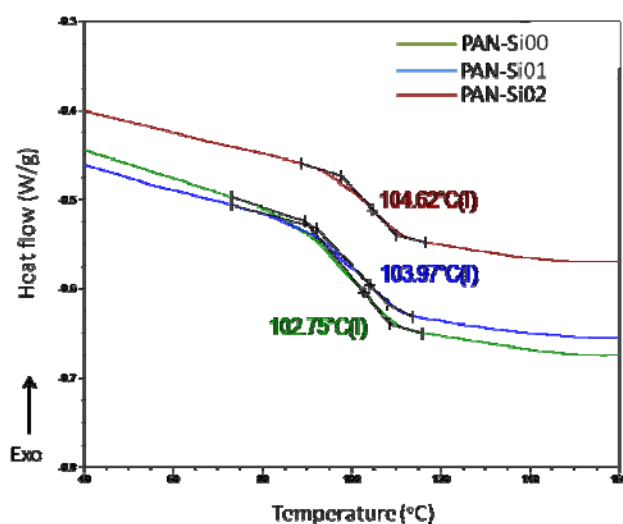
Figure 4.10 : Endothermic shift of pure PAN and PAN/silica nanofibers from DSC analysis.

It has been reported that the exothermic peak of PAN can result from three principal reactions, i.e., dehydrogenation, instantaneous cyclization, and crosslinking reactions, which are exothermic in nature. Among these three reactions, the predominant one is the instantaneous cyclization reaction. The large and sharp peak of pure PAN indicates the instantaneous cyclization of nitrile groups into an extended conjugated ring system in the nitrogen atmosphere. The broadening of the exothermic peak in the presence of silica suggests that silica either works as a

dehydration reagent, or modifies the activity of the free radicals involved in the cyclization reaction [113].
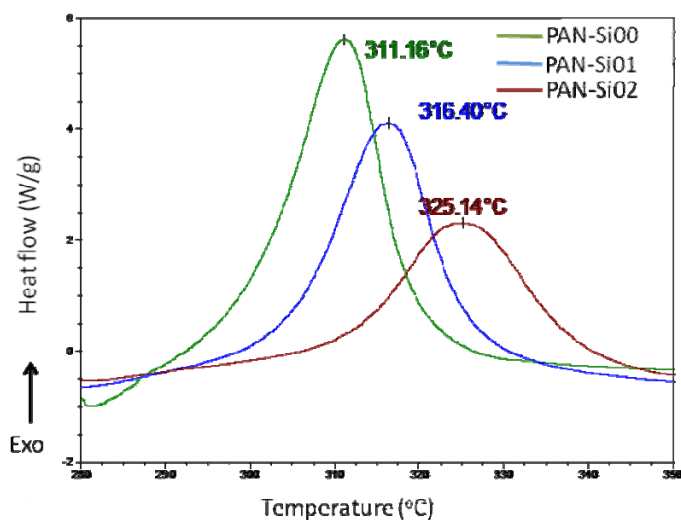
Figure 4.11 : Exothermic shift of pure PAN and PAN/silica nanofibers from DSC analysis.

The reduced reaction heat is caused by the interactions between PAN and silica, which decrease the formation of free radicals on the nitrile groups and subsequently their recombinations. The shifting of the peak to higher temperatures is also attributed to the inhibiting effect of silica on the free radical formation. At higher silica concentrations, the exothermic peak disappears, indicating that the cyclization reaction may cease to occur because of the interactions between PAN molecules and large quantities of silica inhibitor. As a result, it can be concluded that the cyclization of PAN molecules in nitrogen environment is hindered by the addition of silica [113].
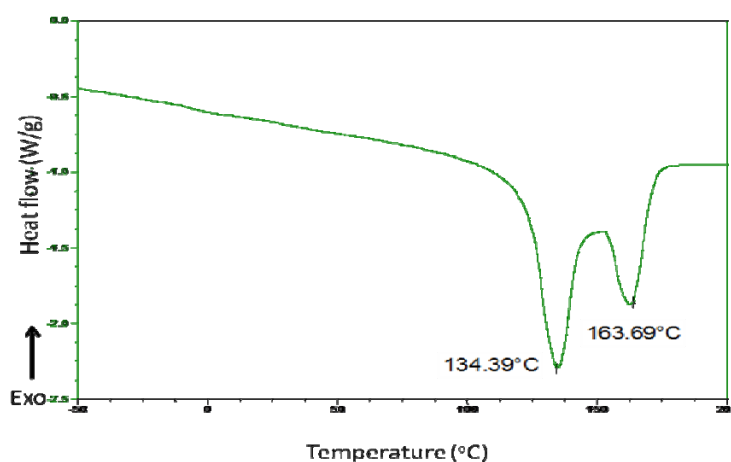
Figure 4.12 : DSC graphic of microporous membrane (Celgard 2020).

DSC thermogram of microporous membrane (Celgard2020) is given in Figure 4.12. Microporous membrane gives two endothermic peaks at 134.4 and 163.7°C. These points are attributed as melting points of polyethylene and polypropylene.

To conclude, pure and silica added PAN nanofiber webs are thermally more stable than the commercially available microporous membrane (Celgard 2020).

4.7.4 Thermal Stability

Microporous, pure PAN and silica added PAN after thermally treated for 36 hour at 120 $^\circ$C is given in Figure 4.13. Microporous membrane lost its spherical shape under heat and it took ellipsoid shape. The reason for this change is attributed to the fact that microporous membrane is produced by stretching method under high temperatures then it stabilized at low temperatures. Therefore, it regains its former shape under high temperatures. Pure PAN nanofibers keep their spherical shape, however specimen lost 16% of its initial diameter in average after 36 hour thermal treatment.
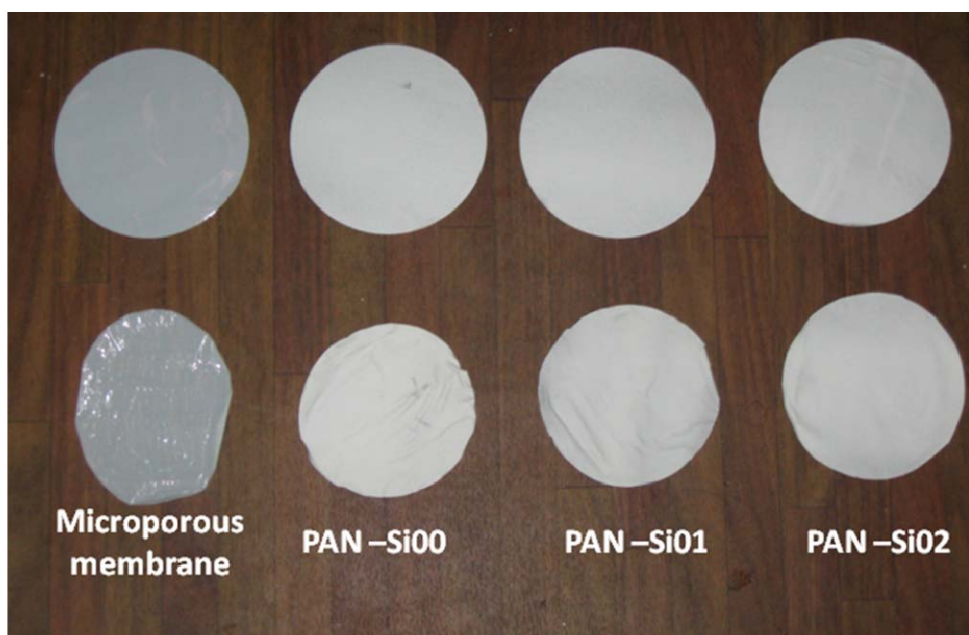
Figure 4.13 : Microporous and nanofiber membranes after thermal treatment with control membranes.

Adding silica to PAN nanofiber improved the thermal stability of PAN nanofiber web as it is verified with DSC analysis. Nanofiber web obtained from 1 wt% silica added PAN/DMF solution, coded as PAN-Si01 kept its average diameter value 5% more than pure nanofiber web.
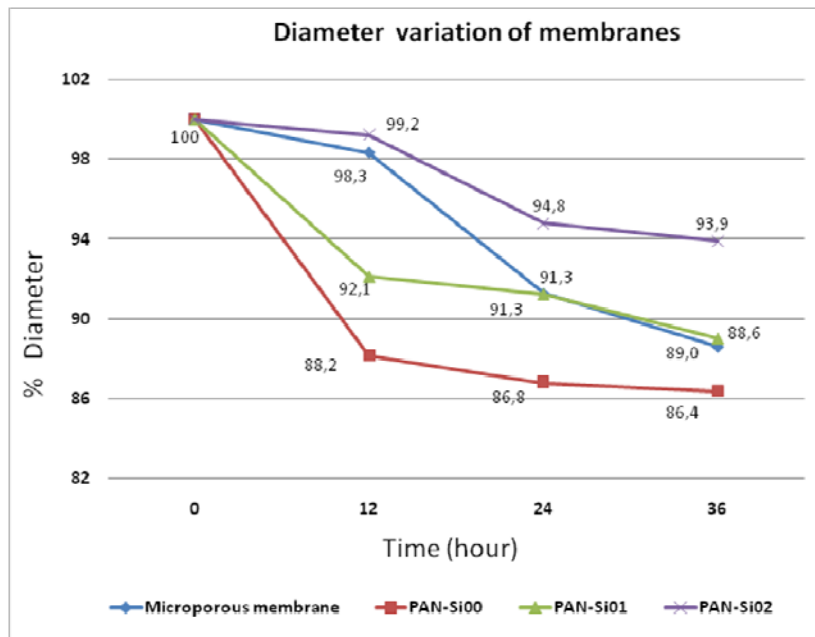
Figure 4.14 : Average diameter variation of membranes during thermal stability test.

Finally, PAN-Si02 specimen that was electrospun from 2 wt% silica added PAN/DMF solution gave the best results. Average diameter of PAN-Si02 nanofiber membrane decreased to 93% of its original diameter after 36 hour thermal test, which is also more stable than commercial microporous membrane.

Average diameter variation of membranes during thermal test is shown in Figure 4.14

5. DESIGN AND MANUFACTURE OF INDUSTRIAL ELECTROSPINNING PILOT MACHINE

5.1 Introduction

In this section of this work, the main aim is to design and manufacture an electrospinning pilot unit for commercial membrane material production. To realize this purpose laboratory experiments, pilot designs and optimization of the pilot electrospinning unit were done.

5.2 Laboratory Scale Experiments for Industrialization of Electrospinning

Before design and manufacturing pilot electrospinning machine, electrospinning tests are conducted in order to figure out the principles of the machine system. The aim of these tests is to reply questions below:

- How does one jet work in electrospinning process?

- What are the necessary parameters for electrospinning process?

- What are the requirements while working with multi jet electrospinning process?

- What are the optimum conditions for increasing production of electrospinning?

5.2.1 One needle electrospinning experiments

For the primary experiments, a one-needle electrospinning set-up is constructed by utilizing early electrospinning set-ups given in the literature. In these experiments 7.5 wt% PVA/water solution was prepared.

Main requirements for electrospinning process were provided by constructing three main component of electrospinning setup

- **High Voltage Power Supply:** A high voltage DC power supply (Gamma ES 100 model) is used for one needle electrospinning set-up which generates up to 100 kV voltage values. Power supply device has two display panels for

voltage and current. Voltage can be manually adjusted and current panel shows the output current of the machine. In addition, power supply can generate maximum 200 µA, so it totally has 20-watt capacity.

- **Solution Feeding System:** Syringes and needles were used which are usually preferred in the literature because of practical and economical properties of them. In order to feeding solution to the electrospinning section with regular control, a syringe pump (Asena GH model) is used. Device can pump solution with 0.1-150 mlh^{-1} flow rate by applying maximum 100 mmHg pressure, also it recognize 5, 10, 20, 50 and 60 ml syringes automatically.

- **Collector:** Aluminum plate is preferred because of high conductivity; it is a cheap material, which can be found in various shapes.

Some process parameters such as voltage, collector to needle distance, flow rate, needle diameter, and position of electrospinning with respect to gravity have been observed with one needle electrospinning system. As a result of these observations, for one needle electrospinning system, PVA/water solution can be regularly electrospun under conditions 12 cm needle to collector distance, 1 ml/min flow rate and 20 kV electric voltage. In this conditions flow rate and voltage are balanced for 0,4 mm inner diameter of needle. If flow rate is reduced, this balance collapses and the needle is clogged.

5.2.2 Multi needle stationary electrospinning set-up

The aim of multi needle electrospinning experiments is that optimizing process parameters such as needle to collector distance, voltage with increasing needle number, observation of path of jets, nanofiber collecting areas and morphological properties of electrospun fibers. In this sense, experiment apparatus is constructed as below (see Figure 5.1).

- 1 mm diameter of holes a were made with 10 mm spaces on 200mm*200mm aluminum plate

- 25 mm PS foam was placed under aluminum plate

- 250 mm diameter aluminum was used as collector
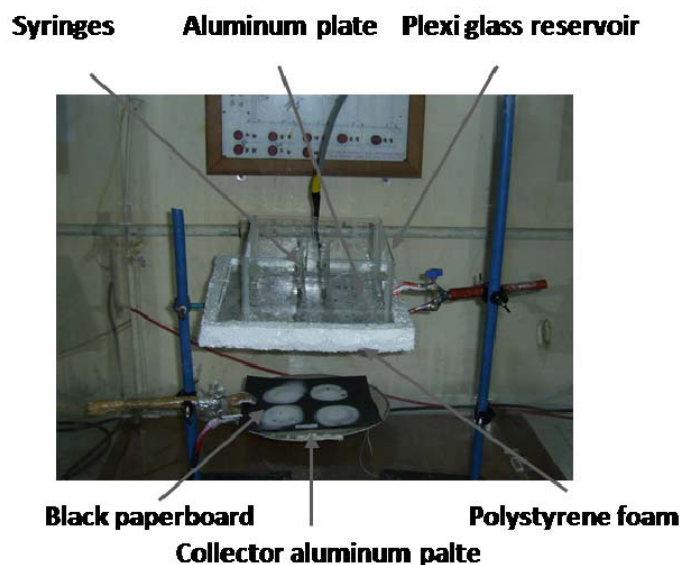
Figure 5.1 : Multi needle electrospinning set-up.

7.5 wt% PVA/water solution is electrospun with 2,4 and 9 needles at 12 cm needle to collector distance in multi needle electrospinning experiments. In this experiment flow rate is adjusted gravimetrically. Production times are observed where total solution volume ejected to system per needle and voltage is applied at a constant value. Results and parameters of these experiments are given in Table 5.1.

Table 5.1 : Results of multi needle experiments.

Parameters and results	2 needle	4 needle	9 needle
Voltage (kV)	25	25	25-30
Needle to collector distance (cm)	12	12	12
Needle spaces (cm)	4	4	2
Production rate (mlmin^{-1})	0.0140	0.0140	0.0135

The most important result of this experiment is that electrospinning jets and electrospinning collecting areas do not mix together. Even though distance between needles is reduced to 2 cm, jets repel each other and they do not produce a homogeneous nanofiber mat with 9-needle electrospinning set-up. The reason of this that jets charged with same polarity repel each other, so they are collected as unconnected nanofiber webs. This phenomenon is one of the biggest problem for industrializing the electrospinning process. In order to increase production rate. Number of needles and needle density must be raised, however effect of electrostatic forces on jets do not permit the increasing needle number. Nanofiber morphologies obtained from this experiment are given in Figure 5.2 below.
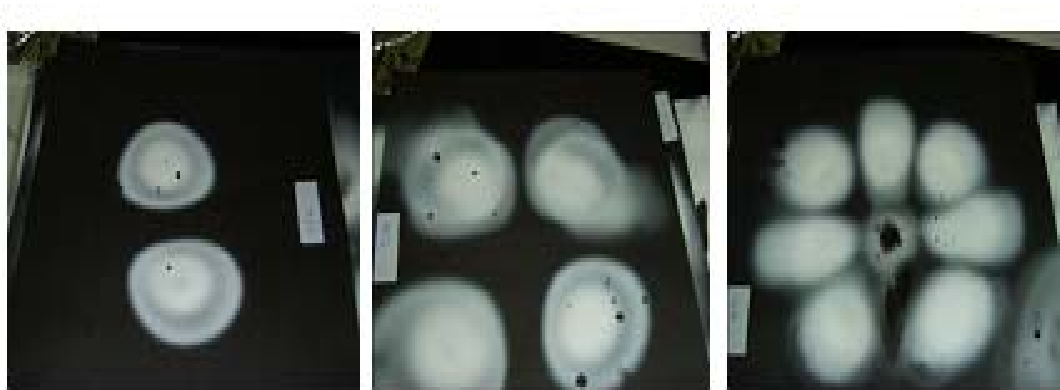
Figure 5.2 : Nanofiber webs produced by 2,4 and 9 needles.

Even though needles were positioned at a narrower area, wider nanofiber webs were collected as a result of repellency of each jet to others. In 9 needle electrospinning experiment with 2 cm needle density, because the central needle was constricted from other jets, central needle could not find enough area for electrospinning process, thus electrospinning for central needle can not be achieved. SEM photographs of nanofiber webs obtained from PVA/water solution are given in Figure 5.3.
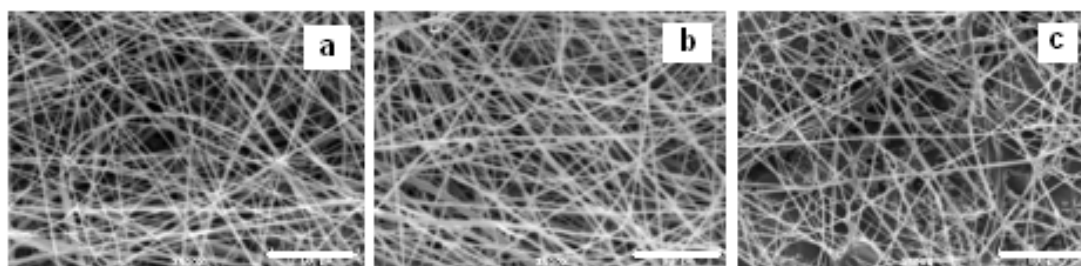
Figure 5.3 : SEM photographs of nanofibers produced by multi needle electrospinning set-up a) 2 needle b) 4 needle c) 9 needle.

5.2.3 16 Needle Electrospinning Set-up Supported Conveyor Belt

Because, jets do not mix or make entanglements, a homogenous web can not be produced by stationary electrospinning set-up. This problem can be solved by making needle system or collector shifting. For this purpose, next experiments were conducted with an electrospinning set-up having a conveyor belt system as collector (see Figure 5.4).

For 16-needle electrospinning set-up, an aluminum collector plate having 400 one millimeter-diameter-holes is manufactured. Distances between holes are 10 millimeter as shown in Figure 5.5.
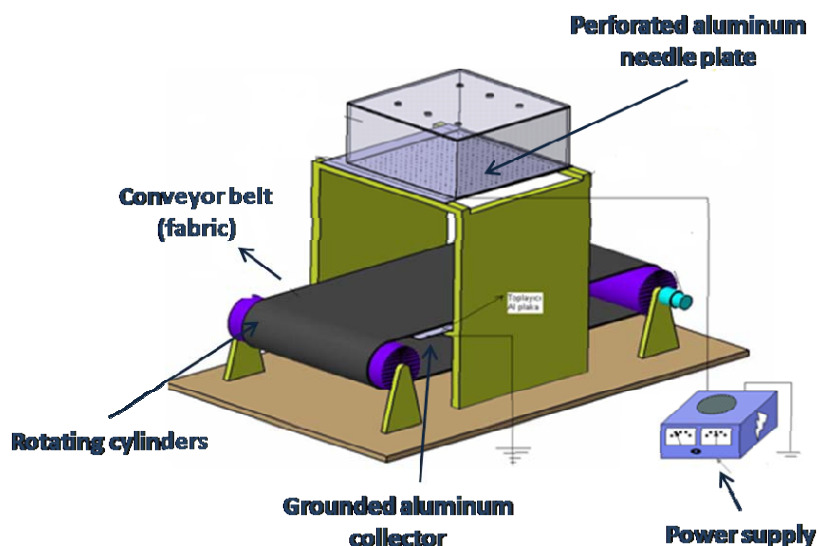
Figure 5.4 : 16 needled electrospinning set-up.

Purpose of manufacturing this plate is that observing interactions between charged needles and jets during electrospinning, also fabricating a homogeneous nanofiber web. That collector plate is located on the top of electrospinning set-up. At the bottom, a conveyor belt system is installed as a substrate material. A nonwoven fabric is used as a substrate which is driven by two rotating cylinder like a conveyor system. An aluminum plate is installed inside of conveyor fabric. As nanofiber accumulating on conveyor fabric, each needle row consists of four needles are shifted 1 cm, in order to inhibit overlapping of spinning jets.
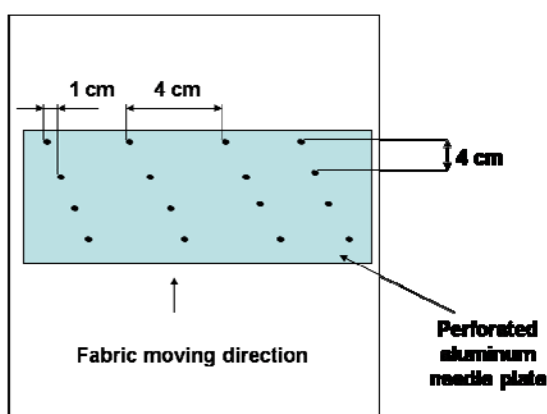
Figure 5.5 : Schematic diagram of needle positions.

Production of four nanofiber product was planned on this electrospinning set-up. 15 wt% PA 6/formic acid solution was used for nanofiber production. Without an external feeding system, flow rate was provided by gravimetric flows. For this purpose, syringes were loaded as much as their capacity. SEM images of produced nanofiber webs are given Figure 5.6.
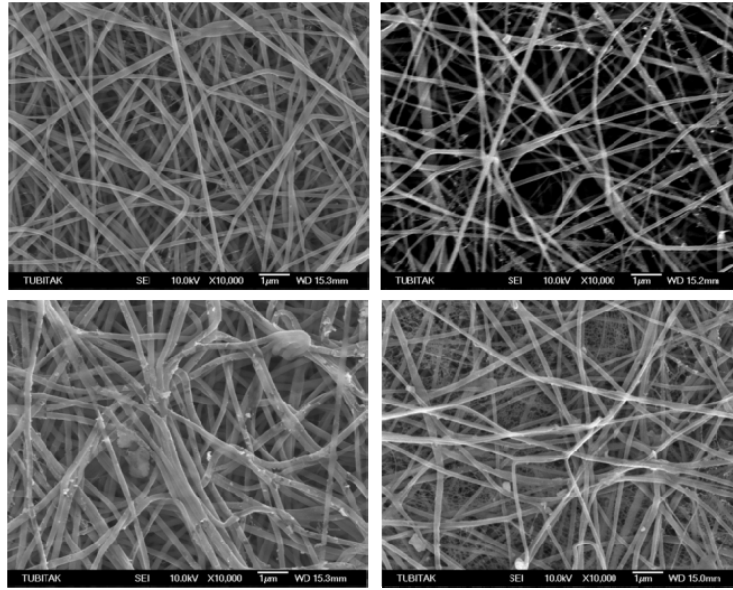
Figure 5.6 : SEM images of PA 6/formic acid solution electrospun on 16 needle-
conveyor belt system.

As a result of experiment, nanofibers that have average diameters about 200 nm were produced. Because feed rate was not control regularly some defects occurred on nanofiber web (see Figure 5.7). In addition, homogeneity of nanofiber web was not provided because of not using a controllable feeding system.
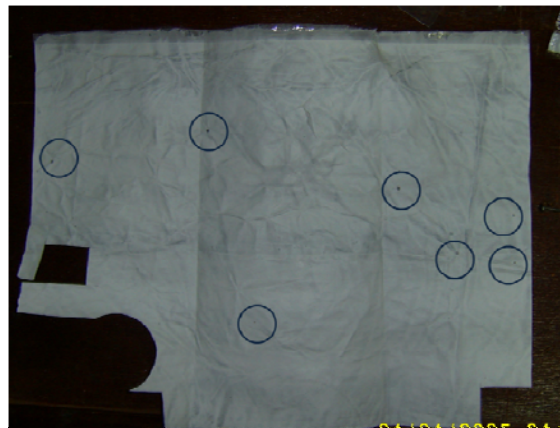
Figure 5.7 : PA 6 nanofiber web on nonwoven fabric, droplet defects are circled.

5.2.4 Bottom to up electrospinning set-up with 24 needle

In order to produce homogeneous nanofiber web and increase the production rate of electrospinning a 24-needle electrospinning set-up was manufactured, the set-up is seen in Figure 5.8). To increase homogeneity of nanofiber web needle layout was spread on the needle block. In this electrospinning set-up bottom-up nanofiber production was applied because of difficulties on controlling of feed rate for each

90

needle. Variations on flow rate of each needle can damage the web by electrospraying of micro or macro droplets on the electrospun web.
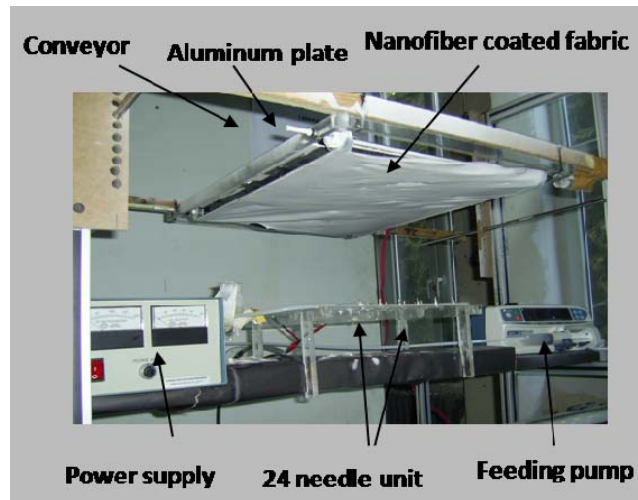
Figure 5.8 : 24-neddle electrospinning set-up.

By bottom-up electrospinning set-up, deformations on the nanofiber web were minimized protecting web from dripping or spraying solution. In the collector part of electrospinning set-up a grounded aluminum is positioned in the continuous a spunbond nonwoven fabric which is also used as a conveyor system. On the counter side of electrospinning system, needles were charged with positive high voltage. By this way, a potential difference is generated between needles and collector.

In addition to 16-needle electrospinning, set-up a feeding pump was used in order to control feed rate. That syringe pump can eject polymer solution with 0.1 milliliter/hour sensitivity.

Observations of this electrospinning set-up are stated below,

- In order to produce nanofiber by electrospinning system voltage, flow rate and needle to collector distance should be adjusted well that is parallel to our experiences that are gained by one needle electrospinning system and information in the electrospinning literature. For the solution of 15% TPU/DMF used in experiments, a collector distance higher than 150 mm and voltage higher than 30 kV are necessary.

- If nanofiber production is realized by grounding one of polar such as needle or collector, grounding must be done well in order to generate better electric field between needle and collector.

- Distance between needles and needle to collector distance are important for drawing, elongating and solidification of polymer jet. Materials used as substrate directly affect electrospinning process or surface morphology of manufactured electrospun product. So, substrate materials should not disrupt charge transmission between needle and collector and contact between substrate and collector plate or cylinder should be homogenous on every point. Irregular air gaps between collector plate and substrate or disorders on the collector plate can result in line faults or inhomogeneous web density from point to point.

- Irregularity of flow rate, which is fed to the each needle, disrupts the homogeneity of nanofiber web or results in clogging some of needles and leaking some of them.

5.2.5 100-Needle Electrospinning Set-up

A 100-needle set-up was designed in order to test the 100-watt power supply if it can endure multi needle electrospinning (see Figure 5.9). 20 needles were constructed on a 10-millimeter-dimater polyethylene pipe. 40 mm space was replaced between every two needles. By preparing five item of that configuration 100 needle set-up is obtained. Needles are connected together by a copper cable, and positive potential is applied by this cable from power supply. Polyethylene pipes are fixed on a plexi glass construction, which has pipe channels. Distance between pipes and channels were 100 mm.
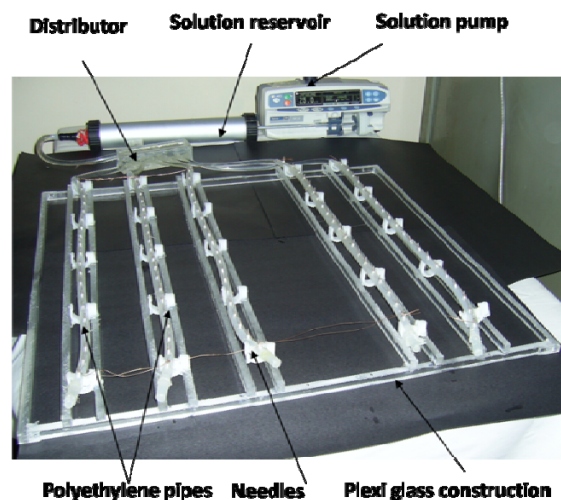
Figure 5.9 : 100-needle electrospinning set-up.

In order to feed the solution regularly, a syringe pump was used with a solution reservoir. In addition, a distributor was designed to distribute solution, which is fed from solution reservoir to five pipes. Plexi glass construction was designed for five pipes and bottom part of pipes on the construction kept open-air structure.
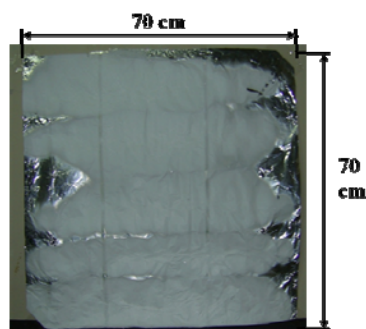
Figure 5.10 : Nanofiber layer produced by 100-needle system on aluminum foil.

If bottom of pipe is closed, solution leaked from needles can cause discharge of charged solution. Thus, electric losses were prohibited. For this electrospinning set-up, there was no moving collector system was used. Nanofiber production was realized by bottom to up electrospinning.

Electrospinning experiments were conducted systematically. Polyethylene pipes are connected to the electrospinning system one by one. At first, 20 needle then consequently 40, 60, 80 and 100 needles were operated. A 70x70 cm aluminum foil is used for this experiment as collector (see Figure 5.10). 15% wt PVA/water solution was electrospun in this electrospinning set-up. Nanofiber web having five rows produced by 100-needle set-up is shown in Figure 5.10. Applied voltages at 15 cm needle to collector distance are shown in Table 5.2 for every polyethylene pipe added to the electrospinning system.

Table 5.2 : Effect of number of needle on required minimum voltage.

Number of needle	Applied Voltage (kV)
20	30
40	33
60	35
80	39
100	41

Here, with increasing needle number applied voltage must be increased as shown in Table 5.2. In theory, needles are connected in parallel and they consume same

energy. If there is no electric losses a 100-watt power supply easily works 100 needle electrospinning set-up. However, with increasing needle discharges from system to air and other spare parts of system limits the usage of power supply. Therefore, electric insulation on the electrospinning system should be well organized.

5.3 Pilot Electrospinning Machine

Before design and manufacture of pilot electrospinning unit, principle of system was carried out by support of some experiences and results of previous experiments on multi needle electrospinning set-ups. Main properties of the pilot electrospinning unit are described below:

- To industrialization of electrospinning system, needle or needless configurations are available. Most of needless systems do not have solution feeding control. Because of the disadvantageous of needless electrospinning set-ups, an electrospinning set-up consists of 416 needles were expected to construct. 26 needle blocks, each of them has 16 needle were planned to design.

- To carry out potential difference between needle blocks and collector, a steel conveyor was placed in the primary designs of pilot electrospinning machine. A rotary steel collector was preferred, because potential difference between the collector and needles generates frictional forces between substrate fabric and metal collector. In order to eliminate the problem a special steel conveyor was designed which is also durable to rotation around cylinder. So any fabric having any strength can be used as a substrate material for electrospun nanofibers.
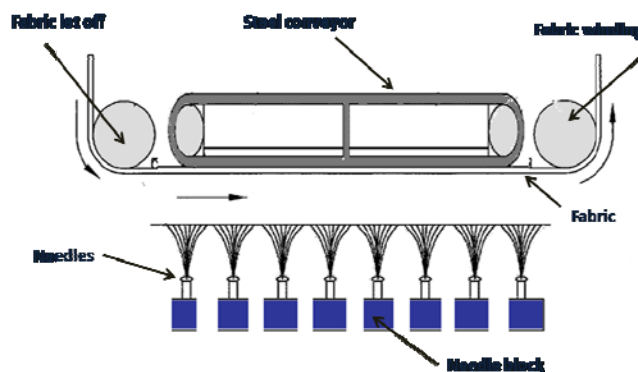
Figure 5.11 : Primary designs for pilot electrospinning machine.

- To realize continuous electrospun nanofibers production a fabric let off and fabric take up system was thought for substrate material. In this configuration, the biggest problem was adjusting the fabric velocity for suitable nanofiber density.

Working principle of pilot electrospinning is shown in Figure 5.11.

5.3.1 Main Frame

It is ideal that main frame of pilot electrospinning should be plastic material because of providing electrical insulation, however plastic materials store static electric on their surface and they lose their mechanical properties under tension load. Thus, sigma aluminum profiles were used for the main frame of electrospinning machine (see Figure 5.12).

Figure 5.12 : 3-D design and photograph of mainframe.

Aluminum profiles, which can be supplied in different size, provide easiness for the aspect of assembly, but aluminum frames have risk of discharging originated from electrospinning zone of the pilot machine during nanofiber production process. Therefore, S-suitable spaces were carried out to solve discharging problems and insulate the frame from electrospinning area of the machine.

5.3.2 Solution Transfer System

A few alternatives were thought for solution transfer system. These are:

- **Needle Block System:** That solution transfer system is constructed from an enclosed solution reservoir on which needles are fixed. Size of needles and position of each needle should be determined and designed well before manufacturing of needle block (see Figure 5.13). A disadvantage of this

system is that it is not practical and flexible. On the other hand, flow rate homogeneity of each needle becomes very good if needle blocks are suitably manufactured. Replacing of one or a few needle blocks easier instead of tens of needles.
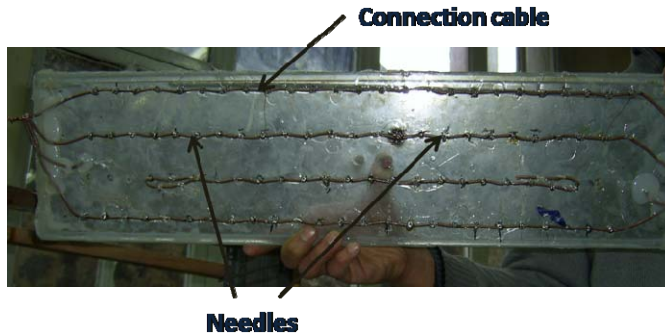
Figure 5.13 : Needle block consists of 100 needles.

- **Solution Reservoir System:** In this solution transfer system, solution is taken from a reservoir without any solution feeding mechanism and it is transferred to electrospinning area. Using a smooth or rough cylinder that immersed into the reservoir, generating droplets on the surface of solution by giving vibrations to the solution reservoir, replacing needle blocks into the solution reservoir in order to generate droplet by utilize of cohesive forces are the main ways to realize electrospinning process without using any controllable feeding system. In this reservoir system there is no possibility of stopping the system because of clogging or flow rate irregularities. However, adjusting of desirable feed rate is very difficult. Increasing the production rate of a developing pilot machine, which has a reservoir solution transfer system, is very difficult.

- **Pipe-Needle System:** This solution transfer system consists of pipes that have a length equivalent to the machine width. Needles are constructed on these pipes in specific spaces. Pipe-needle system can be positioned in any configuration through the machine length. This solution transfer system is very advantageous because of its producibility, low cost and flexibility properties. Difficulty of feeding to each needle on a pipe with same rate is a disadvantage of pipe-needle system.

These three alternative systems were considered, so pipe-needle system was selected. Distance between each needle has determined as seven centimeter by taking account of previous experiences on multi needle electrospinning experiments and optimization practices that would be carried out when pilot unit is constructed.

For the pipe material, PTFE was selected, because PTFE has high dielectric strength, is durable to most aggressive solvents and chemicals, protects its shape long time, is easily processed, it is economic and it is practical. One disadvantage of PTFE pipe is that it necessitates support columns under it when it is placed in the pilot machine because of its flexible structure. During the electrospinning, because solution is indirectly charged, electric power losses appear. Thus, in order to minimize the electric losses diameter of pipe was minimized as much as possible. Size of pipe was chosen as 8 mm for inner diameter and 16 mm for outer diameter. Properties of PTFE pipe are given in Table 5.3.

Table 5.3 : Properties of PTFE pipes used in pilot machine.

PROPERTIES	TEST METHOD	UNIT	PTFE
Specific Gravity	ASTM D 1457/18	$grcm^{-3}$	2,14-2,2
Usage Temperature	-	°C	-260/+260
Melting Temperature	ISO 3146	°C	325-330
Brittleness Temperature	-	°C	-200
Pulling Strength	ASTM D- 1708	$kgcm^{-2}$	250-300
Elongation Upon Breaking	ASTM D- 1708	%	250-300
Resistance To Stroke	ASTM D- 256	$cmkgcm^{-1}$	15,5
Shore D Hard	ASTM D- 2240	-	53-57
Deformity Under Load 230 °C, 1day, 140kgcm⁻²	ASTM D- 621	%	9,5-11
D-Electric Resistance	ASTM D- 149	$kVmm^{-1}$	50-80
Thermal Conductivity	ASTM C- 177	$kcalcm^{-1}°C^{-1}hour^{-1}$	0,035
Thermal Expansion	ASTM E 831	$10^{-5}°C$	12-14
Inflammability Temperature	ASTM D- 1929	°C	530

Needles installed on pipes were designed as a shape, which minimize clogging, electrical losses, and irregular flow rate. For needle pipe system, the smaller needle diameter makes the flow rate more regular for each needle. On the other hand, needle diameter should be as large as possible in order to minimize the clogging. These factors were considered, so needle was designed as shape in Figure 5.14.
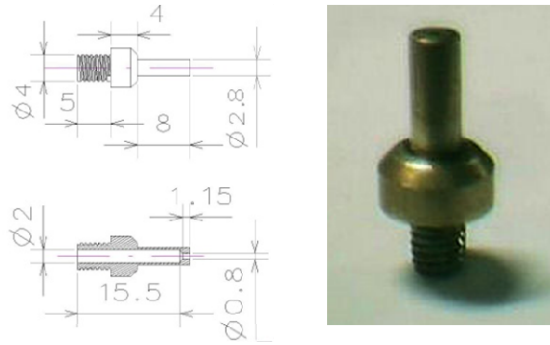
Figure 5.14 : Technical drawing and photograph of brass needle.

As it is seen in the drawing of brass needle, length of needle is 17 mm, outer diameter is 2.8 mm, inner diameter is 2.0 mm and hole diameter of needle is 0.8 mm. Needle was manufactured by CNC turn bench, it is pluggable, cleanable, it should be durable to aggressive chemicals, so it was manufactured from yellow brass.

Figure 5.15 : PTFE pipe-needle solution transfer system.

In order to get effectively 100 cm product from the pilot machine length of PTFE pipes are adjusted to 120 cm. Thus, 16 needles can be settled on a PTFE pipe as shown in Figure 5.15.

5.3.3 Solution Feeding System

A solution feeding system is necessary because of that solution transfer system has been chosen as pipe-needle system. A peristaltic pump was assembled to the pilot machine which replies requirements stated below.

- **Flow rate:** Needle-pipe system for pilot machine contains 16 needles for each pipe. It was understood by multi needle experiments that each needle has approximately 1 ml/h flow rate capacity. Therefore, a pump, which can create

16 ml/h flow rate at least, can be qualitatively sufficient. Having flexibility of chosen solution feeding system can be advantageous for oncoming optimization experiments of pilot unit. The chosen pump can eject solution with 0.1 mlh^{-1} sensitivity.

- **Chemical durability:** Pump must be durable to aggressive chemicals, because hazardous chemicals such as DMF, DMAc, THF, formic acid, toluene is used to solve PU, PA, PAN, PVC polymers for solution electrospinning. In addition to this, any material such as oil, air contaminants, metallic particles that can change solution properties must not get mix into the solution at feeding zone. For peristaltic pumps, there is no directly contact between solution and components of pump.

- **Electrical insulation:** Electric voltage can indirectly affect the solution reservoir and pump parts via solution if there is no interruption on solution transfer system. Electrical and electronic parts should be insulated from high voltage area. For the peristaltic pump, there is no contact between electrical and electronic parts of pump and solution.

Specifications of peristaltic pump are stated below:

- **Speed:** 0.1 to 50.0 rpm, reversible

- **Speed Precision:** 0.1 rpm

- **Speed Control:** Membrane keypad

- **Display:** 3-digit LED displays current rpm

- **Analog Interface:** Start/stop and $cwccw^{-1}$ control

- **Power Supply:** AC 220 V 10% 50/60 Hz (standard)
  AC 110 V 10% 50/60 Hz (optional)

- **Power Consumption:** < 10 W

- **Operating Condition:** Temperature 0 to 40 °C, Relative humidity < 80%

- **Dimensions (L : W : H):** 176 :110: 115 (mm)

- **Drive Weight:** 2.2 kg
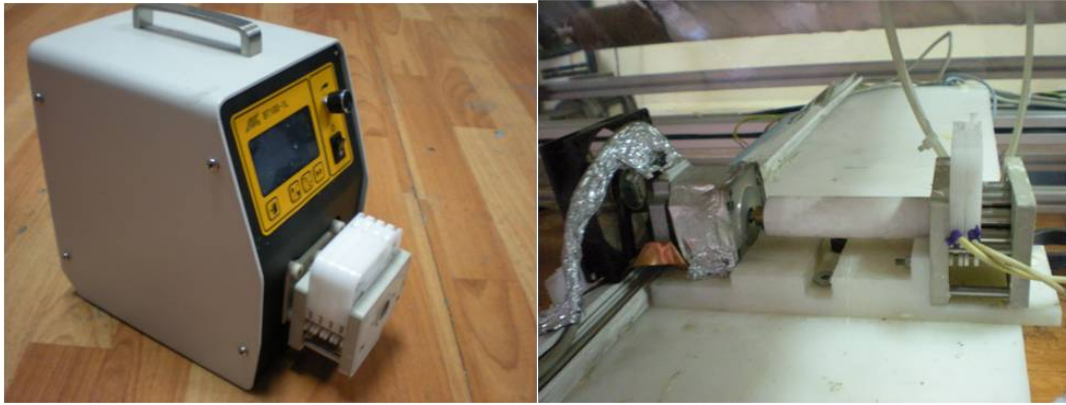
Figure 5.16 : Peristaltic pump and assembly of peristaltic pump for pilot system.
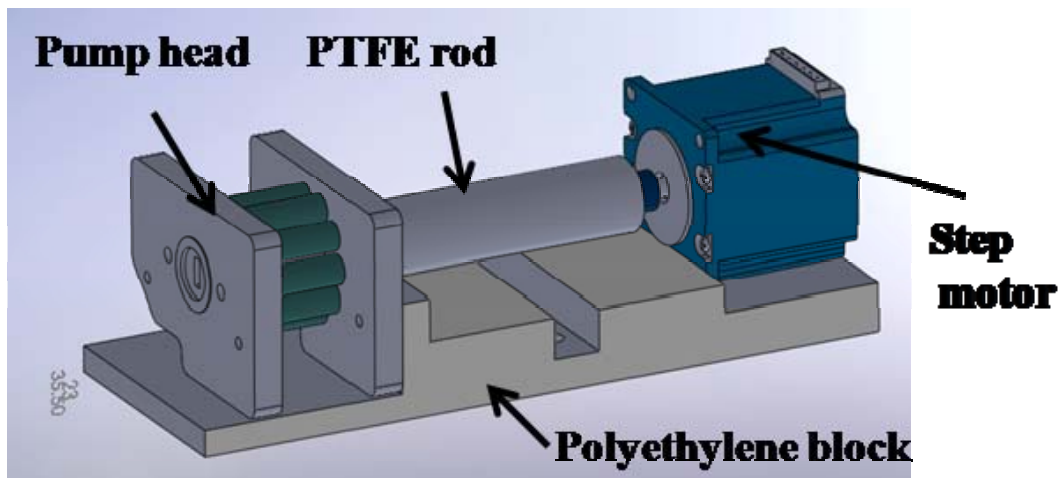
Figure 5.17 : 3-D design of insulated peristaltic pump head.

Because high voltage and magnetic field are existed in the pilot electrospinning machine, electrical and control parts of peristaltic pump was separated from working parts of pump. Head of pump was placed at bottom part of pilot machine. A polyethylene block was designed and manufactured to assemble pump head to the machine (see Figure 5.16 and 5.17).

5.3.4 Power Supply

The most crucial device of the pilot electrospinning system is power supply. High electric field is necessary in order to produce electrospun nanofiber on an area that spreads in 150x400 cm area. A high voltage and a grounded collector can be enough for one needle or small electrospinning units. A positive and a negative high voltage power supplies were used for pilot electrospinning unit to generate direct electric field. Specifications of power supplies were given in Table 5.4 and Table 5.5 below.

Table 5.4 : Specifications of positive-negative power supply.

Input voltage	220 VAC 50-60 Hz
Output voltage	Continuously adjustable from -100 to 100 kV
Regulation	0.05% for ± 10% line change
Ripple	0.1%
Size	5" (H) x 8" (W) x 10" (L)
Metering	Two analog meter read output voltage and output current
Power	20 watt

Table 5.5 : Specifications of positive power supply.

Input voltage	220 VAC
Output voltage	Continuously adjustable from zero to 60 kV
Regulation	0.05% for ± 10% line change
Ripple	0.1%
Size	43.6 mm (H) x 482 mm (W) x 478 mm (L)
Metering	Two digital meter read output voltage and output current

5.3.5 Collector

According to basic working principle of pilot electrospinning, machine collector was installed at the top of machine, and substrate fabric passes through between collector and needles, it is wound by winding cylinder. It was experienced by previous multi needle electrospinning systems that frictional force between substrate fabric and collector increases with increasing voltage. The frictional force can disturb surface regularity of fabric or it makes difficult to wind up the fabric. In addition to this, only high durability fabrics can be used as substrate material, low durability fabrics might tear under high frictions caused by electric field. To solve this problem, studies for designing of a system that substrate fabric and collector synchronously move. As a result of this study, a conductive conveyor system can solve this problem. Additionally, surface of collector should be smooth. Smoothness of collector directly affects the surface morphology of electrospun nanofiber. So collector should be homogeneously conductive and it homogeneously contact with the fabric.
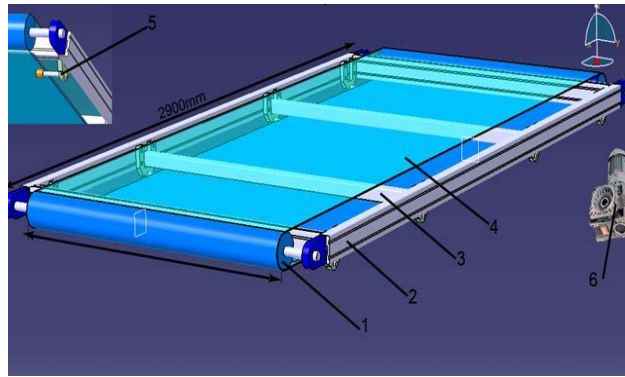
Figure 5.18 : 3-D design Steel mesh- aluminum plate collector.

1) Polyamide cylinder

2) 45x90 mm aluminum sigma profile

3) 45x45 mm aluminum sigma profile

4) Steel mesh

5) Compression pulleys

6) AC motor with reductor

Conveyor system, which had been designed, was not feasible because of economical and producible problems. So a movable conductive conveyor system was manufactured by using aluminum plate and steel mesh instead of steel conveyor system as seen in Figure 5.18. Though steel conveyor system is more efficient for electrospinning process, steel mesh-aluminum plate conveyor system was manufactured because of its low cost. However, steel mesh conveyor has a disadvantage that it must be accurately manufactured, because mesh can tear due to an axial fault of conveyor cylinders. The manufactured steel mesh-aluminum plate conveyor system brake down because of this problem.

Figure 5.19 : Conveyor system as collector.

Finally, a conveyor system containing an aluminum plate and two cylinders was used as collector part of pilot machine (see 5.19).

In pilot machine, negative high potential is applied to the aluminum collector. Therefore, collector must be well isolated from conveyor and mainframe of pilot unit. Aluminum collector plate was isolated from conveyor frame via using ultra high-density polyethylene plates. Specification of high-density polyethylene plate is given Table 5.6.

Table 5.6 : Specifications of high-density polyethylene used for electrical insulation of collector.

PROPERTIES	UNIT	DN	ISO	UHMW -PE
Specific Gravity	gcm^{-3}	53479	1183	0,93
Service Temperature	0 °C	53461	75	70
Melting Point	0 °C	-	-	130-133
Thermal Elongation	$K^{-1}10^{-5}$	53752	-	ca 20
Pull Strength	Nmm^{-2}	53455	527	³20
Pull Elongation	%	53455	527	20
Breaking Strength	Nmm^{-5}	53455	527	40
Breaking Elongation	%	53455	527	350
Stroke Resistance	kjm^{-2}	53453	179	-
Notch Stroke Resistance	kjm^{-2}	53453	179	210
Elasticity Module	Nmm^{-2}	53452	178	600
Water Sucking	%	53495	62	<0,02
Dielectric Resistance	$kVmm^{-1}$	53481	243	>45
Corrosion (Sand Slurry)	%	58836	-	100
Shore	D	53505		D60-70
Marble Notch 358/30	Nmm^{-2}	53456	2039-1	38

5.3.6 Fabric let off and winding system

In order to realize continuous production, a substrate fabric must be passed through the electrospinning zone and it must be stored by a fabric let off and winding system. Fabric let off and winding system was designed as connected to mainframe of electrospinning unit. Actuating the motion of fabric let off and winding system was realized by driving the fabric cloth batch from its surface, so speed of fabric motion is fasten up.
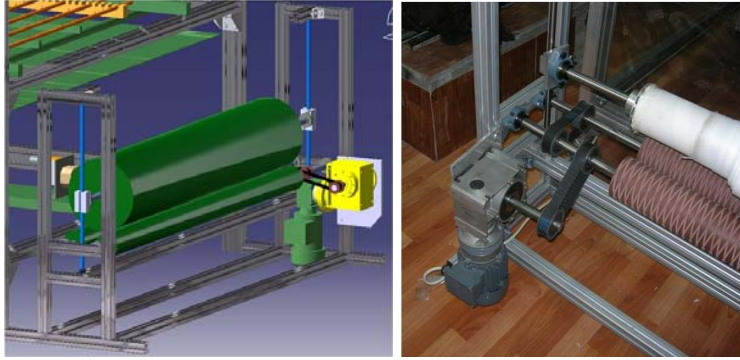
Figure 5.20 : 3-D design and photograph of fabric let-off and winding system.

Fabric speed is inversely proportional to nanofiber density on substrate fabric. Because the production rate of pilot electrospinning machine is not so high, fabric speed must be very slow which is about 1 m/minute and non-stop. To provide low fabric speed, rotation speed of an AC motor, which has 900 rpm, was reduced to required speed by using belt pulley mechanism, reductor and AC motor drives (see Figure 5.20). Motor drives were connected to control panel.

5.3.7 Solvent Exhaust System

Solidification of fiber jet in the solution electrospinning system is realized by evaporation of solvent from polymer-solvent system. At first, the pilot machine was designed consisting of 400 needles. If it is thought that each needle has 1 ml/h solution flow rate, which contains 10% polymer phase, 6 ml solvent, must be continuously removed from electrospinning zone of pilot machine in a minute. To remove solvent from electrospinning zone a pair of exhaust hood was designed which is installed on the top of machine.

(a)   (b)

Figure 5.21 : a) exhaust hood b) flexible aluminum ducts.

Two 2 m x 2 m stainless galvanization sheet iron exhaust hood was manufactured having shape of triangle prism. Two fans, which have 3 m^3min^{-1} airflow capacity, were used to transfer solvent. Connection between fans and exhaust hoods were provided by 20 cm diameter flexible aluminum spiral duct as shown in Figure 5.21.

5.3.8 Control Panel

Since high voltage exists on the machine during electrospinning process, electronic accessories must be electrically insulated from high voltage or they must be combined in an external control unit. A control unit was constructed to isolate electronic parts from high electric potential and control devices such as pumps, motor drives and high voltage power supplies from one panel.

A practical controlling system was designed by putting control units of some equipment stated below:

- 2 power supply

- 7 peristaltic pump

- 3 AC motor drive

- 2 control units for fan motors

Figure 5.22 : Control panel.

Voltage output cables of 100 kV power supplies were lengthened as much as they reach to the machine from the control panel. Mainframes of power supplies were installed in control unit. Voltage and current displays, on/off switches and voltage potentiometers were assembled on control panel door as seen in Figure 5.22 and Figure 5.23.
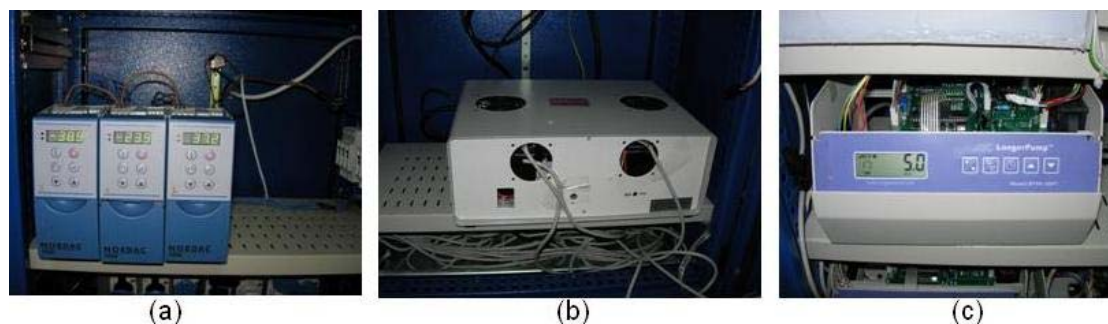
Figure 5.23 : a) Motor drives b) power supply c) peristaltic pump.

Moving parts of peristaltic pumps such as step motors and pump heads were removed from mainframe of peristaltic pump, and they constructed at bottom part of machine. Displays and control pads of pumps were installed on control panel door.

Three items of AC motor drives of fabric let off and winding system were installed in control unit to control them from one point (see Figure 5.23 (a)).

Switches of fan motors, which, are used to evacuation of solvent, are installed on control panel door.

All devices positioned in control panel were connected to main switch by passing through on one fuse for each one. In addition, an emergency button was assembled to the control panel.

5.3.9 Assembly of machine

Each system of machine was assembled into the main frame as shown in Figure 5.24 and Figure 5.25. Two fabric storing system one of them for let off and the other for winding was placed back and forth of the machine.

Conveyor collector system was fixed to the main frame by four shaft-linear bushing systems and two ball screws. By this configuration, collector has vertically 80 cm stroke. Pipe-needle systems are placed in to the machine on two blocks of polyethylene channels. 416 needles were assembled to the machine before production and optimization of electrospinning unit. Seven peristaltic pumps were

assembled under pipe-needle blocks onto a polyethylene block that have 80 mm thickness.
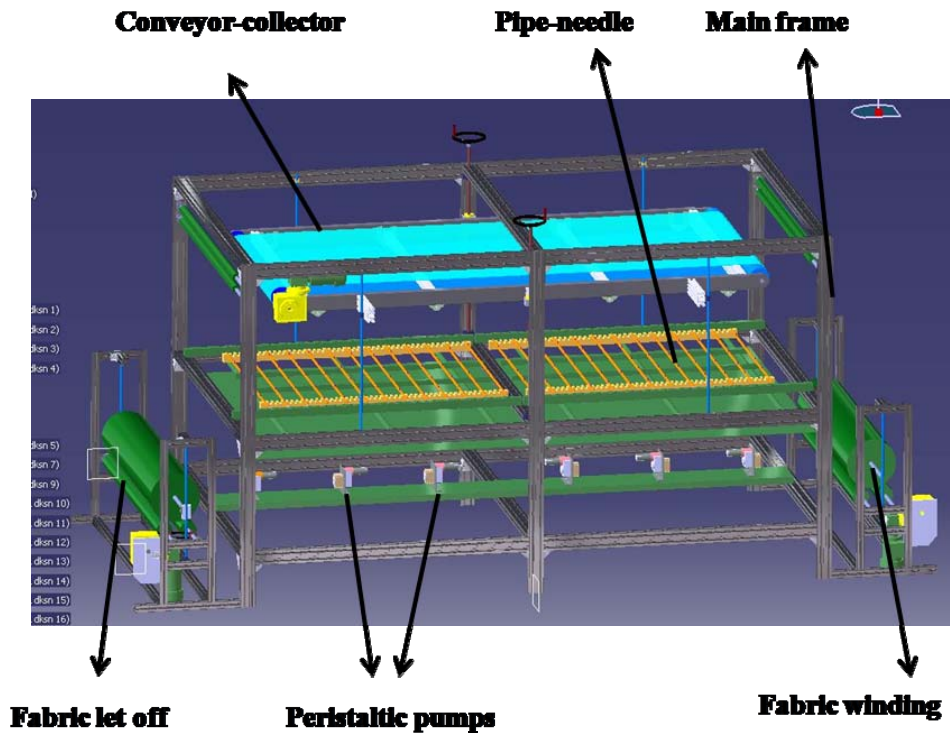
Figure 5.24 : 3-D design of assembled pilot machine.

Figure 5.25 : Photograph of assembled pilot electrospinning unit.

5.4 Electrospinning Process on Pilot Unit

To start electrospun nanofiber production by pilot unit, pipe-needle blocks were configurated to produce homogeneous nanofiber web. Needle-pipe blocks are dislocated, as any needle does not locate as one after another (see Figure 5.26). Another requirement for operating pilot machine is substrate material. Substrate material should be a little conductive for not permitting capacitance between charged aluminum collector and needles. Substrate material has 3.6 m^2 contact area with aluminum collector. When aluminum collector is charged with high voltage, strong frictional force generates between substrate and collector.

Figure 5.26 : Pipe-needle layout in electrospinning pilot unit.

During electrospinning process, substrate material can be torn if it is not resistant to high stress. In addition, elastic substrates do not keep their smooth surface when they move on charged aluminum plate. Therefore, a rigid substrate, which has high tensile strength, is preferable for making experiments on pilot unit. Fabric velocity adjusted to minimum speed, which was 0.2 mmin^{-1} to electrospun thicker nanofiber webs. Collector to needle distance was adjusted in respect of solution properties. Voltage and flow rate was adjusted online to control both parameters according to their potential and rate values. Fans were operated at high speed for efficient solvent removing. 60 grm^{-2} polyester spunbond was used as a substrate for nanofiber web.

Pilot electrospinning was operated with 416 needles at first, so each pipe-needle block was placed with 10 cm spaces. Inner diameter of a pipe is 8 mm and a pipe has 1200 mm length. To operate pilot unit with 416 needles, 9.2 liter polymer solution must be required.

Aliphatic polyether based polyurethane/DMF solution which has 15 wt% polymer content was obtained from Polychem Company. Polyurethane solution has 750 cP viscosity value.

Many experiments were conducted on pilot electrospinning unit with polyurethane solution obtained from Polychem Company. Electrospinning jets were visible when setting adjustment of machine was carried out as stated in Figure 5.27 below.

- Needle to collector distance: 25-45 cm

- Flow rate: 2,15 mlh^{-1}needle^{-1}

- Negative voltage: (-10)- (-40) kV

- Positive voltage: 30-48 kV

Figure 5.27 : Electrospinning jets during electrospinning.

However, every experiment became unsuccessful producing nanofiber because of evaporation rate of solvent during solidification of electrospun jet. Solvent used to prepare solution of polyurethane has 153 $^{\circ}$C boiling point and low evaporation rate [114].
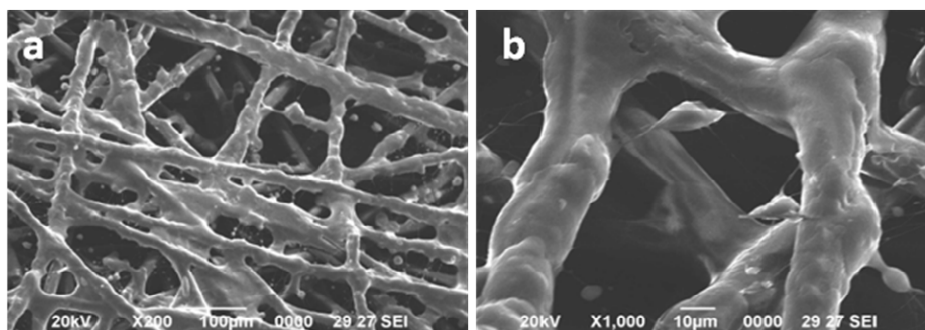
Figure 5.28 : SEM photographs of electrospun products from polyurethane solution on PET spunbond fabric a) 200X magnification b) 1000X magnification.

Electrospinning of this solution gave products in film form (see Figures 5.28 and 5.29) Therefore, mixed solvent systems were prepared for solving thermoplastic polyurethane pellets to increase evaporation rate of solution during solidification phase of electrospinning.
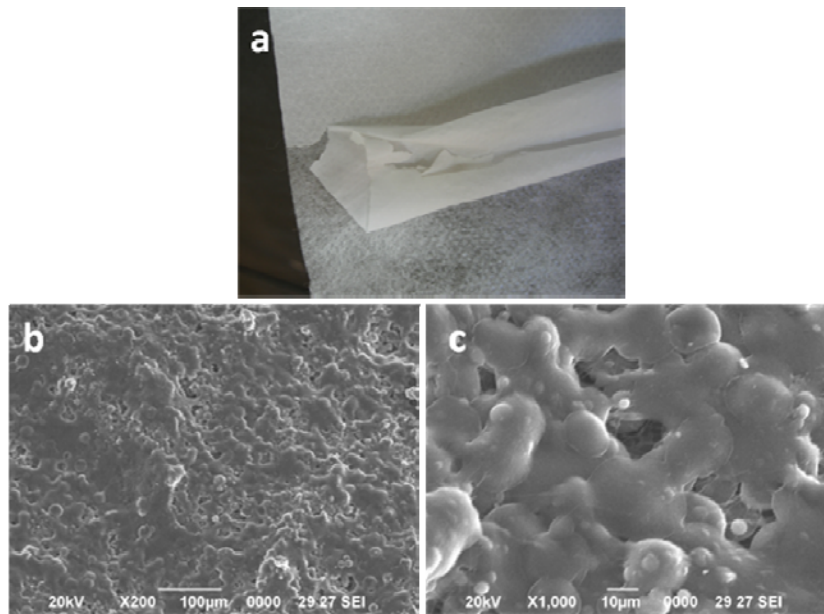
Figure 5.29 : a) Photograph of electrospun layer on PET spunbond fabric b) SEM photograph of electrospun layer at 200X magnification c) 1000X magnification.

Elastollan® B64D11 coded polyester based thermoplastic polyurethane pellets were obtained from ENPAŞ Ltd. and a variety of polyurethane solution which contains different mixed solvent systems at various proportions were electrospun on pilot unit.

- DMF/THF solvent system at 80/20, 60/40/, 50/50and 40/60 ratios

- DMF/DCM solvent system at 80/20, 60/40, 50/50 and 40/60 ratios

- DMF/ethyl acetate solvent system at 80/20, 60/40, 50/50, 40/60 and 30/70 ratios

Mixed solvent systems above were experimented to produce electrospun nanofiber. However, in all experiments wet film layers were produced.

In the electrospinning process, whipping phenomena plays important role on elongation and solidification of polymer jet. Polymer jet goes through hundreds of meters path at a collector distance that can be expressed as a few centimeters by whipping action (see Figure 5.30). Whipping action can be controlled with adjustment of polymer solutions or process parameters.
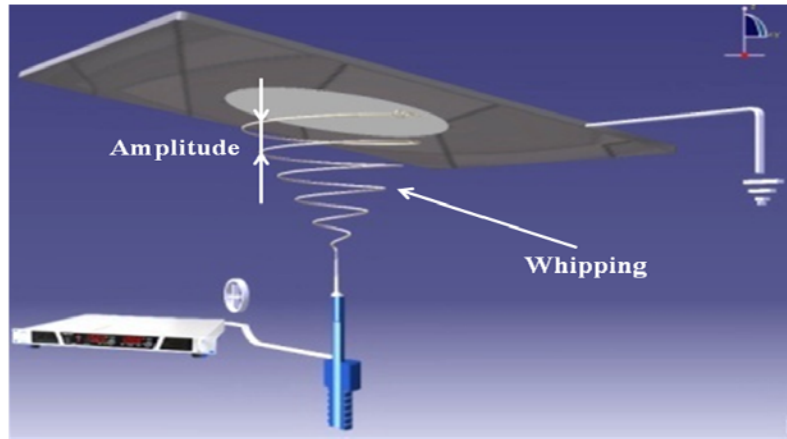
Figure 5.30 : Whipping action during electrospinning.

To increase solidification rate of polymer or evaporation of solvent from the jet, whipping action should form with high speed and low amplitude. That effect can be realized with increasing conductivity of jet by adding a bit of ionic salt compound to the solution. However, high salt content can disturb regime of jets and causes generating fiber bundles between the needles and the collector. These bundles quickly affect jets and can stop whole process on the machine.
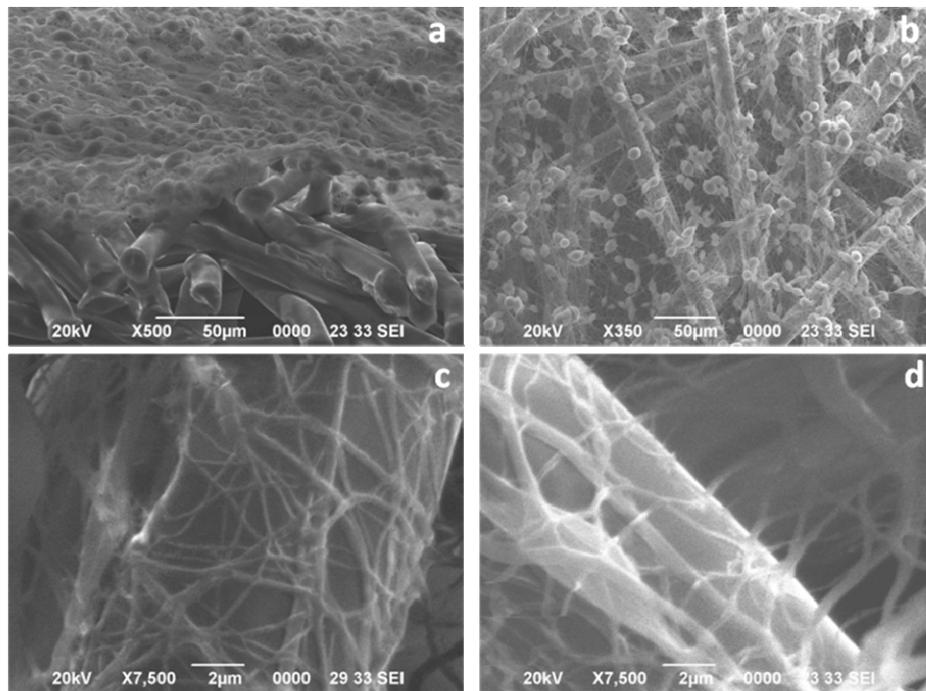
Figure 5.31 : SEM photographs of nanofibers electrospun by 0,005 % wt NaCl added PU/DMF solution.

To prepare more conductive solution 0.008 wt% NaCl was added to the solution, which was obtained from Polychem Company. Many experiments were conducted to optimize the electrospinning process of this solution, the parameters are given below.

- Positive voltage: + 48 kV

- Negative Voltage: - 12 kV

- Needle to collector distance: 27 cm

- Feed rate: 1.4 mlh^{-1} needle

In Figure 5.31, SEM photographs of electrospun PU solution are shown. Many bead defects, which were 5-8 micron diameter, are existed on PET spunbond substrate.

Diameter distribution of PU nanofibers are given in Figure 5.32, average diameter of fiber web is about 360 nm. Diameter distribution spreads from 150 nm to 600 nm. Nanofibers are not smooth and nanofibers adhere with each other on the contact points.
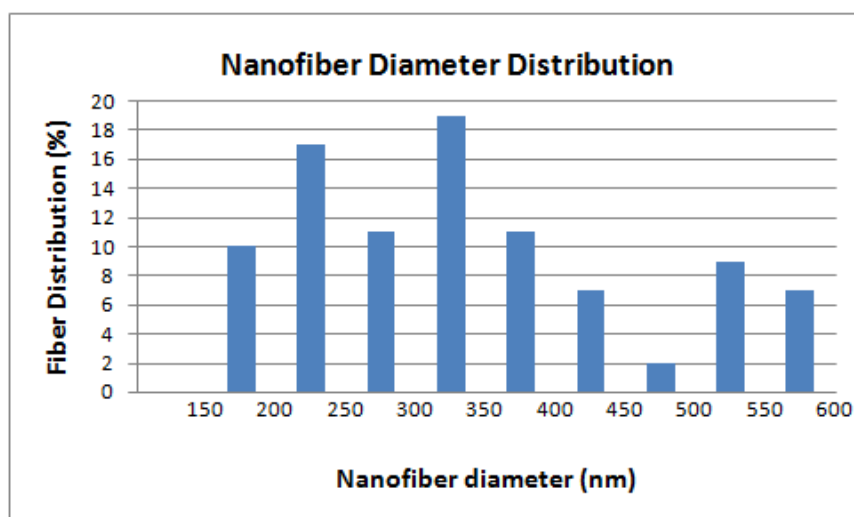
Figure 5.32 : Diameter distribution of PU nanofibers.

Another solution was prepared to minimize the bead defects on nanofiber web. 15%wt TPU pellets were solved in 85 wt% 3/1 ratio of DMF/ethyl acetate solvent blend. 0.008 wt% NaCl was added to the solution in order to increase conductivity. Optimal electrospinning conditions of that polymer solution are given below.

- Positive voltage: + 50 kV

- Negative Voltage: - 20 kV

- Needle to collector distance: 18 cm

- Feed rate: 1.9 mlh^{-1}.needle
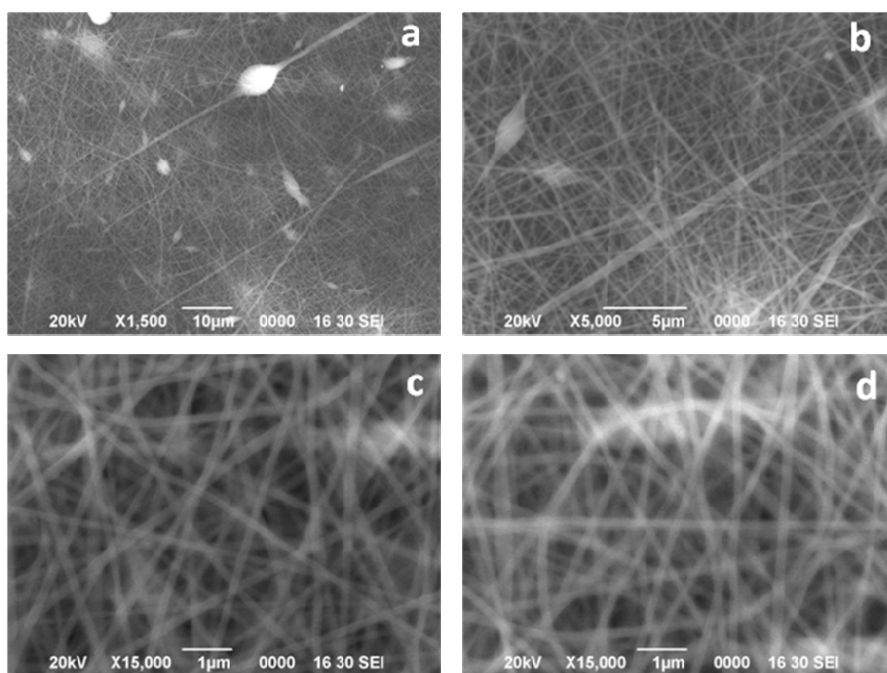
Figure 5.33 : SEM photographs of TPU/DMF/ethyl acetate solution a) 1500X b) 5000X c,d)15000X.
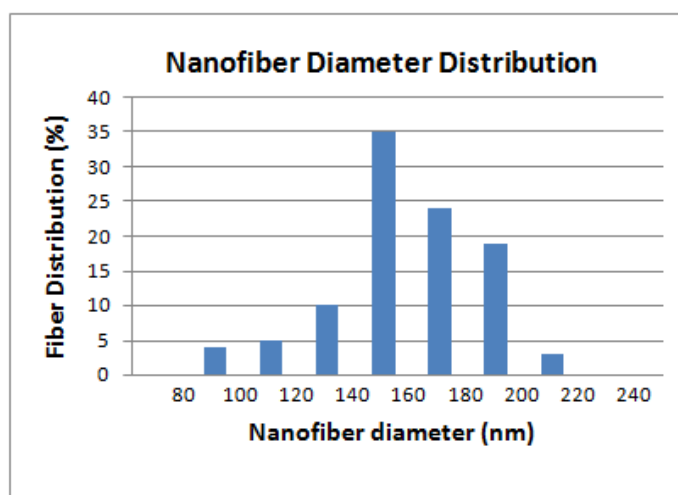
Figure 5.34 : Fiber distribution of TPU/DMF/ethyl acetate solution.

Table 5.7 : Optimization parameters of electrospinning on pilot unit.

Parameters	64 needle	128	256
Negative voltage (kV)	-24	-11	-16
Positive voltage (kV)	46,5	47	50
Needle to collector distance	19	16	18
Positive current (µA)	-200	-200	-200
Negative current (µA)	225	330	520
Feed rate (mlh^{-1}needle^{-1})	4.8	5.3	4.3

Diameters of nanofibers were well distributed and average fiber diameter was about 160 nm (see Figure 5.34). Dielectric constant and conductivity of ethyl acetate is higher than DMF, so fiber was produces smoother and thinner than other solutions (see Figure 5.33).

5.5 Modifications on Pilot Electrospinning System

Plastic pipe material was preferred for solution transfer system in the first design of the pilot machine because of electrical insulation properties of the PTFE material. Although plastic pipe-needle system satisfies expected properties such as chemical durability, electrical insulation and operating temperature, low glass transition temperature and low hardness properties of pipe made some difficulties.

To provide equivalent flow rate for each needle on a pipe-needle block, pipe must be gravimetrically balanced along its length. In addition to this, area under the pipes must be free in order to prevent electric loses and discharges. Elastic structure of PTFE pipe causes bending of pipe if any support material is not placed under pipes (see Figure 5.35). Though two blocks of polyacetal rods were constructed under PTFE pipes, sufficient flow rate regularity for each needle could not be realized. Therefore, aluminum tubes were installed to test of energy loses in the pilot machine as solution transfer system instead of PTFE pipes because of rigid structure of the aluminum tubes (see Figure 5.36). The test was conducted with ampermeter of the power supply. No difference was observed between the PTFE pipes and the aluminum tubes for energy loses. It was concluded that aluminum tubes can be used as solution transfer system if its electrical insulation from the main frame can be effectively achieved.

New needle-aluminum tube solution transfer system was manufactured with same size with former solution transfer system except inner diameter of tube, which is 11.5 mm. Needle-aluminum tubes were assembled on rectangular aluminum sigma profile frame by suitable connection equipments. To insulate frame of needle-aluminum tubes from mainframe of machine cast PA 6 rods were used. Four pieces of PA 6 rods, which has 100 mm diameter and 80 mm length, were assembled under bends of frame of tube needle as shown in Figure 5.37.

Figure 5.35 : PTFE pipe-needle block in pilot unit.

Figure 5.36 : Aluminum tube-needle block in pilot unit.
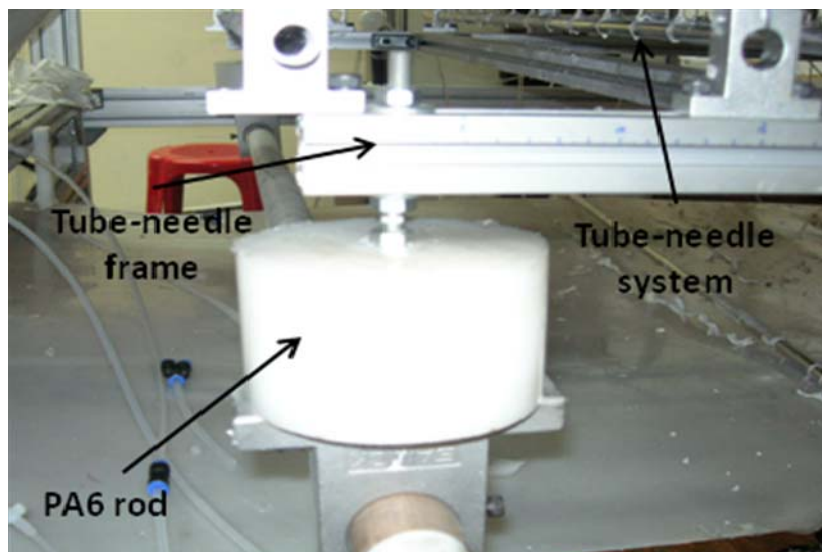
Figure 5.37 : Insulation of solution transfer system form main fame.

Modified solution transfer system provides regular flow rate during electrospinning process. In addition to this, copper tapes were used to connect needles on the PTFE pipe in the former solution transfer system. Because aluminum is conductive, it does not need any connection equipment to contact with needles.

6. OVERALL RESULTS, DISCUSSION AND RECOMMENDATIONS FOR FURTHER WORK

Research and development activities on nanotechnology have been continuously increasing. In parallel with this development, nanofiber production via electrospinning is an attractive topic of research. Nanofiber materials produced by electrospinning method, come into prominence with their high surface area to volume ratio and high porosity properties. In addition to these, nanocomposite materials can be easily produced by adding nanoparticles or nanorods into the continuous nanofiber structure by electrospinning method. In this work, nanofiber membranes, which may be defined as a product of nanotechnology, have been designed. Additionally, design and manufacture of a pilot unit for electrospun nanofiber web production were successfully carried out.

Despite the fact that the electrospinning process is an easily applicable and reproducible nanofiber production method at laboratory scale, the process is affected by numerous parameters which may be easily observed on large scale electrospinning set-ups. Solution viscosity, surface tension, solution conductivity, applied voltage, needle to collector distance and flow rate of the solution are the main group of these parameters. A jet of a polymer solution is converted into a nano-filament by a chaotic process influenced by these and additional parameters. This chaotic process named whipping instability of the polymer jet gives extreme properties to the final nanofiber product with respect to the fiber diameter. High surface area to volume ratio and high porosity are the significant examples of the phenomena. Nanofiber materials produced by electrospinning method are potential alternatives to selectively permeable products by small pore structures with high porosity.

Waterproof breathable membranes chosen as target products for this work have been designed and successfully produced. These types of membranes are used in daily clothes, shoes, sport clothes, building materials and demand for these types of materials continuously increasing. In order to produce such selectively permeable

barrier materials, different types of polyurethane solutions with various additives were prepared. Nanofiber webs were produced from the prepared solutions and they were tested. Nanofibers produced from polyester based thermoplastic polyurethane have smooth structures without bead. On the other hand, polyether based polyurethane and poly(methylphenylsiloxane) added polyester based polyurethane solutions give nanofibers with beaded structures. Nanofiber webs obtained from polyester based polyurethane solution without any additive have higher water penetration resistance than polyether based polyurethane nanofiber webs with no poly(methylphenylsiloxane) addition. Polyether based polyurethane nanofiber webs are able to bear a hydrostatic pressure of 18 cm water, while polyester based nanofiber webs are able to 62 cm water. On the other hand, poly(methylphenylsiloxane) added polyester based polyurethane nanofiber webs are able to bear a hydrostatic pressure of 250 cm water. So medium level water resistant breathable material were produced. A final product electrospun from poly(methylphenylsiloxane) added polyester based polyurethane solution and laminated onto a cotton woven fabric was compared with a commercially best selling waterproof breathable membrane having high water penetration resistance and water vapor transmission rates. Nanofiber web laminated woven product can be grouped in high water resistant materials even though it has not reached the water penetration value of the commercial product.

Water vapor transmission rates of designed nanofiber membrane has the same values as it is compared to commercial product named Gore-Tex® which is highly breathable. The other commercial material with trademark of Eurodach® has much less water vapor transmission rate than the polyurethane nanofiber membrane. In addition to this, increasing thickness of nanofiber web improves the water penetration resistance of the nanofiber membranes while water vapor transmission rate is not significantly affected from the thickness of the fiber web. It can therefore be concluded that this is the result of a fully open pore structure of the nanofiber web.

For some waterproof breathable products, the air permeability is an important requirement. The air permeability of nanofiber membranes is four times higher than commercially available membranes. The air permeability of a nanofiber web laminated cotton woven fabric by polyurethane hotmelt adhesive is low however, it

is higher than the commercially available barrier materials. A waterproof breathable product with these properties may be a potential candidate for membranes used in construction.

The other product designed within this work is a nanofiber battery separator material, which can be also categorized as a nanocomposite material. Commercially available battery separator materials have low porosity and durability problems under high temperatures. The experimental work has done with PAN/SiO$_2$ nanofiber membranes in order to produce highly porous and thermally stable membrane separators. Membranes contains nano sized fibers were successfully produced from 10%wt PAN/DMF solution with different silica content. Morphological, physical and thermal characterizations of membrane material were also carried out. An agglomeration of 21 nm silica nanoparticles is observed on nanofibers, though nanoparticles spread onto nanofibers, so approximately homogeneous separator material was obtained.

The air permeability of PAN/SiO$_2$ nanocomposite membrane is approximately 20 times higher than commercially available micro porous separator material. This means that porosity of nanofiber web is higher than micro porous membrane. Ideal properties of battery separator materials are small pore size, high porosity, selective permeability and thermal stability. The thermal properties of nanofiber membranes compared to the commercially available material gives better results. In fact, nanofiber web electrospun from 2 wt% silica added PAN/DMF solution shows better dimensional stability and total area protection than micro porous membrane separator under high thermal conditions.

The final section of this work is formed with experimental works directed towards industrialization of designed membranes and electrospinning process. The drawbacks of the industrialization of the electrospinning process are the use of very high voltage power supply, the difficulty in measuring the voltage values and inhomogeneous products. Laboratory scale electrospinning set-ups were designed and constructed in order to observe and remove these difficulties. Nanofiber production was successfully carried out on these electrospinning set-ups. A prototype unit of electrospun nanofiber web production machine was also designed and constructed by these results and data obtained from the electrospinning experiments conducted with

the small-scale set-ups. Prototype unit which has 2x2x4 m size can effectively produce 1 meter width nanofiber web.

After many optimization efforts on the electrospinning unit, the final electrospinning pilot machine accommodating 256 needles. Each of these needles can produce nanofiber filaments by consuming 0-5 mlh^{-1} polymer solution. The prototype unit was designed and manufactured with controls of solution flow rate, fabric velocity, voltage and solvent exhaust. The remaining short falls in the design and construction of the pilot machine may be stated as the electrical insulation, voltage discharges and flow rate variations.

Moreover, the adjustment of the solution properties loaded to the machine and configuration of the spinning system are the other requirements for efficient nanofiber production. Especially the viscosity, concentration, conductivity and the volatility of the solution, the distance between spinnerets, applied voltage to the spinnerets and the type of the collector are the parameters, which have to be adjusted accurately.

This work carried out under three main topics was successfully completed. In addition to these efforts, these recommendations for further work may be listed as follows:

- The performance tests of the waterproof breathable membrane were done only once for each specimen. To the improve performance properties of the material water penetration resistance, water vapor transmission rate of the material should be measured many times after use or after washing each specimen. Therefore, modification should be applied to the material after additional tests. In addition to this, poly(methylphenylsiloxane) is added to the thermoplastic polyurethane/DMF solution in order to increase water penetration resistance of the nanofiber membrane. Preparing the solution with suitable homogeneity is very difficult and phase separation of solution with time is the other disadvantage of the polymer/solvent/additive system. Nonhomogeneous solution or disruption of the solution homogeneity with time negatively affects the nanofiber web production on the pilot electrospinning unit. As a solution of this problem and as an alternative method to increase the water penetration resistance of nanofiber web, work

should be conducted with copolymers containing polyurethane and siloxane groups

- The battery separator material designed and manufactured from PAN/silica nanocomposite material accomplished porosity and thermal stability requirements of lithium-ion batteries better than micro porous membranes. However, silica nanoparticles have not homogeneously dissipated into the fibers. Various solution and process parameters should be experienced with more experiments. Agglomeration problem of nanoparticles should be solved by conducting more experiments. In addition to the tests completed with this work, electrical properties and mechanical behavior of nanofiber separator membrane should be measured and necessary optimizations on the nanofiber product should be applied.

- In the designed and manufactured pilot electrospinning unit, electrical insulation of the system should be improved by preparing vacuum chamber for the electrospinning area and making better insulation of electrical parts from the main frame to increase efficiency of the machine. In addition to this, one or two additional high voltage power supply should be added to the system to increase production rate of nanofiber web. A solvent recovery system should be adapted to the pilot unit to decrease the solvent cost and to reduce the emission of the solvent to the environment.

REFERENCES

[1] *<http://www.nanowerk.com/spotlight/spotid=1792.php>*, accessed at 11.12.2008.

[2] *<http://www.nanowerk.com/spotlight/spotid=1328.php>*, accessed at 11.12.2008.

[3] *<http://www.ml.com/media/14504.pdf>*, accessed at 11.12.2008.

[4] *<http://vienna.bioengr.uic.edu/RET/Reports/Final%20Reports/ZufanRETFinal Report.pdf>*, accessed at 11.12.2008.

[5] **Ramakrishna, S., Fujihara, K., Teo, W.E., Yong, T., Ma, Z.W. and Ramaseshan, R.,** 2006: Electrospun nanofibers: solving global issues, *Materials Today*, **9**(3), 40-50.

[6] **Teo, W.E. and Ramakrishna, S. ,** 2006: A review on electrospinning design and nanofibre assemblies, *Nanotechnology*, **17**(14), R89-R106.

[7] **Benjamin, C., S., H.B. and Dufei, F.,** 2006. Apparatus for electro-blowing or blowing-assisted electro-spinning technology and process for post treatment of electrospun or electroblown membranes, *United States Patent*, No: 20060049542 dated 03.09.2006.

[8] **Huang, Z.M., Zhang, Y.Z., Kotaki, M. and Ramakrishna, S.,** 2003: A review on polymer nanofibers by electrospinning and their applications in nanocomposites, *Composites Science and Technology*, **63**(15), 2223-2253.

[9] **Greiner, A. and Wendorff, J.H.,** 2007: Electrospinning: A fascinating method for the preparation of ultrathin fibres, *Angewandte Chemie-International Edition*, **46**(30), 5670-5703.

[10] **Ramakrishna, S., Thavasi, V. and Singh, G.,** 2008: Electrospun nanofibers in energy and environmental applications, *Energy & Environmental Science*, **1**(2), 205-221.

[11] **Gray, S.,** 1731: A letter concerning the electricity of water, from Mr. Stephen Gray to Cromwell Mortimer, *M.D.Secr.R.S Phil. Trans*, **37**, 227.

[12] **Larmor, J.,** 1898: Note on the complete scheme of electrodynamic equations of a moving material medium, and on electrostriction, *Proceedings of the Royal Society of London*, **63**, 365-372.

[13] **Cooley, J.F.,** 1902. Apparatus for electrically dispersing fluids, *United States Patent*, No:692631 dated 04.02.1902.

[14] **Morton, W.J.,** 1902. Method of dispersing fluids. *United States Patent*,No: 705691 dated 29.06.1902.

[15] **Hagiwara, K.,** 1929. Process for manufacturing artificial silk and other filaments by applying electric current, *United States Patent*, No: 1699615 dated 21.01.1929.

[16] **Formhals, A.,** 1934. Process and apparatus for preparing artificial threads, *United States Patent*, No: 1975504 dated 02.10.1934.

[17] **Vonnegut, B. and Neubauer, R.L.,** 1952: Production of monodisperse liquid particles by electrical atomization, *Journal of Colloid Science*, **7**(6), 616-622.

[18] **Drozin, V.G.,** 1955: The electrical dispersion of liquids as aerosols, *Journal of Colloid Science*, **10**, 158-164.

[19] **Simons, H.L.,** 1966. Process and apparatus for producing patterned non-woven fabrics, *United States Patent*, No:3280229 dated 18.10.1966.

[20] **Taylor, G.I.,** 1969: Electrically driven jets, *Proceedings of the Royal Society of London Series A Mathematical and Physical Sciences*, **313**, 453-475.

[21] **Baumgarten, P.,** 1971: Electrostatic Spinning of Acrylic Microfibers, *Journal of Colloid and Interface Science*, **36**(1), 71-79.

[22] **Martin, G.E., Cockshott, I.D. and Fildes, J.T.,** 1977. Fibrillar lining for prosthetic device. *United States Patent*, No: 4044404 dated 30.08.1977.

[23] **Simm, W., Gosling, C., Bonart, R. and VON Falkai, B.,** 1978. Filter made of electrostatically spun fibres, *United States Patent*, No:4069026 dated 17.01.1978.

[24] **Larrondo, L. and Manley, R.S.J.,** 1981: Electrostatic Fiber Spinning from Polymer Melts 2, Examination of the Flow Field in an Electrically Driven Jet. *Journal of Polymer Science Part B-Polymer Physics*, **19**(6), 921-932.

[25] **Bornat, A.,** 1982. Electrostatic spinning of tubular products, *United States Patent*, No:4323525 dated 06.04.1982

[26] **Bornat, R.,** 1987. Production of electrostatically spun products., *United States Patent,,*No: 4689186 dated 25.08.1987.

[27] *<http://www.etpbc.ca/content/view/64/84/>*, accessed at 12.12.2008

[28] **Doshi, J. and Reneker, D.H.,** 1995 Electrospinning Process and Applications of Electrospun Fibers, *Journal of Electrostatics*, **35**(2-3), 151-160.

[29] **Subbiah, T.,** 2004, Development of nanofiber protective substrates,*MSc Thesis*, Texas Tech University, Lubbock

[30] **Ramakrishna, S., Fujihara, K., Teo, W.E., Ma, Z.W. and Lim, T.C.,** 2005: An Introduction to Electrospinning and Nanofibers, World Scientific Publishers, Singapore.

[31] **Demir, A.,** 2007. Elektrospinning Yöntemiyle Nanolif Üretim Teknolojisi, TUBITAK report No:105M045, Ankara, Türkiye.

[32] *<http://en.wikipedia.org/wiki/File:Electrospinning_Diagram.jpg>*, accessed at 02.01.2009

[33] **Heikkila, P. and Harlin, A.,** 2008: Parameter study of electrospinning of polyamide-6, *European Polymer Journal*, **44**(10), 3067-3079.

[34] **Lee, K.H., Kim, H.Y., Bang, H.J., Jung, Y.H. and Lee, S.G.,** 2003: The change of bead morphology formed on electrospun polystyrene fibers, *Polymer*, **44**(14), 4029-4034.

[35] **Deitzel, J.M., Kleinmeyer, J., Harris, D. and Tan, N.C.B.,** 2001: The effect of processing variables on the morphology of electrospun nanofibers and textiles, *Polymer*, **42**(1), 261-272.

[36] **Mit-uppatham, C., Nithitanakul, M. and Supaphol, P.,** 2004: Ultratine electrospun polyamide-6 fibers: Effect of solution conditions on morphology and average fiber diameter, *Macromolecular Chemistry and Physics*, **205**(17), 2327-2338.

[37] **Fong, H., Chun, I. and Reneker, D.H.,** 1999: Beaded nanofibers formed during electrospinning, *Polymer*, **40**(16), 4585-4592.

[38] **Supaphol, P., Mit-Uppatham, C. and Nithitanakul, M.,** 2005: Ultrafine electrospun polyamide-6 fibers: Effect of emitting electrode polarity on morphology and average fiber diameter, *Journal of Polymer Science Part B-Polymer Physics*, **43**(24), 3699-3712.

[39] **Tan, S.H., Inai, R., Kotaki, M. and Ramakrishna, S.,** 2005: Systematic parameter study for ultra-fine fiber fabrication via electrospinning process, *Polymer*, **46**(16), 6128-6134.

[40] **Deitzel, J.M., Tan, N.C.B., Kleinmeyer, J.D., Rehrmann, J., Tevault, D., Reneker, D. and Sendijarevic, I.,** 1999. Generation of Polymer Nanofibers Through Electrospinning, Army Research Laboratory, Adelphi, USA.

[41] **Gomes, D.S., da Silva, A.N.R., Morimoto, N.I., Mendes, L.T.F., Furlan, R. and Ramos, I.,** 2007: Characterization of an electrospinning process using different PAN/DMF concentrations, *Polimeros-Ciencia E Tecnologia*, **17**(3), 206-211.

[42] **Srivastava, Y., Marquez, M. and Thorsen, T.,** 2007: Multijet electrospinning of conducting nanofibers from microfluidic manifolds, *Journal of Applied Polymer Science*, **106**(5), 3171-3178.

[43] **Qin, X.H., Yang, E.L., Li, N. and Wang, S.Y.,** 2007: Effect of different salts on electrospinning of polyacrylonitrile (PAN) polymer solution, *Journal of Applied Polymer Science*, **103**(6), 3865-3870.

[44] **Zong, X.H., Kim, K., Fang, D.F., Ran, S.F., Hsiao, B.S. and Chu, B.** Structure and process relationship of electrospun bioabsorbable nanofiber membranes. *Polymer*, 2002, **43**(16), 4403-4412.

[45] **Demir, M.M., Yilgor, I., Yilgor, E. and Erman, B.,** 2002: Electrospinning of polyurethane fibers, *Polymer*, **43**(11), 3303-3309.

[46] **Son, W.K., Youk, J.H., Lee, T.S. and Park, W.H.,** 2004: The effects of solution properties and polyelectrolyte on electrospinning of ultrafine poly(ethylene oxide) fibers, *Polymer*, **45**(9), 2959-2966.

[47] **Jung, Y.H., Kim, H.Y., Lee, D.R., Park, S.Y. and Khil, M.S.,** 2005: Characterization of PVOH nonwoven mats prepared from surfactant-polymer system via electrospinning, *Macromolecular Research*, **13**(5), 385-390.

[48] **Kataphinan, W.,** 2004, Electrospinning and potential applications, *PhD Thesis*,University of Akron, Ohio.

[49] **Zhao, S.L., Wu, X.H., Wang, L.G. and Huang, Y.,** 2004: Electrospinning of ethyl-cyanoethyl cellulose/tetrahydrofuran solutions, *Journal of Applied Polymer Science*, **91**(1), 242-246.

[50] **Kessick, R., Fenn, J. and Tepper, G.,** 2004: The use of AC potentials in electrospraying and electrospinning processes, *Polymer*, **45**(9), 2981-2984.

[51] **Sano, Y.,** 2001: Drying behavior of acetate filament in dry spinning, *Drying Technology*, **19**(7), 1335-1359.

[52] **Yuan, X.Y., Zhang, Y.Y., Dong, C.H. and Sheng, J.,** 2004: Morphology of ultrafine polysulfone fibers prepared by electrospinning, *Polymer International*, **53**(11), 1704-1710.

[53] **Jalili, R., Hosseini, S.A. and Morshed, M.,** 2005: The effects of operating parameters on the morphology of electrospun polyacrilonitrile nanofibres, *Iranian Polymer Journal*, **14**(12), 1074-1081.

[54] **Macossay, J., Marruffo, A., Rincon, R., Eubanks, T. and Kuang, A.,** 2007: Effect of needle diameter on nanofiber diameter and thermal properties of electrospun poly(methyl methacrylate), *Polymers for Advanced Technologies*, **18**(3), 180-183.

[55] **Mo, X.M., Xu, C.Y., Kotaki, M. and Ramakrishna, S.,** 2004: Electrospun P(LLA-CL) nanofiber: a biomimetic extracellular matrix for smooth muscle cell and endothelial cell proliferation, *Biomaterials*, **25**(10), 1883-1890.

[56] **Mit-uppatham, C., Nithitanakul, M. and Supaphol, P.,** 2004: Effects of solution concentration, emitting electrode polarity, solvent type, and salt addition on electrospun polyamide-6 fibers: A preliminary report, *Macromolecular Symposia*, **216**, 293-299.

[57] **Kilic, A., Oruc, F. and Demir, A.,** 2008: Effects of polarity on electrospinning process, *Textile Research Journal*, **78**(6), 532-539.

[58] **Megelski, S., Stephens, J.S., Chase, D.B. and Rabolt, J.F.,** 2002: Micro- and nanostructured surface morphology on electrospun polymer fibers, *Macromolecules*, **35**(22), 8456-8466.

[59] **Casper, C.L., Stephens, J.S., Tassi, N.G., Chase, D.B. and Rabolt, J.F.** Controlling surface morphology of electrospun polystyrene fibers: Effect of humidity and molecular weight in the electrospinning process. *Macromolecules*, **37**(2), 573-578.

[60] **Kim, G.T., Lee, J.S., Shin, J.H., Ahn, Y.C., Jeong, K.H., Sung, C.M., and Lee, J.K.,** 2004: Effect of humidity on the microstructures of electrospun polystyrene nanofibers, *Microscop. Microanalysis Microstruc.*, **10**, 554-555.

[61] *<http://www.ultrawebisalwaysbetter.com/>*, accessed at 06.01.2009

[62] *<http://www2.dupont.com/Separation_Solutions/en_US/tech_info/hmt/hmt. html>*, accessed at 06.01.2009.

[63] **Graham, K., Ouyang, M., Raether, T., Grafe, T., McDonald, B., Knauf, P.,** 2002. Polymeric Nanofibers in Air Filtration Applications, *Fifteenth Annual Technical Conference & Expo of the American Filtration & Separations Society,*Galveston, Texas,USA, April 9-12.

[64] **Kim, G.T., Ahn, Y.C. and Lee, J.K.,** 2008: Characteristics of Nylon 6 nanofilter for removing ultra fine particles, *Korean Journal of Chemical Engineering*, **25**(2), 368-372.

[65] *<http://www.finetextech.com/ftt_application1_3.jsp>*, accessed at 06.01.2009.

[66] *<http://www.surmodics.com/pdf/What_is_Nanofiber.pdf>*, accessed at 27.12.2008.

[67] *<http://www.surmodics.com/technologies-invitro-ecm.html>*, accessed at 06.01.2009.

[68] *<www.nicast.com>*, accessed at 26.12.2008.

[69] *<http://www.nanowerk.com/news/newsid=1156.php>*, accessed at 27.12.2008.

[70] **Vasita, R. and Katti, D.S.,** 2006: Nanofibers and their applications in tissue engineering, *International Journal of Nanomedicine*, **1**(1), 15-30.

[71] **Venugopal, J.R., Zhang, Y.Z. and Ramakrishna, S.,** 2006: In vitro culture of human dermal fibroblasts on electrospun polycaprolactone collagen nanofibrous membrane, *Artificial Organs*, **30**(6), 440-446.

[72] *<http://www.alltracel.com/Portals/1/hcn08_nanospider-brief_rd3.pdf>*, accessed at 27.12.2008.

[73] **Choi, S.S., Lee, Y.S., Joo, C.W., Lee, S.G., Park, J.K. and Han, K.S.,** 2004: Electrospun PVDF nanofiber web as polymer electrolyte or separator, *Electrochimica Acta*, **50**(2-3), 339-343.

[74] *<http://www2.dupont.com/Energy_Storage/en_US/tech_info/technical _info.html>*, accessed at 06.01.2009

[75] **Takeshi, K., Masaaki, K., Fuminori, K. and Masahiro, A.,** 2007. Separator for electric double layer capacitor and electric double layer capacitor containing same. *United States Patent*, No:20070247785 dated 25.10.2007.

[76] *<http://www2.dupont.com/Allergen_Barrier/en_US/products/benefits.html>*, accessed at 15.03.2008.

[77] *<http://old.elmarco.com/download/Antimicrobeweb_line.pdf>*, accessed at 25.03.2008.

[78] **Ding, B., Yamazaki, M. and Shiratori, S.,** 2005: Electrospun fibrous polyacrylic acid membrane-based gas sensors, *Sensors and Actuators B-Chemical*, **106**(1), 477-483.

[79] **Lomax, G.R.,** 2007: Breathable polyurethane membranes for textile and related industries, *Journal of Materials Chemistry*, **17**(27), 2775-2784.

[80] **Horrocks, A.R., Anand, S.C. and Raton, B.,** 2000: Handbook of technical textiles:Waterproof breathable fabrics, Woodhead Pub. Ltd.,Cambridge.

[81] <*http://www.torayentrant.com*>, accessed at 06.01.2009.

[82] <*http://www2.dupont.com/Tyvek/en_US/index.html*>, accessed at 12.12.2008

[83] <*http://www.albe24.com/tyvek1.jpg*>, accessed at 06.12.2008.

[84] <http://upload.wikimedia.org/wikipedia/commons/1/1d/Tyvek_house_wrap. jpg>, accessed at 06.12.2008.

[85] <*http://upload.wikimedia.org/wikipedia/commons/9/9a/John_wearing_Tyvek_ suit.jpg*>, accessed at 06.12.2008.

[86] **Mukhopadhyay, A. and Midha, V.K.,** 2008: A review on designing the waterproof breathable fabrics part I: Fundamental principles and designing aspects of breathable fabrics, *Journal of Industrial Textiles*, **37**, 225-262.

[87] **Baker, R.W.,** 2004: Membrane Technology and Applications, John Wiley & Sons Ltd, West Sussex.

[88] **Fung, W.,** 2002: Products from coated and laminated fabrics: Coated and laminated textiles, Woodhead Publishing Ltd, Florida.

[89] <*http://www.gore-tex.com/remote/Satellite/content/what-is-gore-tex-membrane*>, accessed at 07.01.2009.

[90] **Brzeziński, S., Malinowska, G., Nowak, T., Schmidt, S., Marcinkowska, D. and Kaleta, A.,** 2005: Structure and properties of microporous polyurethane membranes designed for textile-polymeric composite systems, *Fibres Textiles in Eastern Europe*, **13**(6), 53-58.

[91] <*www.sympatex.com*>, accessed at 12.12.2008.

[92] <*http://prospector.ides.com/DataView.aspx?E=84376*>, accessed at 11.01.2009.

[93] <*http://prospector.ides.com/DataView.aspx?E=83945*>, accessed at 11.01.2009.

[94] **CEN EN 20811,** 1992. Textiles — Determination of resistance to water penetration — Hydrostatic pressure test, E*uropean Committee for Standardization,* Brussels.

[95] **ASTM E96**, 2005. Standard test methods for water vapor transmission of materials, American Society for Testing and Materials, West Conshohocken.

[96] **ISO 9237,** 1995. Textiles - Determination of the permeability of fabrics to air first edition, *International Organization for Standardization*, Geneva.

[97] <http://www.textest.ch/pages_en/3300-III_en.htm>, accessed at 12.01.2009.

[98] **R.W. Gore**., 1980: Porous products and process therefor, *United States Patent,* No:4187390 dated 05.02.1980.

[99] **Danino, A.M., Malka, G., Revol, M. and Servant, J.M.,** 2005: A scanning electron microscopical study of the two sides of polypropylene mesh (Marlex[®]) and PTFE (Gore Tex[®]) mesh 2 years after complete abdominal wall reconstruction. A study of 15 cases, *British Journal of Plastic Surgery*, **58**(3), 384-388.

[100] **Kang, Y.K., Park, C.H., Kim, J. and Kang, T.J.,** 2007: Application of electrospun polyurethane web to breathable water-proof fabrics, *Fibers and Polymers*, **8**(5), 564-570.

[101] **Holmer, I.,** 2005: Textiles for protection against cold: Textiles for protection, p. 390, Woodhead Publishing Ltd Cambridge.

[102] *<http://www.allbusiness.com/automotive/automotive-industry-environment/11506958-1.html>*, accessed at 28.12.2008.

[103] **Chen, H.S., Cong, T.N., Yang, W., Tan, C.Q., Li, Y.L. and Ding, Y.L.,** 2009: Progress in electrical energy storage system: A critical review, *Progress in Natural Science*, **19**(3), 291-312.

[104] **Wang, C., M., Chen, J., M.,** 2003. Nanotechnology Prospect for Rechargeable Li-ion Batteries, *Materials Science and Technology in Engineering Conference,* Hong Kong, January 15-17.

[105] **Zhang, S.S.,** 2007: A review on the separators of liquid electrolyte Li-ion batteries. *Journal of Power Sources*, **164**, 351-364.

[106] **Bohnstedt, W.,** 1999: Separators. In Besenhard: Handbook of Battery Materials, Wiley-VCH, Graz.

[107] *<rsbook.googlepages.com/sszhang.pdf>*, accessed at 06.01.2009.

[108] **Spotnitz, R.,** 1999: Separators for Lithium-Ion Batteries: Handbook of Battery Materials, Wiley-VCH Graz.

[109] **Kritzer, P.,** 2006: Nonwoven support material for improved separators in Li-ion polymer batteries, *Journal of Power Sources*, **161**(2), 1335-1340.

[110] **Cho, T.H., Tanaka, M., Onishi, H., Kondo, Y., Nakamura, T., Yamazaki, H., Tanase, S. and Sakai, T.,** 2008: Battery performances and thermal stability of polyacrylonitrile nano-fiber-based nonwoven separators for Li-ion battery, *Journal of Power Sources*, **181**(1), 155-160.

[111] *<http://www.csc-jaekle.de/fileadmin/MeBl/150/MeBl_150053_EN.pdf>*, accessed at 14.03.2009.

[112] *<http://www.celgard.net/documents/2320_Data_Sheet_2008-12_20002.pdf>*, accessed at 14.03.2009.

[113] **Ji, L., Medford, A.J. and Zhang, X.,** 2009: Electrospun polyacrylonitrile /zinc chloride composite nanofibers and their response to hydrogen sulfide, *Polymer*, **50**, 605-612.

[114] *<http://www.jtbaker.com/msds/englishhtml/d6408.htm>*, accessed at 12.04.2009.

CURRICULUM VITAE

Candidate's full name:	**Tuncay GÜMÜŞ**
Place and date of birth:	**DÜZCE - 01.09.1983**
Permanent Address:	**Kürkçübaşı M. Sulubostan S. No:21/17 Cerrahpaşa/İSTANBUL**
Universities and Colleges attended:	**ITU Textile Technology and Design Faculty, Textile Engineering**
	Düzce Anatolian Teacher Training High School